COMPRESSIBILITY EFFECTS IN HELICOPTER

ROTOR BLADE FLUTTER

A THESIS

Presented to

The Faculty of the Division of Graduate

Studies and Research

by

Charles Eugene Hammond

In Partial Fulfillment

of the Requirements for the Degree

Doctor of Philosophy

in the School of Aerospace Engineering

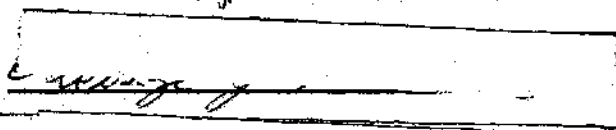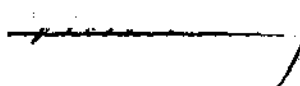
Georgia Institute of Technology

December, 1969

In presenting the dissertation as a partial fulfillment of
the requirements for an advanced degree from the Georgia
Institute of Technology, I agree that the Library of the
Institute shall make it available for inspection and
circulation in accordance with its regulations governing
materials of this type. I agree that permission to copy
from, or to publish from, this dissertation may be granted
by the professor under whose direction it was written, or,
in his absence, by the Dean of the Graduate Division when
such copying or publication is solely for scholarly purposes
and does not involve potential financial gain. It is under-
stood that any copying from, or publication of, this dis-
sertation which involves potential financial gain will not
be allowed without written permission.

7/25/68

COMPRESSIBILITY EFFECTS IN HELICOPTER
ROTOR BLADE FLUTTER

Approved:

Chairman

Date approved by Chairman: 12·19·69

ACKNOWLEDGMENTS

also wish to thank Mrs. Rae Sperry for her careful examination of the final draft.

To Mr. Jerry W. Segers, the staff, and machine operators of the Rich Electronic Computer Center I owe a special debt of gratitude. The advice of Mr. Segers concerning programming difficulties encountered during the course of this research has been indispensable. The efficient operation of the CALCOMP plotter by Messrs. Hugh Lewis, Andy Callahan, and others greatly reduced the formidable task of plotting the many velocity-damping curves required in the investigation.

The financial assistance of the U. S. Naval Weapons Laboratory, Dahlgren, Virginia, the U. S. Army Research Office, Durham, and the Vertical Flight Foundation is gratefully acknowledged. Without the assistance of the Naval Weapons Laboratory through their Full Time Advanced Study Program, my graduate academic career would have been delayed considerably.

To my parents I owe my entire career. For their many sacrifices during my undergraduate academic program and for impressing upon me the value of higher education, I express my deepest appreciation.

My wife Mae has contribued most significantly to the successful completion of this thesis and my entire graduate program through her patience, understanding, and encouragement. My daughter Cynthia, who will soon learn that fathers have occupations other than going to school, has always been a source of encouragement and joy.

TABLE OF CONTENTS

Unsteady Aerodynamic Development
    Comparison with Jones and Rao
    Comparison with Loewy's Incompressible Theory
    The Equivalent Single Bladed Rotor
    Convergence of the Wake Series

Two Degree of Freedom Flutter Analysis
    Structural Damping
    Generalized Forces

Static Divergence

Numerical Solution of the Unsteady Aerodynamic Problem
    Numerical Procedures

Numerical Solution of the Two Degree of Freedom
 Flutter Problem
    Discussion of the Velocity-Damping Plot

Static Divergence

LIST OF TABLES

LIST OF ILLUSTRATIONS

NOMENCLATURE

Roman Symbols

A	doublet strength for three-dimensional pulsating doublet, defined by Equation (A-25)
A_j	coefficient in the pressure series
$\bar{A}_j$	modified pressure series coefficient, defined by Equation (94)
a	nondimensional location of the reference airfoil elastic axis relative to midchord, measured positive aft
a_∞	free stream sound speed
b	semichord length of reference airfoil section
$Ci(\nu)$	cosine integral
D	dissipation function
D_1, D_2	dummy variables defined by Equations (H-9) and (H-10) respectively
D_n, D_{nq}	distances by which wake airfoils lead the reference airfoil, defined by Equations (E-6)
$E_1(\nu)$	exponential integral
$E^*(\nu)$	modified exponential integral

g	structural damping
g_h	structural damping in bending
g_α	structural damping in torsion
$H_\nu^{(p)}$	Hankel function of pth kind and ν^{th} order
h	inflow ratio, nondimensional h', $h = h'/b$
h'	vertical spacing between adjacent wake layers, $h' = 2\pi u/Q\Omega$
h_{eq}	equivalent single bladed inflow ratio for a multibladed rotor
$\bar{h}$	deflection of the reference airfoil elastic axis, positive down
$\mathcal{I}$	denotes the imaginary part of a complex quantity
I	used at various places to denote the value of an integral which is being manipulated
I_g	generalized integral, defined by Equation (19)
I_α	mass moment of inertia of reference airfoil
i	complex number, $i = \sqrt{-1}$
J	total number of terms from the pressure series
J_ν	Bessel function of first kind and ν^{th} order

j	summation index for pressure series
K	kernel of the integral equation, defined by Equation (21)
$K(x)$	distribution function, defined by Equation (E-3)
K_f	kernel of the fixed wing portion of the downwash equation, defined by Equation (62)
$\bar{K}_f$	kernel obtained by subtracting out the singular portion of K_f, defined by Equation (72)
K_h	bending stiffness of reference airfoil section
$\bar{K}_h$	kernel defined by Equation (H-3)
K_α	torsional stiffness of reference airfoil section
K_o	singular portion of K_f
$K_{oo}(x)$	distribution function, defined by Equation (E-5)
k	reduced frequency, $k = b\omega/U$
L	aerodynamic lift, positive down
L_h, L_α	aerodynamic coefficients, defined by Equations (49)
ℓ_h, ℓ_α	aerodynamic coefficients, defined by Equations (90)
$\bar{\ell}_z, \bar{\ell}_{\dot{z}}, \bar{\ell}_\alpha, \bar{\ell}_{\dot{\alpha}}$	aerodynamic coefficients, defined by Equations (124)

ℓ_{α_0}	value of ℓ_α at zero reduced frequency
M	Mach number
$M_{c/4}$	aerodynamic moment about quarter-chord point, positive nose-up
$M_{e.a.}$	aerodynamic moment about the elastic axis, positive nose-up
M_h, M_α	aerodynamic coefficients, defined by Equations (49)
m	frequency ratio, $m = \omega/\Omega$
m_{eq}	equivalent single bladed frequency ratio for a multibladed rotor
m_h, m_α	aerodynamic coefficients, defined by Equations (90)
$\bar{m}_z$, $\bar{m}_{\dot{z}}$, $\bar{m}_\alpha$, $\bar{m}_{\dot{\alpha}}$	aerodynamic coefficients, defined by Equations (124)
$\bar{m}$	mass per unit chord of reference airfoil
$\tilde{m}$	total mass of reference airfoil
N	total number of wake terms
NIP	number of integration points
n	rotor revolution index
P	dummy variable, defined by Equation (H-7)
p	local pressure
p_L	pressure on lower surface of reference airfoil

p_U pressure on upper surface of reference airfoil

$\Delta \bar{p}_a(x)$ pressure differential across reference airfoil, $\Delta \bar{p}_a(x) = p_U(x) - p_L(x)$

p_∞ free stream pressure

Q total number of blades in rotor

Q_h generalized force, bending

Q_α generalized force, torsion

q blade index for multibladed rotor

q_1, q_2 source strength

$\mathcal{R}$ denotes the real part of a complex quantity

r radial location of reference airfoil from center of rotation of the rotor

r_f radius of spherical propagation front, defined by Equation (A-9)

r_α nondimensional radius of gyration of the reference airfoil section

$\bar{r}, \theta$ polar coordinates, defined by Equations (D-4)

$Si(\nu)$ sine integral

S_α static unbalance of reference airfoil

S_1, S_2, S_3	series defined respectively by Equations (H-4), (H-5), and (H-6)
S_{1n}, S_{2n}, S_{3n}	n^{th} term of the series S_1, S_2, S_3
T	kinetic energy
t	time variable
U	free stream velocity which reference airfoil sees
U_D	static divergence speed
U_F	flutter speed
u	inflow velocity through rotor disc
V	potential energy
δw	virtual work
W	downwash function, defined by Equation (E-10)
W_i	downwash function for infinite system of wakes, defined by Equation (E-12)
w	downwash velocity at a general field point in the flow
w_a	total downwash velocity at the reference airfoil surface
w_f	downwash velocity at the reference airfoil due to the reference airfoil itself

w_h downwash velocity at the reference airfoil due to the infinite system of wakes

w' dummy variable, defined by Equation (B-2)

w'', w''' dummy variables, defined by Equations (B-6)

X, Z nondimensional coordinates, defined by Equations (E-10)

x, y, z Cartesian coordinate system; x positive downstream, y positive outboard, z positive up

x_j chordwise location of the jth collocation point

x_α nondimensional location of the reference airfoil center of gravity relative to the elastic axis, measured positive aft

Y_ν Bessel function of second kind and ν^{th} order

z_a displacement of a point on the midsurface of the reference airfoil

Greek Symbols

α angle of attack of reference airfoil, positive nose-up

β $\sqrt{1 - M^2}$

$\bar{\Gamma}$ total circulation for reference airfoil in incompressible flow, defined by Equation (G-7)

$\bar{\gamma}_a(x)$ vorticity distribution on reference airfoil in incompressible flow, defined by Equation (G-3)

γ_E constant related to Euler's constant by the relation, $\ln\gamma_E$ = Euler's constant

δ integer for convergence criteria, defined by Equation (32)

ϵ small distance between a source-sink pair

ζ dummy variable, defined alternately by Equations (A-34), (C-2), (D-2), and (H-8)

θ chordwise angle variable, defined by Equation (57)

Λ complex eigenvalue of the flutter problem, defined by Equation (110)

μ density ratio

μ_D doublet strength/U, i.e., $\mu_D U$ = doublet strength

ξ streamwise coordinate

ρ_∞ free stream density

τ time variable, defined alternately by Equations (A-8) and (D-2)

φ disturbance velocity potential

φ_c^s disturbance velocity potential for compressible source flow, defined by Equation (A-5)

φ_i^s disturbance velocity potential for incompressible source flow, defined by Equation (A-6)

Ψ acceleration potential

Ψ_q phase angle by which the motions of the qth blade lead the motions of the reference blade

Ψ_s acceleration potential for source flow

Ω rotational speed of rotor

ω_h uncoupled natural frequency in bending

ω_α uncoupled natural frequency in torsion

SUMMARY

An analytical study is presented of the effect which compressibility of the airstream has on the flutter condition of rotary wings. An unsteady, compressible aerodynamic theory is first developed. By assuming axial flight and low inflow conditions for the helicopter rotor, the complicated three-dimensional flow field is reduced to the more easily managed two-dimensional one used successfully by other investigators studying incompressible rotor flow.

The aerodynamics of the two-dimensional flow model are formulated using a kernel function approach. Using an acceleration potential the governing integral equation for the flow together with its attendant downwash boundary condition are developed. In solving the integral equation numerically, a pressure mode assumption in conjunction with a collocation technique is used. The pressure distribution thus determined is integrated to give the usual two-dimensional aerodynamic coefficients.

The flutter model used for the study is a rigid two-dimensional airfoil section free to pitch and plunge. The equations of motion for this model are established using a Lagrangian approach and are solved using the velocity-damping technique typical of most flutter analyses. The aerodynamic forcing functions necessary for the flutter analysis are taken from the previously developed aerodynamic theory.

The compressible aerodynamic theory is compared analytically with two other existing theories, one incompressible and one compressible,

and shown to agree with these theories provided the flow models used are made to agree. The difference in flow models comes about as a result of the kernel function approach used in this study. The effect of the difference in flow models is evaluated by comparing the numerical results of the different theories. The aerodynamic coefficients from the three theories are compared and shown to be in good agreement for values of the frequency ratio parameter near unity, but the disagreement is substantial for lower values of frequency ratio. The frequency ratio parameter is shown to be an indication of the degree of difference in the flow models; the higher the frequency ratio, the better the agreement.

The many parameters entering the flutter problem are varied systematically and their effect on the flutter condition under compressible flow conditions presented. A comparison is also made of the flutter speeds obtained using the aerodynamic theory of this study for zero Mach number with those obtained using a previous incompressible theory. The agreement between the two sets of flutter results is excellent for all values of the structural parameters investigated. However, for low values of the frequency ratio parameter it is shown that differences in the results exist. This again is due to the increasing difference in flow models as the frequency ratio is decreased. Comparison could not be made with flutter results obtained using the other recently developed compressible aerodynamic theory due to unavailability of the necessary aerodynamic data.

The variation of the flutter speed with the various flutter

parameters was found to be essentially the same for compressible as for incompressible flow. However, it is shown that the flutter speed for almost all conditions is decreased when the Mach number of the airstream is increased. The exceptions to this trend occur when the elastic axis and center of gravity locations coincide. For this case static divergence is shown to be more critical than flutter for certain combinations of the remaining parameters. Static divergence was not important when the center of gravity was shifted aft of the elastic axis by one-tenth of a semi-chord.

CHAPTER I

INTRODUCTION

The determination of the aerodynamics associated with a helicopter rotor has presented a challenge to the helicopter analyst since the conception of helicopters. Due to the complexity of this problem, helicopter aerodynamicists and aeroelasticians are still striving to obtain a satisfactory incompressible theory — even though helicopters are presently flying with rotor tip Mach numbers in excess of unity (see, for example, Reference [1]). This lack of adequate aerodynamic theories has led helicopter designers to rely heavily on experimental data and past experience in designing new helicopters. However, with the advent of higher helicopter speeds it is imperative that adequate theories be developed in order to cope with problems similar to those which have arisen in conjunction with fixed wing vehicles as a result of high speed.

Aeroelastic analyses depend heavily on the knowledge of unsteady aerodynamics. As fixed wing vehicles have progressed from low subsonic speeds through high subsonic speeds to supersonic speeds and even to hypersonic speeds in the case of missiles, appropriate unsteady aerodynamic theories have been developed to assist in predicting any aeroelastic instabilities which might occur. Unfortunately, the state-of-the-art in unsteady helicopter aerodynamics has not progressed as rapidly as that for unsteady fixed wing aerodynamics. This is due

in part to the fact that the rotary wing, especially in the forward
flight mode, is not as amenable to analysis as its fixed wing
counterpart. In dealing with the unsteady flow fields associated with
helicopter rotors, the analyses developed for fixed wings must be
drastically modified or abandoned altogether as a result of the rotor
blade being forced to pass in proximity to its wake on each revolution.

Many of the first attempts to analyze the unsteady rotor blade
aerodynamic problem were based on the supposition that the rotor blade
could be replaced by an equivalent fixed wing with an appropriate free
stream velocity. The important fact that the helicopter blade is
forced to pass over its wake was neglected. (It might be noted here
that this same procedure is currently being employed by some helicopter
companies in attempting to ascertain the effect of compressibility on
the aeroelastic instabilities of rotor blades). The first significant
unsteady approach to the rotor blade aerodynamic problem which
considered the rotor blade to be a separate entity from the fixed wing
was made by Loewy [2], Jones [3], and Timman and van de Vooren [4].
In this approach, which considered the flow to be incompressible,
certain assumptions were made in order to make the mathematical
analysis more tractable. The rotor was first considered to be operating
in axial flight or in a hovering condition. Further, it was assumed
that the rotor inflow velocity was low compared to the rotational
velocity. With these assumptions it was possible to reduce the
complicated three-dimensional rotor flow field to a more manageable
two-dimensional flow field. The resulting two-dimensional mathematical
model included a reference airfoil together with a complete system of

wakes shed by other blades in the rotor as well as the wake shed by the reference blade on previous revolutions. This system of wakes is the one thing which makes the helicopter aerodynamic analysis so much more complicated than the fixed wing aerodynamic problem. Whereas for the fixed wing the wake is assumed to lie in the same plane as the wing, the helicopter rotor wake is blown below the plane of the rotor by the inflow velocity and the determination of the blade loading depends on knowing the location of the wake. Using this two-dimensional approximation to the rotor flow field, Loewy [2] was able to show that the two-dimensional loading on the reference airfoil could be written in the same form as the loading on a two-dimensional fixed wing airfoil with the stipulation that Theodorsen's [5] lift deficiency function be replaced by a modified lift deficiency function applicable to rotor aerodynamics.

In a recent study, Hammond [6] has presented a comparison between the flutter speed obtained for a two degree of freedom system using Loewy's aerodynamics and the flutter speed for the same system using Theodorsen's [5] fixed wing aerodynamics. The results of this study indicated that given the same inertial conditions the flutter speed obtained using Loewy's aerodynamics was generally lower than the flutter speed obtained using Theodorsen's aerodynamics. The implications of this result are that the rotor wake which lies below the reference airfoil exerts a destabilizing influence on the two degree of freedom flutter condition and hence that the use of unsteady fixed wing aerodynamics in rotor blade flutter calculations will lead to unconservative results.

Miller [7] has presented a summary of many of the past approaches taken in obtaining rotor blade harmonic air loads. In addition he presents a technique for obtaining the three-dimensional unsteady aerodynamics for a rotor in forward flight. In this approach the flow is considered incompressible and the air loads on the blade resulting from the near wake are treated using lifting surface theories, while the far wake is treated using the lifting line approximation.

In a recent publication Ichikawa [8] presents a comprehensive lifting surface theory for a helicopter rotor in forward flight through an incompressible medium. In this theory the lifting surface equations are developed for a rotor in forward flight and then a reduction to the lifting line equations is made through approximations equivalent to those of Weissinger's [9] L-method. It was shown that agreement with experimental results was fairly good and stated that disagreement was probably caused by wake roll-up which was neglected in the theory. The wake roll-up problem which appears to be a significant source of error in helicopter aerodynamic theories has been treated very successfully and efficiently by Landgrebe [10].

In all the aerodynamic theories mentioned above the flow is assumed to be incompressible. However, as indicated by Reference [1], present day helicopters operate with tip speeds in the high subsonic speed range, thus suggesting that compressibility effects should be included in any realistic analysis of helicopter rotor blade loads. Unlike the steady flow case, the transition from incompressible to compressible unsteady flow results cannot be accomplished by simple transformations such as the Prandtl-Glauert transformation. This

difficulty follows from the result that in an incompressible fluid a disturbance is propagated at an infinite velocity and thus no time lag occurs between the initiation of a disturbance and its effect at some other point in the flow. However, in a compressible medium a definite time is required for a signal to reach a distant field point so that both a phase lag and a change in magnitude result.

The compressible flow results for a two-dimensional oscillating fixed wing have been known for some time. The first theoretical development of the problem was presented by Possio [11]. Dietze [12], Shade [13], Küssner [14], and others presented refinements of Possio's derivation and method of solution. Most of these early works are summarized by Karp, Shu, and Weil [15]. In more recent years Fettis [16], Frazer [17], Jordan [18], Jones [19], and a multitude of others have published papers on the oscillating airfoil in a compressible stream using basically the same integral equation developed by Possio. A different type of solution which essentially presents a closed form solution in terms of an infinite series of Mathieu functions has been published by Reissner and Sherman [20], Haskind [21], and Timman et al [22,23] among others.

In this thesis an unsteady aerodynamic theory for helicopter rotors which allows for the compressibility of the fluid medium is presented. Since the logical development of complex problems proceeds from the relatively simple to the more difficult problems, the approach taken here is to develop a compressible aerodynamic theory based on the assumptions made by Loewy [2]. The result is a two-dimensional unsteady compressible aerodynamic theory for rotor blades.

The method used to obtain the two-dimensional oscillatory loading on a reference airfoil section of the rotor is essentially the same as that used in many of the above mentioned fixed wing analyses. An acceleration potential is employed in developing the integral relation between the downwash and pressure distribution on the reference airfoil. The integral equation thus obtained, which is the same as Possio's [11] fixed wing integral equation with the addition of a correction term to account for the helicopter wake, is finally solved by collocation for the unknown pressure distribution.

Jones and Rao [24] have recently published a similar theory for the compressible aerodynamic loading on rotor blades. This theory differs from the theory developed in the present research in that a velocity potential approach was used in conjunction with the identical flow model used by Loewy [2]. One of the major conclusions reached in Reference [24] was that the helicopter wake had exactly the same effect on the unsteady aerodynamic blade loading in both compressible and incompressible flows. As will be shown later, this conclusion was a direct consequence of the flow model employed. The flow model used in the present study is a modified version of the two-dimensional model used by Loewy [2], and Jones and Rao [24]; the modifications being necessary to accommodate the acceleration potential approach.

The purpose of this research is to establish the effect of compressibility on the flutter condition for rotary wings operating in hovering or axial flight conditions. The major portion of the research is the development of the unsteady two-dimensional compressible aerodynamic theory discussed above. Also presented is a classical two

degree of freedom flutter analysis. The compressible unsteady aerodynamics are used in conjunction with the flutter analysis and a variation of the parameters occurring in the flutter problem is made to evaluate the effect of these parameters on the flutter condition when compressibility is included in the aerodynamics. Further, the results of this analysis are compared with the results obtained by Hammond [6] using Loewy's incompressible aerodynamics in order to demonstrate the overall effect of compressibility on the flutter condition for rotary wings.

CHAPTER II

THEORETICAL DEVELOPMENT

In this chapter the theoretical development necessary for computation of the compressible aerodynamic loading on the reference blade of a helicopter rotor is presented. Appropriate simplifying assumptions are made so that the complicated three-dimensional rotor flow field is reduced to a more tractable two-dimensional flow field. Finally using this two-dimensional mathematical model of the flow the integral relation between the downwash at the reference airfoil and the pressure differential across the reference airfoil is established.

Also included in this Chapter is the theoretical development underlying a classical two degree of freedom flutter analysis. The reference airfoil of the two-dimensional approximation to the rotor flow field is assumed to have two degrees of freedom, pitching and plunging, and the characteristic equation is developed for the double eigenvalue flutter problem.

Unsteady Aerodynamic Development

The general flow phenomena associated with a helicopter rotor has been described in some detail by Loewy [2]. With the assumptions of axial flight and low inflow velocity Loewy was able to reduce the complicated three-dimensional flow to a more tractable two-dimensional flow. The basic premise underlying this reduction is that under axial

flight and low inflow conditions, only that vorticity which lies in a small azimuth angle on either side of the reference blade significantly affects the loading on that blade. This assumption allows one to take a pie-shaped cut through the plane of rotation and on down through the helical vortex sheet which forms the wake from the blade. If then a vertical slice is taken perpendicular to the radial line passing from the center of rotation out along the reference blade, a plane is formed in which the flow may be considered to be two-dimensional. For low inflow the inclination of the vortex wake layers below the reference section may also be neglected. These assumptions thus lead to a two-dimensional representation of the flow made up of a reference airfoil section and its immediate trailing wake (both in the same horizontal plane) together with a system of horizontal wake layers lying at regularly spaced intervals below the reference section. These wake layers below the reference section account for the wake which has been shed by other blades in the rotor as well as for that shed by the reference blade in previous revolutions, with the spacing between the layers being determined by the inflow and rotational velocities. This flow model is shown in Figure 1 where it should be noted that the horizontal length of the vortex layers below the reference airfoil is finite. The length of the layers is determined by the azimuth angle on each side of the reference blade, inside of which the wake vorticity has a significant influence on the blade loading. In order to make the problem more mathematically manageable Loewy allowed the wake layers to extend to infinity both upstream and downstream. This final step is justified by the following argument. If the blade loading is
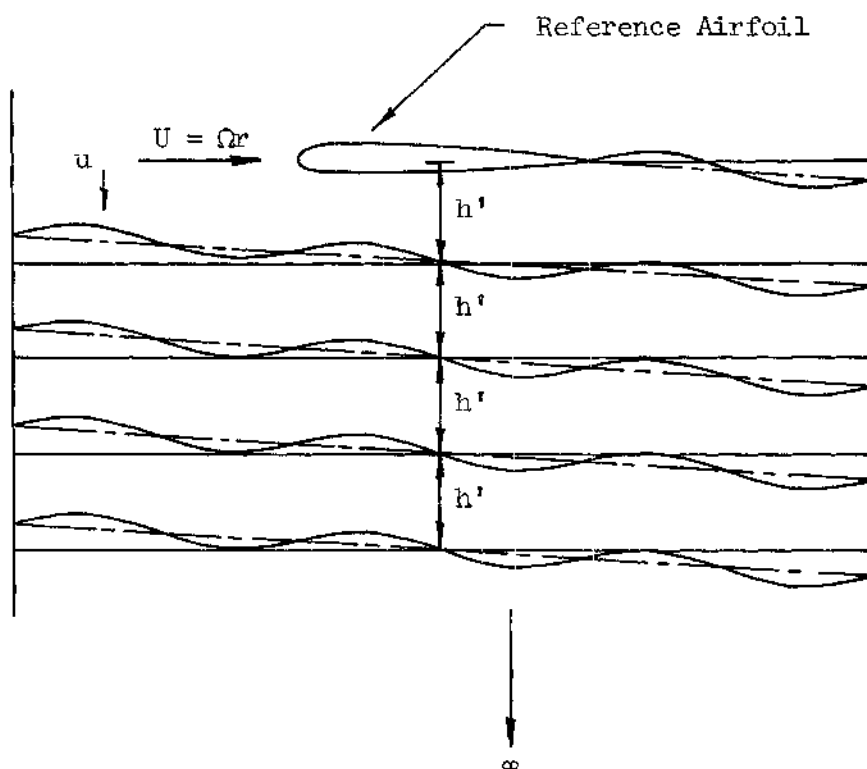
Figure 1. Two-Dimensional Model of the Unsteady Rotor
          Flow Field Under Assumptions of Axial Flight
          and Low Inflow

significantly affected by only that vorticity within a small azimuth angle on either side of the blade, then the vorticity added by allowing the horizontal rows of wake to extend to infinity both upstream and downstream cannot have any appreciable effect on blade loading and thus this device is acceptable. Loewy's final two-dimensional representation of the flow is shown in Figure 2.

In Loewy's analysis the flow is considered to be incompressible and a velocity potential approach is used to obtain the nonstationary loading on the reference blade. In a recent paper Jones and Rao [24] have used the velocity potential approach in conjunction with Loewy's flow model and included compressibility effects. They obtained the result that the effect of the infinite layers of wake below the reference airfoil was exactly the same for both compressible and incompressible flow. This result is due to the fact that the infinite layers of wake below the reference airfoil can be considered as wake layers shed by fixed wing airfoils regularly spaced below the reference airfoil and leading it by an infinite distance. The important concept which distinguishes compressible from incompressible unsteady flows, that of a time delay between the initiation of a disturbance and the time it is felt at some other point in the flow, is thus lost and the wake layers indeed appear as incompressible wakes.

In the present dissertation Loewy's work is extended to include the effect of compressibility, but the theoretical approach taken to the problem of determining the unsteady aerodynamic reactions on the reference airfoil differs in technique and, as a result, in flow model from the approach taken by Jones and Rao. The acceleration potential
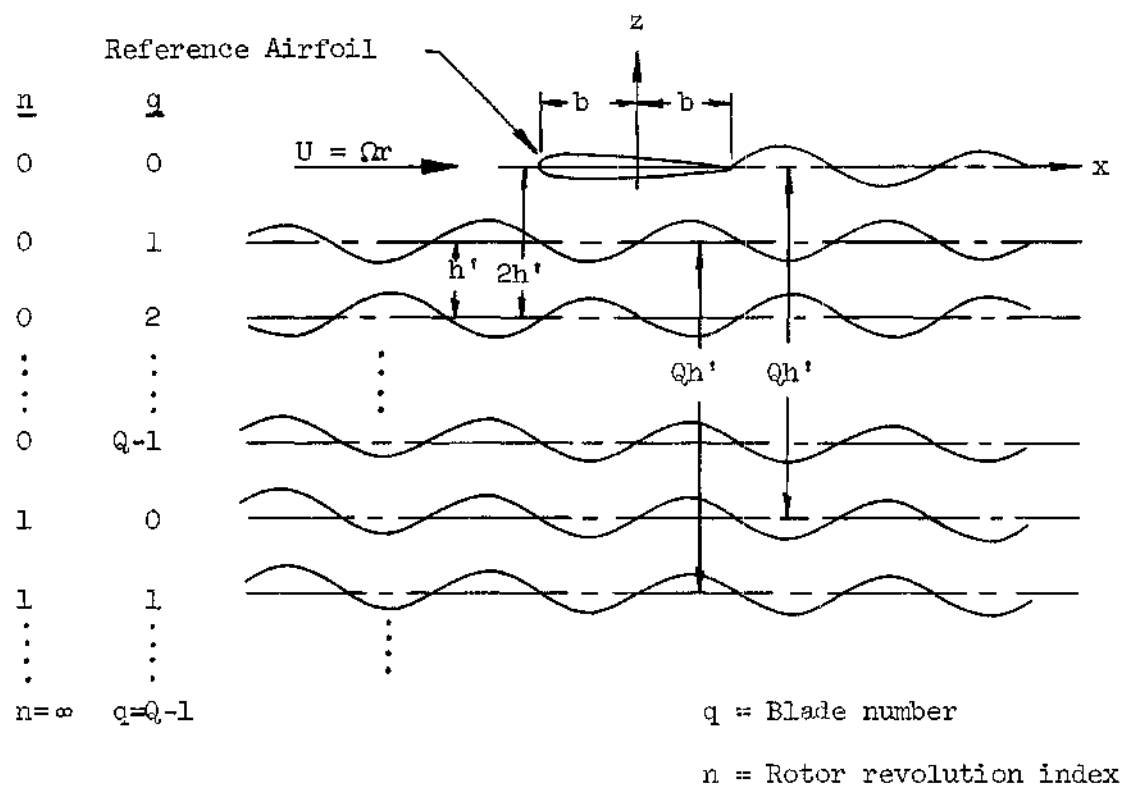
Figure 2. Loewy's Incompressible Aerodynamic Model

approach which has proved fruitful in fixed wing compressible flow analyses is adopted as the basic method of attacking the problem. The use of the acceleration potential approach, however, leads to difficulties when one attempts to apply the method to Loewy's flow model.

With a velocity potential approach such as that used by Loewy, and Jones and Rao, the elemental flows from which the overall flow is to be developed must be distributed in the wake as well as on the airfoil itself in order to account for the velocity discontinuity which exists across the wake and across the airfoil. In contrast, however, the acceleration potential is associated with a pressure discontinuity and thus the elemental flows may be distributed on the airfoil only since no pressure discontinuity is allowed to exist in the wake. With the acceleration potential approach, therefore, it is necessary to introduce a device by which the layers of wake lying below the reference airfoil can be taken into account.

Consider first a single bladed rotor and a reference blade section lying a radial distance r from the axis of rotation. As the blade traverses the azimuth it trails a wake which is blown below the blade by the inflow velocity and forms a helical sheet. (Loewy's model would give an infinite number of wake layers below the reference airfoil). Now when the reference section has made one complete revolution it has traveled a distance of $2\pi r$. As the blade makes its second revolution it sees a wake which was shed on its first revolution and which has been blown downward by the inflow velocity. This wake can be thought of as being shed by an airfoil identical to the reference airfoil which is flying under the reference airfoil and

leading it by a distance of $2\pi r$. On the third revolution the reference airfoil sees two layers of wake; the lowermost layer being shed on the first revolution and the upper layer being shed on the second revolution. The reference section has now traveled a distance of $4\pi r$ since the wake was shed on the first revolution and a distance of $2\pi r$ since the wake was shed on the second revolution. To account for these wake layers, two airfoils are placed below the reference airfoil; the lowermost one leading the reference airfoil by a distance of $4\pi r$ and the upper one leading the reference airfoil by a distance of $2\pi r$. The vertical spacing of the individual layers is governed by the inflow and rotational velocities and is the same as for Loewy's model. By continuing the above process the entire wake can be represented by a semi-infinite cascade of airfoils regularly spaced below the reference airfoil and leading it by integer multiples of $2\pi r$.

The argument for a multibladed rotor is precisely the same as for a single bladed rotor. The passage of blades other than the reference blade is accounted for by airfoils below the reference airfoil and interspersed between the "wake airfoils" representing previous passages of the reference airfoil. The resulting two-dimensional flow model for a multibladed rotor which will be used in the mathematical development to follow is shown in Figure 3.

With the mathematical flow model thus established the problem remains to determine the nonstationary lift and moment on the reference airfoil when it is permitted to oscillate with simple harmonic motion as it moves through a compressible medium. The
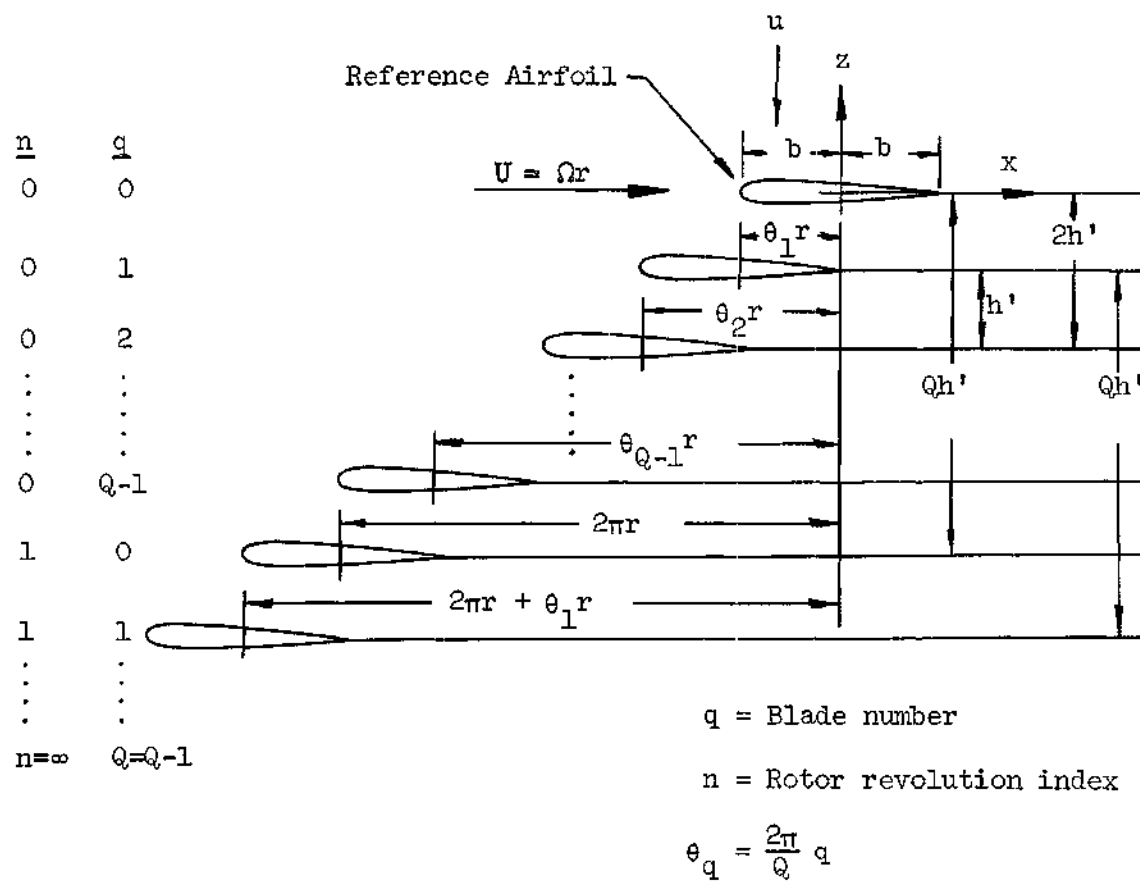
Figure 3. Compressible Aerodynamic Model for a Multibladed
Rotor Showing Notation for Mathematical Analysis

classical small disturbance assumptions are made so that the governing partial differential equation for the flow may be taken as the linearized acceleration potential equation

$$\frac{\partial^2 \Psi}{\partial x^2} + \frac{\partial^2 \Psi}{\partial z^2} - \frac{1}{a_\infty^2} \left[\frac{\partial^2 \Psi}{\partial t^2} + 2U \frac{\partial^2 \Psi}{\partial t \partial x} + U^2 \frac{\partial^2 \Psi}{\partial x^2} \right] = 0 \tag{1}$$

The acceleration potential, Ψ, is related to the disturbance velocity potential, φ, by

$$\Psi = \frac{\partial \varphi}{\partial t} + U \frac{\partial \varphi}{\partial x} \tag{2}$$

which is seen to be the linearized form of the substantial derivative of φ with respect to time. The acceleration potential is related also to the pressure at any point in the flow through the equation

$$p - p_\infty = - \rho_\infty \Psi \tag{3}$$

The pressure on the reference airfoil is obtained in the manner typical of most linearized aerodynamic analyses. An elementary flow solution is first found for the governing differential Equation (1). The total flow solution is then found by superimposing the elemental flow solutions and satisfying the two boundary conditions for potential flows: (1) all disturbances must vanish at field points far removed from the body with the exception of the wake, and (2) the flow at the body must be tangent to the body.

In this case, as in most compressible flow analyses, the elementary flow solution is taken to be the doublet. Since oscillatory motions of the reference airfoil are to be permitted, the strength of the doublet must also pulsate with time. The acceleration potential of such a pulsating doublet located at the origin of the coordinate system is developed in Appendix A to be

$$\Psi_D = U\mu_D \frac{\partial \overline{\Psi}_s}{\partial z} \tag{4}$$

where

$$\overline{\Psi}_s = \frac{i}{4\beta} e^{i\omega \left(t + \frac{M^2}{\beta^2} \frac{x}{U} \right)} H_o^{(2)} \left(\frac{\omega M}{\beta^2 U} \sqrt{x^2 + \beta^2 z^2} \right)$$

$U\mu_D$ = doublet strength.

It may be noted here that the pulsating doublet solution also satisfies the boundary condition that disturbances vanish at points far away from the doublet.

In order to obtain the complete flow solution, these pulsating doublets are distributed over the chord of the reference airfoil and over the chords of the airfoils below the reference airfoil which account for the rotor wake. The total acceleration potential at any field point (x,z) in the flow is then found by integrating the acceleration potentials of the distributed doublets. That is

$$\Psi(x,z;t) = \int_{-b}^{b} U\mu_{D}(\xi,o) \; \frac{\partial}{\partial z} \left\{ \frac{i}{4\beta} e^{i\omega\{t + [M^2(x-\xi)/\beta^2 U]\}} \right. \tag{5}$$

$$\left. \cdot H_{o}^{(2)} \left(\frac{\omega M}{\beta^2 U} \sqrt{(x-\xi)^2 + \beta^2 z^2} \right) \right\} d\xi$$

$$+ \sum_{n=o}^{\infty} \sum_{q=1}^{Q-1} \int_{-b-\frac{2\pi}{Q} qr -2n\pi r}^{b-\frac{2\pi}{Q} qr-2n\pi r} U\mu_{D}(\xi, -(nQ + q)h') \frac{\partial}{\partial z} \left\{ \frac{i}{4\beta} e^{i\omega\{t + [M^2(x-\xi)/\beta^2 U]\} + i\Psi_{q}} \right.$$

$$\left. \cdot H_{o}^{(2)} \left(\frac{\omega M}{\beta^2 U} \sqrt{(x-\xi)^2 + \beta^2 [z + (nQ + q)h']^2} \right) \right\} d\xi$$

$$+ \sum_{n=1}^{\infty} \int_{-b-2n\pi r}^{b-2n\pi r} U\mu_{D}(\xi,o) \frac{\partial}{\partial z} \left\{ \frac{i}{4\beta} e^{i\omega\{t + [M^2(x-\xi)/\beta^2 U]\}} \right.$$

$$\left. \cdot H_{o}^{(2)} \left(\frac{\omega M}{\beta^2 U} \sqrt{(x-\xi)^2 + \beta^2 (z + nQh')^2} \right) \right\} d\xi$$

The $e^{i\Psi_q}$ was introduced in the second integral above to allow for the fact that other blades in the rotor might be oscillating out of phase with the reference blade. The assumption is now made that the strength of the doublet distribution on all the airfoils in the cascade is the same. This is equivalent to saying that the motions of all the blades are identical which in turn implies that all blades of the rotor are identical, and this condition met as nearly as manufacturing tolerances will allow on most helicopter rotors. Now in the second integral let

$$\xi_o = \xi + \frac{2\pi}{Q} qr + 2n\pi r$$

and in the third integral let

$$\xi_o = \xi + 2n\pi r$$

so that the total acceleration potential becomes

$$\Psi(x,z;t) = \frac{iU}{4\beta} e^{i\omega t} \left\{ \int_{-b}^{b} \mu_D(\xi) e^{i\omega M^2 (x-\xi)/\beta^2 U} \right. \tag{6}$$

$$\left. \cdot \frac{\partial}{\partial z} H_o^{(2)} \left(\frac{\omega M}{\beta^2 U} \sqrt{(x-\xi)^2 + \beta^2 z^2} \right) d\xi \right.$$

$$+ \sum_{n=o}^{\infty} \sum_{q=1}^{Q-1} e^{i\Psi_q + i2\pi\omega M^2 r(nQ+q)/Q\beta^2 U} \int_{-b}^{b} \mu_D(\xi_o) e^{i\omega M^2(x-\xi_o)/\beta^2 U}$$

$$\cdot \frac{\partial}{\partial z} H_o^{(2)} \left(\frac{\omega M}{\beta^2 U} \sqrt{\left[(x - \xi_o) + \frac{2\pi r}{Q}(nQ + q) \right]^2 + \beta^2 \left[z + (nQ + q)h' \right]^2} \right) d\xi_o$$

$$+ \sum_{n=1}^{\infty} e^{i2n\pi r(\omega M^2/\beta^2 U)} \int_{-b}^{b} \mu_D(\xi_o) e^{i\omega M^2(x-\xi_o)/\beta^2 U}$$

$$\cdot \frac{\partial}{\partial z} H_o^{(2)} \left(\frac{\omega M}{\beta^2 U} \sqrt{(x - \xi_o + 2n\pi r)^2 + \beta^2(z + nQh')^2} \right) d\xi_o \Bigg\}$$

In Appendix B it is shown that the pressure discontinuity across the reference airfoil is related to the doublet distribution strength by

$$\Delta \bar{p}_a(x) = - \rho_\infty U\mu_D(x) \tag{7}$$

where

$$\Delta p_a(x;t) = \Delta \bar{p}_a(x) e^{i\omega t}$$

Using this fact and defining the parameters

$$k = \text{reduced frequency} = \frac{b\omega}{U} = \frac{b\omega}{\Omega r} \tag{8}$$

$$m = \text{frequency ratio} = \frac{\omega}{\Omega} = \frac{kr}{b}$$

$$h = \text{inflow ratio} = \frac{h'}{b}$$

the total acceleration potential becomes

$$\Psi(x,z;t) = -\frac{ie^{i\omega t}}{4\rho_\infty \beta} \left\{ \int_{-b}^{b} \Delta\bar{p}_a(\xi) e^{ikM^2(x-\xi)/\beta^2 b} \right. \tag{9}$$

$$\cdot \frac{\partial}{\partial z} H_o^{(2)} \left(\frac{kM}{\beta^2} \sqrt{\left(\frac{x-\xi}{b}\right)^2 + \beta^2\left(\frac{z}{b}\right)^2} \right) d\xi$$

$$+ \sum_{n=o}^{\infty} \sum_{q=1}^{Q-1} e^{i\Psi_q + i[2\pi m M^2(nQ+q)/\beta^2 Q]} \int_{-b}^{b} \Delta\bar{p}_a(\xi) e^{ikM^2(x-\xi)/\beta^2 b}$$

$$\cdot \frac{\partial}{\partial z} H_o^{(2)} \left(\frac{M}{\beta^2} \sqrt{\left[\frac{k(x-\xi)}{b} + \frac{2\pi m}{Q}(nQ+q)\right]^2 + \beta^2\left[\frac{kz}{b} + (nQ+q)kh\right]^2} \right) d\xi$$

$$+ \sum_{n=1}^{\infty} e^{i2n\pi m M^2/\beta^2} \int_{-b}^{b} \Delta \vec{p}_a(\xi) e^{ikM^2(x-\xi)/\beta^2 b}$$

$$\cdot \frac{\partial}{\partial z} H_o^{(2)} \left(\frac{M}{\beta^2} \sqrt{\left[\frac{k(x-\xi)}{b} + 2n\pi m \right]^2 + \beta^2 \left[\frac{kz}{b} + nQkh \right]^2} \right) d\xi \Bigg\}$$

The second boundary condition on the flow, namely that the flow be tangent to the body, is specified in terms of the downwash velocity at the body. The boundary condition is

$$w_a(x,t) = \frac{\partial z_a}{\partial t} + U \frac{\partial z_a}{\partial x} \quad \text{for} \quad z = 0, \ -b \leq x \leq b \qquad (10)$$

Thus in order to apply the boundary condition the relationship between the total acceleration potential, $\Psi(x,z;t)$, and the downwash velocity, $w(x,z;t)$, must be known. The downwash may be expressed in terms of the disturbance velocity potential, φ, as

$$w = \frac{\partial \varphi}{\partial z} \qquad (11)$$

The acceleration potential and disturbance velocity potential are also related and the relationship is given by Equation (2). Since Ψ, and therefore φ, are simple harmonic time dependent functions (due to the linearity of the problem)

$$\Psi(x,z;t) = \overline{\Psi}(x,z)e^{i\omega t}$$

$$\varphi(x,z;t) = \overline{\varphi}(x,z)e^{i\omega t} \tag{12}$$

and Equation (2) may be written

$$\overline{\Psi}(x,z) = i\omega\,\overline{\varphi}(x,z) + U\frac{\partial\overline{\varphi}}{\partial x} \tag{13}$$

This last equation can be integrated along a path of constant z to obtain

$$\overline{\varphi}(x,z) = \int_{-\infty}^{x} \frac{\overline{\Psi}(\xi,z)}{U}\, e^{\,i\,\frac{\omega}{U}(\xi-x)}\, d\xi + C(z) \tag{14}$$

The function $C(z)$ is set equal to zero in order to satisfy the first boundary condition that all disturbances vanish at points far from the body. Thus

$$\varphi(x,z;t) = \frac{1}{U} \int_{-\infty}^{x} \Psi(\xi,z;t)e^{-i\,\frac{\omega}{U}(x-\xi)}\, d\xi \tag{15}$$

The downwash at any point in the flow is now given by

$$w(x,z;t) = \frac{1}{U} \int_{-\infty}^{x} \frac{\partial\Psi(x,z;t)}{\partial z}\, e^{-i\,\frac{\omega}{U}(x-\xi)}\, d\xi \tag{16}$$

Introducing the acceleration potential

$$w(x,z;t) = -\frac{ie^{i\omega t}}{4\rho_\infty U\beta} \left\{ \int_{-\infty}^{x} \int_{-b}^{b} \Delta\bar{p}_a(\xi)e^{ikM^2(\xi'-\xi)/\beta^2 b} \; e^{-i\omega(x-\xi')/U} \right. \tag{17}$$

$$\cdot \frac{\partial^2}{\partial z^2} H_o^{(2)}\left(\frac{kM}{\beta^2}\sqrt{\left(\frac{\xi'-\xi}{b}\right)^2 + \beta^2\left(\frac{z}{b}\right)^2} \right) d\xi \; d\xi'$$

$$+ \sum_{n=0}^{\infty} \sum_{q=1}^{Q-1} e^{i\Psi_q + i[2\pi m M^2(nQ+q)/\beta^2 Q]} \int_{-\infty}^{x} \int_{-b}^{b} \Delta\bar{p}_a(\xi) \; e^{ikM^2(\xi'-\xi)/\beta^2 b} \; e^{-i\omega(x-\xi')/U}$$

$$\cdot \frac{\partial^2}{\partial z^2} H_o^{(2)}\left(\frac{M}{\beta^2}\sqrt{\left[\frac{k(\xi'-\xi)}{b} + \frac{2\pi m}{Q}(nQ+q)\right]^2 + \beta^2\left[\frac{kz}{b} + (nQ+q)kh\right]^2} \right) d\xi \; d\xi'$$

$$+ \sum_{n=1}^{\infty} e^{i2n\pi m M^2/\beta^2} \int_{-\infty}^{x} \int_{-b}^{b} \Delta\bar{p}_a(\xi) \; e^{ikM^2(\xi'-\xi)/\beta^2 b} \; e^{-i\omega(x-\xi')/U}$$

$$\cdot \frac{\partial^2}{\partial z^2} H_o^{(2)}\left(\frac{M}{\beta^2}\sqrt{\left[\frac{k(\xi'-\xi)}{b} + 2n\pi m\right]^2 + \beta^2\left[\frac{kz}{b} + nQkh\right]^2} \right) d\xi \; d\xi' \left. \right\}$$

Reversing the order of integration and collecting the exponentials

$$
w(x,z;t) = -\frac{ie^{i\omega t}}{4\rho_\infty U\beta} \left\{ \int_{-b}^{b} \Delta\bar{p}_a(\xi)\, e^{-ik(x-\xi)/b} \int_{-\infty}^{x} e^{ik(\xi'-\xi)/\beta^2 b} \right. \tag{18}
$$

$$
\cdot \frac{\partial^2}{\partial z^2} H_o^{(2)}\left(\frac{kM}{\beta^2}\sqrt{\left(\frac{\xi'-\xi}{b}\right)^2 + \beta^2\left(\frac{z}{b}\right)^2} \right) d\xi'\, d\xi
$$

$$
+ \sum_{n=o}^{\infty} \sum_{q=1}^{Q-1} e^{i\Psi_q + i[2\pi m M^2(nQ+q)/\beta^2 Q]} \int_{-b}^{b} \Delta\bar{p}_a(\xi)\, e^{-ik(x-\xi)/b} \int_{-\infty}^{x} e^{ik(\xi'-\xi)/\beta^2 b}
$$

$$
\cdot \frac{\partial^2}{\partial z^2} H_o^{(2)}\left(\frac{M}{\beta^2}\sqrt{\left[\frac{k(\xi'-\xi)}{b} + \frac{2\pi m}{Q}(nQ+q)\right]^2 + \beta^2\left[\frac{kz}{b} + (nQ+q)kh\right]^2} \right) d\xi'\, d\xi
$$

$$
+ \sum_{n=1}^{\infty} e^{i2n\pi m M^2/\beta^2} \int_{-b}^{b} \Delta\bar{p}_a(\xi)\, e^{-ik(x-\xi)/b} \int_{-\infty}^{x} e^{ik(\xi'-\xi)/\beta^2 b}
$$

$$
\left. \cdot \frac{\partial^2}{\partial z^2} H_o^{(2)}\left(\frac{M}{\beta^2}\sqrt{\left[\frac{k(\xi'-\xi)}{b} + 2n\pi m\right]^2 + \beta^2\left[\frac{kz}{b} + nQkh\right]^2} \right) d\xi'\, d\xi \right\}
$$

The three interior integrals appearing in the above equation may be simplified somewhat to produce the kernel of the integral equation. These three integrals may be evaluated by considering a generalized form which encompasses all three integrals, namely

$$I_g = \int_{-\infty}^{x} e^{ik(\xi'-\xi)/\beta^2 b} \frac{\partial^2}{\partial z^2} H_o^{(2)} \left(\frac{M}{\beta^2} \sqrt{\left[\frac{k(\xi'-\xi)}{b} + A\right]^2 + \beta^2 \left[\frac{kz}{b} + B\right]^2} \right) d\xi'$$

(19)

where A and B are constants with respect to the integration. This integral is evaluated in Appendix C where it is shown that

$$I_g = \frac{\omega M}{U} \frac{\left[\frac{k(x-\xi)}{b} + A\right] e^{ik(x-\xi)/\beta^2 b} H_1^{(2)} \left(\frac{M}{\beta^2}\sqrt{\left[\frac{k(x-\xi)}{b}+A\right]^2 + \beta^2\left[\frac{kz}{b}+B\right]^2}\right)}{\sqrt{\left[\frac{k(x-\xi)}{b} + A\right]^2 + \beta^2 \left[\frac{kz}{b} + B\right]^2}}$$

(20)

$$+ \frac{i\omega}{U} e^{ik(x-\xi)/\beta^2 b} H_o^{(2)}\left(\frac{M}{\beta^2}\sqrt{\left[\frac{k(x-\xi)}{b} + A\right]^2 + \beta^2 \left[\frac{kz}{b} + B\right]^2} \right)$$

$$+ \frac{\omega}{U} e^{-iA/\beta^2} \int_{-\infty}^{[k(x-\xi)/b]+A} e^{i\eta/\beta^2} H_o^{(2)}\left(\frac{M}{\beta^2}\sqrt{\eta^2 + \beta^2\left[\frac{kz}{b} + B\right]^2} \right) d\eta$$

Using this result and defining the following kernel

$$K\left[M, \frac{k(x-\xi)}{b}, \frac{kz}{b}\right] = \frac{iM}{4\beta}\left[\frac{k(x-\xi)}{b}\right] e^{ikM^2(x-\xi)/\beta^2 b} \tag{21}$$

$$\cdot H_1^{(2)}\left(\frac{M}{\beta^2}\sqrt{\left[\frac{k(x-\xi)}{b}\right]^2 + \beta^2\left[\frac{kz}{b}\right]^2}\right) \bigg/ \sqrt{\left[\frac{k(x-\xi)}{b}\right]^2 + \beta^2\left[\frac{kz}{b}\right]^2}$$

$$- \frac{1}{4\beta} e^{ikM^2(x-\xi)/\beta^2 b} H_0^{(2)}\left(\frac{M}{\beta^2}\sqrt{\left[\frac{k(x-\xi)}{b}\right]^2 + \beta^2\left[\frac{kz}{b}\right]^2}\right)$$

$$+ \frac{i}{4\beta} e^{-ik(x-\xi)/b}\int_{-\infty}^{k(x-\xi)/b} e^{i\eta/\beta^2} H_0^{(2)}\left(\frac{M}{\beta^2}\sqrt{\eta^2 + \beta^2\left[\frac{kz}{b}\right]^2}\right) d\eta$$

the downwash may be written as

$$w(x,z;t) = -\frac{\omega e^{i\omega t}}{\rho_\infty U^2}\left\{\int_{-b}^{b} \Delta\bar{p}_a(\xi) K\left[M, \frac{k(x-\xi)}{b}, \frac{kz}{b}\right] d\xi \tag{22}\right.$$

$$+ \sum_{n=0}^{\infty}\sum_{q=1}^{Q-1} e^{i\Psi_q}\int_{-b}^{b}\Delta\bar{p}_a(\xi) K\left[M, \frac{k(x-\xi)}{b} + 2\pi(nQ+q)\frac{m}{Q}, \frac{kz}{b} + (nQ+q)kh\right] d\xi$$

$$+ \sum_{n=1}^{\infty}\int_{-b}^{b}\Delta\bar{p}_a(\xi) K\left[M, \frac{k(x-\xi)}{b} + 2\pi m, \frac{kz}{b} + nQkh\right] d\xi\bigg\}$$

The downwash at the reference airfoil may now be found by allowing z to go to zero, i.e.

$$w_a(x;t) = \lim_{z \to 0} w(x,z;t) \tag{23}$$

Requiring the downwash to vary harmonically with time

$$w_a(x,t) = \bar{w}_a(x) \ e^{i\omega t} \tag{24}$$

the downwash at the reference airfoil becomes

$$\bar{w}_a(x) = -\frac{\omega}{\rho_\infty U^2} \left\{ \int_{-b}^{b} \Delta\bar{p}_a(\xi) \ K\left[M, \frac{k(x-\xi)}{b}, 0\right] d\xi \right. \tag{25}$$

$$+ \sum_{n=0}^{\infty} \sum_{q=1}^{Q-1} e^{i\Psi_q} \int_{-b}^{b} \Delta\bar{p}_a(\xi) \ K\left[M, \frac{k(x-\xi)}{b} + 2\pi(nQ+q)\frac{m}{Q}, (nQ+q)kh\right]d\xi$$

$$\left. + \sum_{n=1}^{\infty} \int_{-b}^{b} \Delta\bar{p}_a(\xi) \ K\left[M, \frac{k(x-\xi)}{b} + 2n\pi m, nQkh\right] d\xi \right\}$$

The first integral above is precisely the integral derived first by Possio [11] for a two-dimensional fixed wing airfoil oscillating in a compressible medium. The second term represents the downwash at the reference airfoil caused by previous passages of blades in the rotor other than the reference blade. Finally, the third term represents the downwash at the reference airfoil due to previous passages of the reference airfoil.

Comparison with Jones and Rao

As was stated earlier Jones and Rao [24] have presented an analysis of the same aerodynamic problem considered here using a different flow model and a different mathematical approach. It is shown in Appendix E that the downwash equation, Equation (18), can be made equivalent to the downwash equation given by Jones and Rao provided that the flow model of Figure 3 is made to agree with the flow model which they used, namely the same model used by Loewy and shown in Figure 2. The model of Figure 3 is made to agree with that of Figure 2 by forcing the "wake airfoils" to lead the reference airfoil by an infinite distance. This presents no real problem in the case of incompressible flow; however, the situation is somewhat different in compressible flow. Whereas a disturbance is propagated at an infinite velocity in an incompressible fluid, the speed of propagation is finite in a compressible medium so that both a time lag and a decay in the magnitude of the disturbance result as the disturbance is transmitted through the fluid. When the "wake airfoils" are allowed to go to infinity this means that the perturbations in the flow caused

by each "wake airfoil" must travel an infinite distance before reaching the reference airfoil. This in effect means that as far as the reference airfoil is concerned the wakes which are trailed by the "wake airfoils" are the same as the ones which would occur if the flow were incompressible. This is indeed one of the major conclusions of Reference [24]. That is, Jones and Rao found that the infinite layers of wake below the reference airfoil, as shown in Figure 2, had exactly the same influence on the downwash at the reference airfoil in compressible flow as in incompressible flow.

This conclusion of an incompressible wake is not possible when the flow model of Figure 3 is used. The dependence of the wake terms on Mach number is shown explicitly by Equations (21) and (25).

Comparison with Loewy's Incompressible Theory

It is desirable to reduce the kernel of Equation (21) for zero Mach number so that comparison with Loewy's work can subsequently be made. This reduction is accomplished in Appendix F where it is shown that for zero Mach number the kernel given by Equation (21) reduces to

$$
K\left[0, \frac{k(x-\xi)}{b}, \frac{kz}{b}\right] = -\frac{1}{2\pi} \frac{\frac{k(x-\xi)}{b}}{\left[\frac{k(x-\xi)}{b}\right]^2 + \left[\frac{kz}{b}\right]^2} - \frac{1}{2} e^{-(kz/b)-i[k(x-\xi)/b]}
$$

$$(26)$$

$$
-\frac{i}{4\pi} e^{-(kz/b) - i[k(x-\xi)/b]} E_1\left[-\frac{kz}{b} - i\frac{k(x-\xi)}{b}\right]
$$

$$- \frac{i}{4\pi} e^{(kz/b) - i[k(x-\xi)/b]} E_1 \left[\frac{kz}{b} - i \frac{k(x-\xi)}{b} \right]$$

Using this kernel it can be shown, as is done in Appendix G, that for zero Mach number the downwash relation of Equation (25) reduces to that given by Loewy provided, of course, that the flow model of Figure 3 is made to agree with that used by Loewy (Figure 2) by forcing the "wake airfoils" to lead the reference airfoils by an infinite distance.

The Equivalent Single Bladed Rotor

Up to this point in the theoretical development all blades of the rotor have been permitted to oscillate out of phase; the phasing being determined by the $e^{i\Psi_q}$ factor in the second term of Equation (25). If, however, it is assumed that all the blades are oscillating in phase, then the second term of Equation (25) containing the double sum can be combined with the third term and the downwash written

$$\bar{w}_a(x) = - \frac{\omega}{\rho_\infty U^2} \left\{ \int_{-b}^{b} \Delta \bar{p}_a(\xi) \, K \left[M, \frac{k(x-\xi)}{b}, 0 \right] d\xi \right. \tag{27}$$

$$\left. + \sum_{n=1}^{\infty} \int_{-b}^{b} \Delta \bar{p}_a(\xi) \, K \left[M, \frac{k(x-\xi)}{b} + 2n\pi \frac{m}{Q}, nkh \right] d\xi \right\}$$

It may be noted that this last expression is exactly the same as the downwash expression one would obtain for a single bladed rotor having a frequency ratio $\frac{m}{Q}$ and an inflow ratio h. Thus with the assumption that all the blades are oscillating in phase the aerodynamic development for a multibladed rotor can be reduced to the consideration of an equivalent single bladed rotor with

$$
\left.
\begin{aligned}
m_{eq} &= \frac{m}{Q} \\[2em]
h_{eq} &= h
\end{aligned}
\right\} \tag{28}
$$

Since this reduction to an equivalent single bladed rotor is possible, all further considerations will be restricted to a single bladed rotor. The integral equation to be solved for the pressure distribution on the reference airfoil thus becomes

$$
\bar{w}_a(x) = -\frac{\omega}{\rho_\infty U^2} \left\{ \int_{-b}^{b} \Delta\bar{p}_a(\xi) \; K\left[M, \frac{k(x-\xi)}{b}, 0\right] d\xi \right. \tag{29}
$$

$$
\left. + \sum_{n=1}^{\infty} \int_{-b}^{b} \Delta\bar{p}_a(\xi) \; K\left[M, \frac{k(x-\xi)}{b} + 2n\pi m, nkh\right] d\xi \right\}
$$

subject to the boundary condition

$$\bar{w}_a(x) = i\omega \bar{z}_a(x) + U \frac{d\bar{z}_a(x)}{dx} , \qquad -b \leq x \leq b \qquad (30)$$

where simple harmonic motion has been assumed for the reference airfoil, i.e.,

$$z_a(x;t) = \bar{z}_a(x) \, e^{i\omega t} \qquad (31)$$

Convergence of the Wake Series

The downwash equation, Equation (29), which is to be solved for the unknown pressure distribution on the reference airfoil contains an infinite series and hence some discussion is in order concerning the convergence of this series. In Appendix H it is shown that the series appearing in Equation (29) converges except for those values of the flow parameters where the relation

$$m \frac{M^2}{\beta^2} - \frac{M}{2\pi\beta^2} \sqrt{(2\pi m)^2 + (\beta k h)^2} = \delta, \qquad \delta = 0,1,2,\ldots \qquad (32)$$

is satisfied.

A condition similar to that of Equation (32) has been encountered by Runyan and Watkins [25] and by Carta [26]. Runyan and Watkins were investigating the unsteady flow over a two-dimensional airfoil in a compressible wind-tunnel stream while Carta was studying the compressible flow over an infinite cascade of oscillating airfoils representing

the compressor blades of a turbine engine. In each of these cases the condition similar to Equation (32) was interpreted as an acoustical resonance condition.

For the present study, however, the interpretation of Equation (32) as an acoustical resonance condition in the physical flow is not justified. Whereas in References [25] and [26] there were present in the physical flow field objects from which pressure waves could be initiated or reflected and thus create a resonance condition, there are no such objects in the physical rotor flow field. The "wake airfoils" in Figure 3 were introduced simply to account for the phase relationship between the reference airfoil and the wake, and to accommodate the mathematical analysis. Therefore, Equation (32) must be interpreted as only a mathematical instability associated with the flow model.

Two Degree of Freedom Flutter Analysis

When an elastic body is placed in an airstream the reaction of the aerodynamic forces on the body will cause the body to deform. This distortion of the body in turn causes an alteration of the aerodynamic reactions, and under most conditions the resulting aerodynamic forces tend to return the body to its original configuration. However, under some conditions the aerodynamic forces can cause the body to deform even more so that an instability of the body motion occurs. The instability of the motion may be either static or dynamic.

Flutter is a case of dynamic instability of an elastic body in an airstream. The flutter speed and flutter frequency are defined

respectively as the airspeed and corresponding circular frequency at which a given elastic body flying at given atmospheric conditions will exhibit self-sustained simple harmonic motion. This definition of flutter allows one to find the flutter boundary between stability and instability by assuming the body to be undergoing simple harmonic motion, calculating the unsteady aerodynamic forces based on simple harmonic motion of the body, and finally calculating the two eigenvalues of the flutter problem — flutter speed and frequency.

In this section the classical two degree of freedom flutter analysis is presented for the reference airfoil shown in Figure 3. The airfoil is considered to be restrained by springs against independent vertical motion (bending) and angular motion (torsion) as shown in Figure 4. No chordwise bending of the airfoil section is permitted. In the development which follows a Lagrangian approach is taken in arriving at the equations of motion for the two degree of freedom system shown in Figure 4.

The kinetic energy of the system is given by

$$T = \frac{1}{2} \int_{-b}^{b} \left(\frac{\partial z_a}{\partial t}\right)^2 \bar{m} \, dx \tag{33}$$

where $\bar{m}$ is the mass per unit chord and z_a is the deflection of some point on the airfoil midsurface from its equilibrium position. From Figure 4

$$z_a = -\left[\bar{h} + (x - ab)\alpha\right] \tag{34}$$
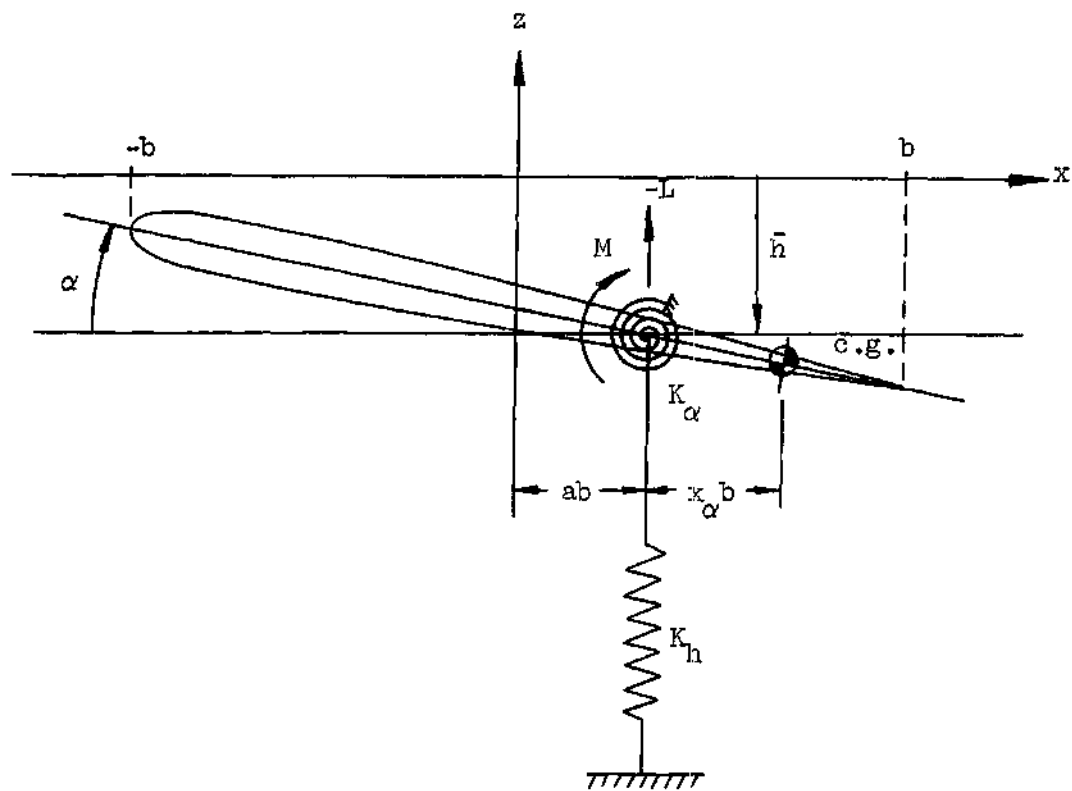
Figure 4. Two Degree of Freedom Flutter Model Showing
Notation for Mathematical Analysis

and

$$\frac{\partial z_a}{\partial t} = - \left[\dot{h} + (x - ab)\dot{\alpha} \right] \tag{35}$$

The kinetic energy thus becomes

$$T = \frac{1}{2} \int_{-b}^{b} \left[\dot{h}^2 + 2\dot{\alpha}\,\dot{h}\,(x - ab) + \dot{\alpha}^2(x - ab)^2 \right] \bar{m}\, dx \tag{36}$$

Now define the parameters

$$\left. \begin{array}{l} \tilde{m} = \displaystyle\int_{-b}^{b} \bar{m}\, dx \\[2em] S_\alpha = \displaystyle\int_{-b}^{b} (x - ab)\, \bar{m}\, dx \\[2em] I_\alpha = \displaystyle\int_{-b}^{b} (x - ab)^2\, \bar{m}\, dx \end{array} \right\} \tag{37}$$

With these substitutions the kinetic energy may be written as

$$T = \frac{1}{2} \left(\tilde{m}\, \dot{h}^2 + 2 S_\alpha\, \dot{\alpha}\, \dot{h} + I_\alpha\, \dot{\alpha}^2 \right) \tag{38}$$

The potential energy is simply the energy stored in the springs, or

$$V = \frac{1}{2}\left(K_\alpha \alpha^2 + K_h \bar{h}^2\right) \tag{39}$$

Using Lagrange's equations for a conservative system the equations of motion for the system become

$$\left.\begin{aligned}
\tilde{m}\,\ddot{\bar{h}} + S_\alpha \ddot{\alpha} + K_h \bar{h} = Q_h \\
\\
I_\alpha \ddot{\alpha} + S_\alpha \ddot{\bar{h}} + K_\alpha \alpha = Q_\alpha
\end{aligned}\right\} \tag{40}$$

Introducing the uncoupled free vibration frequencies

$$\left.\begin{aligned}
\omega_h^2 = \frac{K_h}{\tilde{m}} \\
\\
\omega_\alpha^2 = \frac{K_\alpha}{I_\alpha}
\end{aligned}\right\} \tag{41}$$

the equations become

$$\left.\begin{aligned}
\tilde{m}\,\ddot{\bar{h}} + S_\alpha \ddot{\alpha} + \tilde{m}\,\omega_h^2 \bar{h} = Q_h \\
\\
I_\alpha \ddot{\alpha} + S_\alpha \ddot{\bar{h}} + I_\alpha \omega_\alpha^2 \alpha = Q_\alpha
\end{aligned}\right\} \tag{42}$$

Structural Damping

It can be shown (see for example Baker, Woolam and Young [27])
that the structural damping force in an elastic system is proportional
to the amplitude and in phase with the velocity of oscillation. Also,
it can be shown experimentally that the energy dissipated per cycle is
proportional to the square of the amplitude and independent of the
frequency of oscillation.

In the usual derivation of the equations of motion, structural
damping is introduced in the following manner. The Lagrangian equations
of motion are set up and then the restoring force terms are modified by
replacing $\tilde{m}\, \omega_h^2\, \bar{h}$ by $(1 + ig_h)\, \tilde{m}\, \omega_h^2\, \bar{h}$, and $I_\alpha \omega_\alpha^2 \alpha$ by $(1 + ig_\alpha)\, I_\alpha \omega_\alpha^2 \alpha$
where the terms $ig_h \tilde{m}\, \omega_h^2\, \bar{h}$ and $ig_\alpha I_\alpha \omega_\alpha^2 \alpha$ are seen to be proportional to
amplitude and in phase with velocity under the assumption of simple
harmonic motion.

Scanlan and Rosenbaum [28] point out that for the simple
harmonic motions being considered here, a dissipation function may be
defined as follows

$$D = \frac{1}{2}\left[\frac{\tilde{m}g_h \omega_h^2}{\omega}\, \dot{h}^2 + \frac{I_\alpha g_\alpha \omega_\alpha^2}{\omega}\, \dot{\alpha}^2 \right] \tag{43}$$

where ω is the coupled frequency of the system.

In either case, when structural damping is introduced the
equations of motion become

$$\tilde{m}\,\ddot{\bar{h}} + S_\alpha\ddot{\alpha} + (1 + ig_h)\,\tilde{m}\,\omega_h^2\,\bar{h} = Q_h$$

$$I_\alpha\ddot{\alpha} + S_\alpha\ddot{\bar{h}} + (1 + ig_\alpha)\,I_\alpha\omega_\alpha^2\alpha = Q_\alpha$$

$$(44)$$

Generalized Forces

The generalized force is defined as the virtual work done during a virtual displacement. Thus

$$\delta w = Q_h\delta\bar{h} + Q_\alpha\delta\alpha \tag{45}$$

But

$$\delta w = \int_{-b}^{b} (p_U - p_L)\,\delta\bar{h}\,dz + \int_{-b}^{b} (p_U - p_L)(x - ab)\,\delta\alpha\,dx \tag{46}$$

so that

$$Q_h = \int_{-b}^{b} (p_U - p_L)\,dx = L$$

$$Q_\alpha = \int_{-b}^{b} (p_U - p_L)(x - ab)\,dx = M_{e.a.}$$

$$(47)$$

where the total lift, L, has been defined as positive down and the moment about the elastic axis, $M_{e.a.}$, has been defined as positive nose-up. Using the results of Equations (47) the equations of motion become

$$\tilde{m}\, \ddot{\bar{h}} + S_\alpha \ddot{\alpha} + (1 + ig_h)\, \tilde{m}\, \omega_h^2\, \bar{h} = L$$

$$I_\alpha \ddot{\alpha} + S_\alpha \ddot{\bar{h}} + (1 + ig_\alpha)\, I_\alpha \omega_\alpha^2 \alpha = M_{e.a.}$$

$$\left. \right\} \quad (48)$$

In unsteady aerodynamic analyses it is customary to write the total lift and moment in component form so that the lift and moment due to each of the degrees of freedom can readily be determined. The expressions used most often in this country are those given by Smilg and Wasserman [29] and shown below in terms of the displacement of the quarter-chord point and rotation about the quarter chord point

$$L = \pi \rho_\infty b^3 \omega^2 \left[L_h \left(\frac{\bar{h}}{b} \right)_{c/4} + L_\alpha (\alpha)_{c/4} \right]$$

$$M_{c/4} = \pi \rho_\infty b^4 \omega^2 \left[M_h \left(\frac{\bar{h}}{b} \right)_{c/4} + M_\alpha (\alpha)_{c/4} \right]$$

$$\left. \right\} \quad (49)$$

These expressions with the lift and moment referenced to the quarter chord point are used in conjunction with the unsteady aerodynamic analysis presented in the first part of this chapter and the aerodynamic coefficients L_h, L_α, M_h, and M_α are calculated numerically. The lift and moment expressions needed in the equations of motion, Equations (48), must be referenced to the elastic axis. This transformation is easily made and in terms of the displacement of the elastic axis and rotation about the elastic axis the lift and moment expressions become

$$L = \pi\rho_\infty b^3 \omega^2 \left\{ L_h \frac{\bar{h}}{b} + \left[L_\alpha - L_h \left(\frac{1}{2} + a \right) \right]\alpha \right\}$$

$$M_{e.a.} = \pi\rho_\infty b^4 \omega^2 \left\{ \left[M_h - L_h \left(\frac{1}{2} + a \right) \right] \frac{\bar{h}}{b} \right.$$

$$\left. + \left[M_\alpha - \left(L_\alpha + M_h \right)\left(\frac{1}{2} + a \right) + L_h \left(\frac{1}{2} + a \right)^2 \right]\alpha \right\} \tag{50}$$

Now restrict all considerations to simple harmonic motion in order to establish the flutter boundary. The displacement of the elastic axis and rotation about the elastic axis are thus written

$$\tilde{h} = \bar{h}_o e^{i\omega t}$$

$$\alpha = \bar{\alpha}_o e^{i\omega t} \tag{51}$$

where $\bar{\alpha}_0$ may be complex to denote the phase relationship between $\bar{h}$ and α. Substituting this restriction and the expressions for lift and moment, Equations (48) become

$$
\begin{array}{l}
- \omega^2 \tilde{m} \, \bar{h} - \omega^2 S_\alpha \alpha + \left(1 + ig_h\right) \tilde{m} \, \omega_h^2 \, \bar{h} \\[3em]
\qquad = \pi \rho_\infty b^3 \, \omega^2 \left\{ L_h \, \frac{\bar{h}}{b} + \left[L_\alpha - L_h \left(\frac{1}{2} + a\right)\right] \alpha \right\} \\[3em]
- \omega^2 I_\alpha \alpha - \omega^2 S_\alpha \bar{h} + \left(1 + ig_\alpha\right) I_\alpha \omega_\alpha^2 \alpha \\[3em]
\qquad = \pi \rho_\infty b^4 \omega^2 \left\{ \left[M_h - L_h \left(\frac{1}{2} + a\right)\right] \frac{\bar{h}}{b} \right. \\[3em]
+ \left. \left[M_\alpha - \left(L_\alpha + M_h\right)\left(\frac{1}{2} + a\right) + L_h \left(\frac{1}{2} + a\right)^2 \right] \alpha \right\}
\end{array}
\right\} \quad (52)
$$

Divinding the first of Equations (52) by $\pi \rho_\infty b^3 \omega^2$ and the second by $\pi \rho_\infty b^4 \omega^2$ and collecting terms the equations may be written in the following form

$$\left\{ \frac{\tilde{m}}{\pi\rho_\infty b^2} \left[1 - \left(\frac{\omega_h}{\omega}\right)^2 \left(1 + ig_h\right)\right] + L_h \right\} \frac{\bar{h}}{b}$$

$$+ \left\{ \frac{S_\alpha}{\pi\rho_\infty b^3} + \left[L_\alpha - L_h \left(\frac{1}{2} + a\right)\right]\right\} \alpha = 0$$

$$\left\{ \frac{S_\alpha}{\pi\rho_\infty b^3} + \left[M_h - L_h \left(\frac{1}{2} + a\right)\right]\right\} \frac{\bar{h}}{b}$$

$$+ \left\{ \frac{I_\alpha}{\pi\rho_\infty b^4} \left[1 - \left(\frac{\omega_\alpha}{\omega}\right)^2 \left(1 + ig_\alpha\right)\right]\right.$$

$$+ \left.\left[M_\alpha - \left(L_\alpha + M_h\right)\left(\frac{1}{2} + a\right) + L_h \left(\frac{1}{2} + a\right)^2 \right]\right\} \alpha = 0$$

$$\left.\begin{array}{c} \\ \\ \\ \\ \\ \\ \\ \end{array}\right\} \quad (53)$$

The problem has now been reduced to that of solving a system of two homogeneous algebraic equations. A nontrivial solution can thus exist only if the determinant of the coefficients vanishes. This determinant is called the "flutter determinant" and for this two degree of freedom problem it is given by

$$\begin{vmatrix} A & B \\ C & D \end{vmatrix} = 0 \qquad (54)$$

where

$$A = \mu \left[1 - \left(\frac{\omega_h}{\omega} \right)^2 \left(1 + ig_h \right) \right] + L_h$$

$$B = \mu x_\alpha + L_\alpha - L_h \left(\frac{1}{2} + a \right)$$

$$C = \mu x_\alpha + M_h - L_h \left(\frac{1}{2} + a \right) \tag{55}$$

$$D = \mu r_\alpha^2 \left[1 - \left(\frac{\omega_\alpha}{\omega} \right)^2 \left(1 + ig_\alpha \right) \right]$$

$$+ \left[M_\alpha - \left(L_\alpha + M_h \right) \left(\frac{1}{2} + a \right) + L_h \left(\frac{1}{2} + a \right)^2 \right]$$

and the following nondimensional parameters have been introduced

$$\mu = \frac{\tilde{m}}{\pi \rho_\infty b^2}$$

$$x_\alpha = \frac{S_\alpha}{\tilde{m} b} \tag{56}$$

$$r_\alpha^2 = \frac{I_\alpha}{\tilde{m} b^2}$$

Equation (54) represents the characteristic equation for the flutter problem and it is a complex quadratic equation. Since the

characteristic equation is complex, the flutter problem is thus seen to be a double eigenvalue problem, the eigenvalues being the flutter speed and flutter frequency. The aerodynamic coefficients appearing in Equation (54) are complicated trancendental functions of both speed and frequency and must be calculated numerically using the unsteady aerodynamic analysis presented in the first part of this chapter. Thus a trial and error process must be used in solving the characteristic equation, Equation (54), for the flutter speed and flutter frequency. The process used is described in detail in Chapter III.

Static Divergence

As stated earlier, an elastic body in an airstream can experience either static or dynamic instabilities of motion. Divergence is a case of static instability. The static divergence speed is found by allowing the reduced frequency to go to zero in the equations of motion, Equations (48). When this is done, all the inertial terms as well as the damping terms g_h and g_α go to zero. The equations of motion for static divergence thus become

$$\tilde{m}\omega_h^2 \, \bar{h} = L$$

$$I_\alpha \, \omega_\alpha^2 \alpha = M_{e.a.}$$

where the lift and moment expressions are evaluated at zero reduced frequency. A more complete discussion of the divergence condition is presented in Chapter III.

In summary, a compressible aerodynamic theory has been presented

for the determination of unsteady aerodynamic loads on rotary wings.
Under the assumptions of axial flight and low inflow conditions, the
three-dimensional rotor flow field was reduced to a two-dimensional
flow field which was used for the mathematical development. The
integral equation relating downwash on the reference airfoil to the
pressure distribution on the reference airfoil was subsequently
developed and the downwash boundary condition stated. This integral
equation with its boundary condition represents the governing equation
which must be solved for the unknown pressure distribution on the
reference airfoil.

A classical two degree of freedom flutter analysis was also
presented in this chapter. This flutter analysis is used later in the
thesis with aerodynamic data computed using the aerodynamic analysis
presented in this chapter to establish the effect of compressibility on
the flutter condition for rotary wings.

CHAPTER III

FORMULATION OF THE NUMERICAL SOLUTIONS

In the previous chapter an integral equation and its attendant boundary condition were developed to relate the downwash on a reference airfoil section of a helicopter rotor blade to the pressure differential across the reference section. In the present chapter a numerical method of solving the integral equation for the unknown pressure distribution on the reference airfoil section is presented. The difficulties involved in this method of solution are discussed along with techniques used for surmounting the difficulties.

The numerical procedure employed in solving the two degree of freedom flutter problem is also discussed in this chapter. Since one of the eigenvalues of the flutter problem appears only implicitly in the unsteady aerodynamic derivatives it is necessary to solve the problem indirectly. This is done by taking oscillatory frequency and structural damping as unknowns, varying reduced frequency, and plotting structural damping versus nondimensional velocity to obtain the flutter speed.

Numerical Solution of the Unsteady Aerodynamic Problem

In Chapter II an integral equation was developed for the down-wash in terms of the pressure distribution on a reference airfoil section of an equivalent single bladed rotor. The downwash equation is

given by Equation (29) and its boundary condition by Equation (30). It is the purpose of this section to describe the method used in solving the integral equation for the unknown pressure distribution subject to the given boundary condition.

First note that the unknown in Equation (29), $\Delta \bar{p}_a(x)$, is contained under the integrals on the right side of the equation and the downwash on the left side of the equation is known through the boundary condition. If somehow the equation could be inverted so that the pressure distribution $\Delta \bar{p}_a(x)$ appeared on the left side and the downwash appeared under the integral, the integrals could be evaluated directly to obtain the pressure distribution. However, since no inversion formula is known for Equation (29) a collocation technique in conjunction with a pressure mode assumption is employed in extracting the solution.

It is first assumed that the pressure distribution may be written in the form of a Fourier type series given by

$$\Delta \bar{p}_a(\theta) = A_o \cot \frac{\theta}{2} + \sum_{j=1}^{\infty} A_j \sin j\,\theta \qquad (57)$$

$$\cos \theta = -\frac{x}{b}$$

The form of this series is based somewhat on physical reasoning. It is known that in subsonic small disturbance theory the linearizing assumptions break down at the leading edge of the airfoil and cause a

singularity in the pressure distribution. This fact is accounted for by the first term of Equation (57). Also, the pressure distribution must go to zero at the trailing edge to satisfy Kutta's hypothesis that the flow traverse the trailing edge smoothly. This requirement is satisfied by using the Fourier sine series instead of the cosine series. In the numerical computations it is necessary to truncate the series after J terms, so in the analysis which follows the finite series

$$\Delta \bar{p}_a(\theta) = A_o \cot \frac{\theta}{2} + \sum_{j=1}^{J-1} A_j \sin j\, \theta \tag{58}$$

is used.

If the pressure distribution series, Equation (58), is substituted in the downwash integral equation, the integrals appearing on the right side of Equation (29) can be evaluated in terms of the J pressure series coefficients. If the boundary condition, Equation (30), is then evaluated at J points on the chord of the reference airfoil there results a system of J algebraic equations which may be solved for the J unknown coefficients of the pressure series. The location of the collocation points, as the points at which the boundary condition is to be satisfied are called, is somewhat arbitrary. Two spacings which are popular in fixed wing analyses are the equal spacing and the Multhopp spacing. The Multhopp spacing is obtained by writing

$$\frac{x_j}{b} = - \cos \theta_j \qquad 0 \le \theta_j \le \pi \qquad (59)$$

and using an equal spacing on the θ_j. This type of spacing results in a higher density of points near the leading and trailing edge than in the center of the chord. Although the spacing of the collocation points is arbitrary, Hsu [30] has shown that for the fixed wing airfoil an optimum set of collocation points exists and is given by

$$\frac{x_j}{b} = - \cos \left(\frac{2j\pi}{2J+1} \right) \qquad j = 1, 2, \ldots , J \qquad (60)$$

where J is the total number of collocation points being used. It will be noted that the optimum distribution for the collocation points is very much similar to the Multhopp spacing, since for the Multhopp spacing

$$\theta_j = \frac{j\pi}{J+1} \qquad j = 1, 2, \ldots , J \qquad (61)$$

The method used by Hsu in obtaining the optimum distribution of collocation points was general enough so that his result can be used equally well in the present study of two dimensional flow over rotary wings. During the course of the present research all three of the above mentioned collocation point distributions (equal, Multhopp, and optimum) were used and it was found that all three yielded

essentially the same results. However, in computing the final results presented in Chapter IV the optimum distribution was used.

With the pressure mode assumption, Equation (58), the integrals occurring in Equation (29) can be evaluated numerically. However, it will be noted that the first integral of Equation (29) contains a singularity at the point $\xi = x$. This is a strong singularity and can seriously affect the numerical results if not handled properly. Since this integral is precisely the one which occurs in the fixed wing theory, the works of the many fixed wing investigators cited in Chapter I can be employed advantageously here. The method of handling the singularity adopted for the present analysis is that used by Frazer [17].

Let the kernel of the first integral of Equation (29) be written as follows

$$K_f\left[M, \frac{k(x-\xi)}{b}\right] = K\left[M, \frac{k(x-\xi)}{b}, 0\right] \tag{62}$$

$$K_f\left[M, \frac{k(x-\xi)}{b}\right] = \frac{1}{4\beta}\left\{e^{ikM^2(x-\xi)/\beta^2 b}\left[iM\frac{(x-\xi)}{|x-\xi|}H_1^{(2)}\left(\frac{kM|x-\xi|}{\beta^2 b}\right)\right.\right.$$

$$\left.\left. - H_0^{(2)}\left(\frac{kM|x-\xi|}{\beta^2 b}\right)\right] + i\beta^2 e^{-ik(x-\xi)/b}\int_{-\infty}^{k(x-\xi)/\beta^2 b}H_0^{(2)}\left(M|\eta|\right)e^{i\eta}\,d\eta\right\}$$

The infinite portion of the integral appearing in Equation (62) can be evaluated in closed form and has been shown by Fung [31] to be

$$\int_{-\infty}^{0} H_0^{(2)}\left(M|\eta|\right)e^{i\eta}\,d\eta = \frac{2}{\pi\beta}\,\ell n\,\frac{1+\beta}{M} \tag{63}$$

With this substitution Equation (62) becomes

$$K_f\left[M, \frac{k(x-\xi)}{b}\right] = \frac{1}{4\beta}\left\{e^{ikM^2(x-\xi)/\beta^2 b}\left[iM\,\frac{(x-\xi)}{|x-\xi|}\,H_1^{(2)}\left(\frac{kM\,|x-\xi|}{\beta^2 b}\right)\right.\right. \tag{64}$$

$$-H_0^{(2)}\left(\frac{kM\,|x-\xi|}{\beta^2 b}\right)\right] + i\beta^2 e^{-ik(x-\xi)/b}\left[\frac{2}{\pi\beta}\,\ell n\,\frac{1+\beta}{M} + \int_0^{k(x-\xi)/\beta^2 b}H_0^{(2)}\left(M|\eta|\right)e^{i\eta}d\eta\right]\right\}$$

Now write Equation (29) in two parts; a part due to the reference airfoil itself (which is analogous to the fixed wing downwash equation), and a part due to the infinite system of wakes. The following notation will be used

$$\bar{w}_a(x) = w_f(x) + w_h(x) \tag{65}$$

where

$$w_f(x) = -\frac{\omega}{\rho_\infty U^2}\int_{-b}^{b}\Delta\bar{p}_a(\xi)\,K_f\left[M, \frac{k(x-\xi)}{b}\right]\,d\xi \tag{66}$$

$$w_h(x) = - \frac{\omega}{\rho_\infty U^2} \sum_{n=1}^{\infty} \int_{-b}^{b} \Delta \bar{p}_a(\xi) \, K\left[M, \frac{k(x-\xi)}{b} + 2n\pi m, \, nkh\right] d\xi \qquad (67)$$

The only singularity of the downwash integral equation, Equation (65), occurs in Equation (66) when $\xi = x$. This singularity is treated as follows. First make the change of variables

$$\xi = - b \cos \theta \qquad (68)$$

Equation (66) then becomes

$$w_f(x) = - \frac{\omega b}{\rho_\infty U^2} \int_0^{\pi} \Delta \bar{p}_a(\theta) \, K_f\left[M, k\left(\frac{x}{b} + \cos \theta\right)\right] \sin \theta \, d\theta \qquad (69)$$

The singularity occurs when the second argument of K_f becomes zero. The procedure used is to subtract out the singular portion of the kernel and then integrate the singular portion in closed form. If K_o represents the asymptotic expression for K_f when the second argument of K_f becomes small, then Frazer [17] shows that

$$K_o\left[M, \, s\right] = \left[- \frac{\beta}{2\pi s} - \frac{1}{4\beta}\right]$$

$$+ i \left\{\frac{\ln|s|}{2\pi\beta} + \frac{1}{2\pi\beta}\left[\beta \ln \frac{M}{1-\beta} + \ln \frac{\gamma_E M}{2\beta^2} - M^2\right]\right\}$$

(70)

where

$$s = k \left(\frac{x}{b} + \cos \theta \right)$$

$$\ln \gamma_E = \text{Euler's constant} = 0.57721566...$$

Equation (66) is now written as follows

$$w_f(x) = - \frac{\omega b}{\rho_\infty U^2} \left\{ \int_0^\pi \Delta \bar{p}_a(\theta) \, \bar{K}_f \left[M, k \left(\frac{x}{b} + \cos \theta \right) \right] \sin \theta \, d\theta \right. \tag{71}$$

$$\left. + \int_0^\pi \Delta \bar{p}_a(\theta) \, K_0 \left[M, k \left(\frac{x}{b} + \cos \theta \right) \right] \sin \theta \, d\theta \right\}$$

where

$$\bar{K}_f \left[M, k \left(\frac{x}{b} + \cos \theta \right) \right] = K_f \left[M, k \left(\frac{x}{b} + \cos \theta \right) \right] - K_0 \left[M, k \left(\frac{x}{b} + \cos \theta \right) \right] \tag{72}$$

The first integral of Equation (71) is now free of singularities because when the second argument of $\bar{K}_f$ approaches zero, $\bar{K}_f$ approaches zero as well. The second integral of Equation (71) contains a singularity, but this integral has been evaluated by Frazer [17]. When the series expression assumed for $\Delta \bar{p}_a(\theta)$, Equation (58), is substituted into the second integral of Equation (71) the integral can be evaluated in terms of the pressure series coefficients and Equation (71) becomes

$$w_f(x) = - \frac{\omega b}{\rho_\infty U^2} \left\{ \int_0^\pi \Delta \bar{p}_a(\theta) \; \bar{K}_f \left[M, \, k \left(\frac{x}{b} + \cos \theta \right) \right] \sin \theta \; d\theta \right. \tag{73}$$

$$\left. + \frac{\beta}{2\pi k} I_0 + \frac{i}{2\pi \beta} I_1 + \left[\frac{i \; \ell n \; k}{2\pi \beta} - \frac{1}{4\beta} + \frac{i}{2\pi \beta} \left(\beta \; \ell n \; \frac{M}{1-\beta} + \ell n \; \frac{\gamma_E M}{2\beta^2} - M^2 \right) \right] I_2 \right\}$$

where

$$I_0 = - \pi A_o + \pi \sum_{j=1}^{J-1} A_j \cos j\theta_r$$

$$I_1 = - \pi \left(A_o + \frac{1}{2} A_1 \right) \ell n \; 2 - \pi A_o \cos \theta_r + \frac{\pi}{4} \cos 2 \; \theta_r$$

$$+ \frac{\pi}{2} \sum_{j=1}^{J-1} A_n \left[\frac{\cos(j+1)\theta_r}{j+1} - \frac{\cos(j-1)\theta_r}{j-1} \right]$$

$$I_2 = \pi \left(A_o + \frac{1}{2} A_1 \right)$$

$$x_r = - b \cos \theta_r = \text{location of rth collocation point}$$

For a given collocation point location Equation (73) can be evaluated numerically to give the first part of Equation (65). No particular difficulty is involved in evaluating the second part of Equation (65) given by Equation (67) since the kernel of Equation (67) contains no

singularities. However, for the numerical computations only a finite number of wake terms can be used so that Equation (67) must be written as

$$w_h(x) = - \frac{\omega b}{\rho_\infty U^2} \sum_{n=1}^{N} \int_o^\pi \Delta \bar{p}_a(\theta) \ K \left[M, \ k \left(\frac{x}{b} + \cos \theta \right) + 2n\pi m, \ nkh \right] \quad (74)$$

$$\cdot \sin \theta \ d\theta$$

It should be noted here that the number of wake terms taken is independent of the number of collocation points taken so that $w_h(x)$ can be computed to any desired degree of accuracy for a given number of collocation points.

With the method of handling the singularity thus established the pressure series can be substituted into Equations (73) and (74). Then if a point x_r on the chord is picked, the right hand side of Equation (65) can be evaluated in terms of the pressure series coefficients. The left side of Equation (65) can also be evaluated by applying the boundary condition, Equation (30). In evaluating the boundary condition, the reference airfoil is assumed to be undergoing plunging and pitching oscillations referenced to the quarter-chord point as shown in Figure 5. From this figure the displacement of any point on the reference airfoil midsurface is seen to be

$$z_a(x;t) = - \bar{h}_{c/4} - (x + \frac{b}{2}) \ \alpha \quad (75)$$

Assuming simple harmonic motion
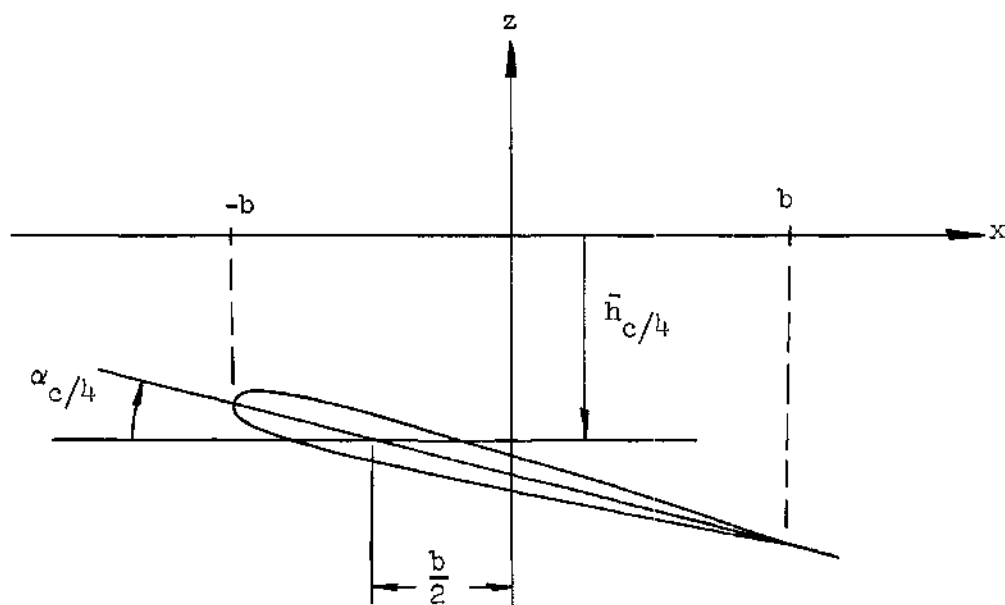
Figure 5. Assumed Motion of Reference Airfoil Used to Calculate Aerodynamic Coefficients

$$\bar{h}_{c/4} = h_o \, e^{i\omega t}$$

$$\alpha = \alpha_o e^{i\omega t} \qquad \Biggr\} \qquad (76)$$

the downwash expression becomes

$$\frac{\bar{w}_a(x)}{U} = - ik \left(\frac{h_o}{b}\right)_{c/4} - \left[1 + ik \left(\frac{x}{b} + \frac{1}{2}\right)\right] \alpha_o \qquad (77)$$

The ultimate goal of the aerodynamic analysis is the determination of the unsteady lift and moment on the reference airfoil. These quantities are obtained by integrating the pressure distribution. The total lift on the reference airfoil (measured positive down) is given by

$$L = \int_{-b}^{b} \left(p_U - p_L\right) dx \qquad (78)$$

Since the airfoil is undergoing simple harmonic motions the pressure varies simple harmonically and hence the lift must vary harmonically as

$$L = \bar{L} \, e^{i\omega t} \qquad (79)$$

Thus

$$\bar{L} = \int_{-b}^{b} \Delta \bar{p}_a(x) \, dx \qquad (80)$$

Making the change of variables

$$x = - b \cos \theta \tag{81}$$

and substituting the pressure series assumption the lift becomes

$$\bar{L} = b \left\{ 2 A_o \int_o^\pi \cos^2 \frac{\theta}{2} \, d\theta + \sum_{j=1}^\infty A_j \int_o^\pi \sin j\theta \sin \theta \, d\theta \right\} \tag{82}$$

Because of the orthogonality of the sine functions, all the integrals except the first in the infinite series are zero and the lift becomes

$$\bar{L} = b \left\{ 2 A_o \int_o^\pi \cos^2 \frac{\theta}{2} \, d\theta + A_1 \int_o^\pi \sin^2 \theta \, d\theta \right\} \tag{83}$$

Performing the necessary integrations

$$\bar{L} = \pi b \left(A_o + \frac{1}{2} A_1 \right) \tag{84}$$

The aerodynamic moment about the quarter-chord point (measured positive nose up) is given by

$$M_{c/4} = \int_{-b}^b \left(p_U - p_L \right)\left(x + \frac{b}{2} \right) dx \tag{85}$$

Again, since the pressure varies simple harmonically the moment must vary simple harmonically as

$$M_{c/4} = \bar{M}_{c/4} \, e^{i\omega t} \tag{86}$$

so that Equation (85) becomes

$$\bar{M}_{c/4} = \int_{-b}^{b} \Delta \bar{p}_a(x) \left(x + \frac{b}{2}\right) dx \tag{87}$$

Making the change of variables given by Equation (81) and substituting the pressure series assumption

$$\bar{M}_{c/4} = b^2 \left\{ \int_{0}^{\pi} A_o \cot \frac{\theta}{2} \left(\frac{1}{2} - \cos \theta\right) \sin \theta \, d\theta \right. \tag{88}$$

$$\left. + \sum_{j=1}^{\infty} A_j \int_{0}^{\pi} \sin j\theta \left(\frac{1}{2} - \cos \theta\right) \sin \theta \, d\theta \right\}$$

Performing the integrations

$$\bar{M}_{c/4} = \frac{1}{4} \pi \, b^2 \left(A_1 - A_2\right) \tag{89}$$

It is of interest to note here that the aerodynamic lift and moment on the reference airfoil section given by Equations (84) and (89) depend only on the first three terms of the pressure series. This does not mean, however, that one needs only to use the first three

terms of the series and hence only three collocation points. The values of the first three coefficients of the series will change as more and more collocation points and terms in the series are used and the boundary condition is satisfied more exactly. The advantage of Equations (84) and (89) is that the lift and moment expressions do not contain a series involving all the coefficients of the pressure series.

As stated in Chapter II it is customary to write the lift and moment on the reference airfoil in the form given by Equations (49). However, it was found that the coefficients L_h, L_α, M_h, and M_α become relatively large for small values of reduced frequency and thus for the numerical computations it was better to write the lift moment expressions as

$$\left. \begin{array}{l} L = \pi \rho_\infty U^2 b \left[\ell_h \left(\dfrac{\bar{h}}{b} \right)_{c/_4} + \ell_\alpha \alpha \right] \\[30pt] M_{c/_4} = \pi \rho_\infty U^2 b^2 \left[m_h \left(\dfrac{\bar{h}}{b} \right)_{c/_4} + m_\alpha \alpha \right] \end{array} \right\} \qquad (90)$$

where

$$\ell_h = k^2 L_h$$
$$\ell_\alpha = k^2 L_\alpha$$
$$m_h = k^2 M_h$$
$$m_\alpha = k^2 M_\alpha$$

Consistent with the preceding analysis the lift in Equations (90) is measured positive down and the moment is measured positive nose-up.

The aerodynamic coefficients ℓ_h, ℓ_α, m_h, and m_α are now obtained as follows. By evaluating the boundary condition, Equation (77), at each of J collocation points there results from Equation (65) a set of J simultaneous equations with the coefficients of the pressure series as unknowns. These equations can be written in matrix form as

$$\left\{ \frac{\bar{w}_a}{U} \right\} = - \frac{\pi}{\rho_\infty U^2} [C] \{A\} \tag{91}$$

Then the coefficients of the pressure series are given by

$$\{A\} = - \frac{1}{\pi} \rho_\infty U^2 [C]^{-1} \left\{ \frac{\bar{w}_a}{U} \right\} \tag{92}$$

or

$$\{\bar{A}\} = [C]^{-1} \left\{ \frac{\bar{w}_a}{U} \right\} \tag{93}$$

where

$$\{\bar{A}\} = - \frac{\pi}{\rho_\infty U^2} \{A\} \tag{94}$$

The coefficient matrix, $[C]$, appearing on the right hand side of Equation (91) can be evaluated independent of the motions which the reference airfoil is performing. The left hand side of the equation depends on the motion. First consider that the reference airfoil is performing only a plunging motion of unit nondimensional amplitude

$$\left(\frac{\bar{h}}{b} \right)_{c/4} = 1 \ e^{i\omega t} \\[20pt] \left. \alpha = 0 \right\} \tag{95}$$

The downwash boundary condition then becomes

$$\frac{\bar{w}_a(x)}{U} = - ik \tag{96}$$

and the lift and moment become

$$\bar{L} = \pi \rho_\infty U^2 b \ \ell_h \\[20pt] \left. \bar{M}_{c/4} = \pi \rho_\infty U^2 b^2 \ m_h \right\} \tag{97}$$

Using the boundary condition Equation (96) in Equation (93) the $\{\bar{A}\}$ coefficients can be obtained, and denoted by $\{\bar{A}\}_{\bar{h}}$. Then from Equations (84) and (89)

$$\bar{L} = -\rho_\infty U^2 b \left(\bar{A}_o + \frac{1}{2} \bar{A}_1 \right)$$

$$\bar{M}_{c/4} = -\frac{1}{4} \rho_\infty U^2 b^2 \left(\bar{A}_1 - \bar{A}_2 \right) \tag{98}$$

Comparing Equations (97) and (98) the aerodynamic coefficients ℓ_h and m_h are given by

$$\ell_h = -\frac{1}{\pi} \left(\bar{A}_o + \frac{1}{2} \bar{A}_1 \right)_{\bar{h}}$$

$$m_h = -\frac{1}{4\pi} \left(\bar{A}_1 - \bar{A}_2 \right)_{\ddot{h}} \tag{99}$$

Similarily, by using the same process as that above and assuming that the reference airfoil is performing only a pitching motion of unit amplitude the remaining aerodynamic coefficients ℓ_α and m_α can be determined.

Numerical Procedures

The above procedures were programmed in FORTRAN V for the UNIVAC 1108 digital computer. Since all the numerical techniques used are completely described in the literature only a brief mention of some of the more important aspects of the numerical computations will be given here.

All finite integrals involved in the computations were evaluated using a Gaussian quadrature technique. It was found that for evaluating

the chordwise integrals of Equations (66) and (67) ten integration
points were needed to yield accurate results. Ten integration points
were also found to be satisfactory for evaluating the finite integral
appearing in Equation (64). In evaluating the kernel of Equation (67)
it is necessary to evaluate finite integrals of the form

$$I = \int_0^{[k(x-\xi)/b]+2n\pi m} H_0^{(2)} \left(\frac{M}{\beta^2} \sqrt{\eta^2 + (\beta nkh)^2} \right) e^{i\eta/\beta^2} \, d\eta \qquad (100)$$

Separating into real and imaginary parts

$$\mathcal{R}(I) = \int_0^{[k(x-\xi)/b]+2n\pi m} J_0 \left(\frac{M}{\beta^2} \sqrt{\eta^2 + (\beta nkh)^2} \right) \cos \frac{\eta}{\beta^2} \, d\eta \qquad (101)$$

$$+ \int_0^{[k(x-\xi)/b]+2n\pi m} Y_0 \left(\frac{M}{\beta^2} \sqrt{\eta^2 + (\beta nkh)^2} \right) \sin \frac{\eta}{\beta^2} \, d\eta$$

$$\mathcal{J}(I) = \int_0^{[k(x-\xi)/b]+2n\pi m} J_0 \left(\frac{M}{\beta^2} \sqrt{\eta^2 + (\beta nkh)^2} \right) \sin \frac{\eta}{\beta^2} \, d\eta \qquad (102)$$

$$- \int_0^{[k(x-\xi)/b]+2n\pi m} Y_0 \left(\frac{M}{\beta^2} \sqrt{\eta^2 + (\beta nkh)^2} \right) \cos \frac{\eta}{\beta^2} \, d\eta$$

It was found that as the summation index n increases more and more integration points are necessary to compute these integrals accurately. To illustrate the process used in establishing the number of points needed, consider the first integral of Equation (101). This integral may be written as

$$I^{R1} = \int_{0}^{2n\pi m} J_{0}\left(\frac{M}{\beta^2}\sqrt{\eta^2 + (\beta nkh)^2}\right) \cos \frac{\eta}{\beta^2} \, d\eta \tag{103}$$

$$+ \cos (2n\pi m/\beta^2) \int_{0}^{k(x-\xi)/b} J_{0}\left(\frac{M}{\beta^2}\sqrt{(\eta + 2n\pi m)^2 + (\beta nkh)^2}\right) \cos \frac{\eta}{\beta^2} \, d\eta$$

$$- \sin (2n\pi m/\beta^2) \int_{0}^{k(x-\xi)/b} J_{0}\left(\frac{M}{\beta^2}\sqrt{(\eta + 2n\pi m)^2 + (\beta nkh)^2}\right) \sin \frac{\eta}{\beta^2} \, d\eta$$

It was found that integrals similar to the last two in Equation (103) could be evaluated accurately for all n with only six integration points. However, due to the oscillatory nature of the integrand, integrals similar to the first of Equation (103) required the use of at least four integration points per period of the trigonometric function. This was necessary because the trigonometric function is the primary contributor to the oscillatory character of the integrand and as the summation index n becomes large, more and more oscillations of the integrand occur. Thus for evaluating integrals similar to the

first integral in Equation (103) the number of integration points needed is given by

$$NIP = 4(2n\pi m)/(2\pi\beta^2) = 4n\,\frac{m}{\beta^2} \tag{104}$$

Also in the evaluation of the kernel of Equation (67) it is necessary to evaluate an integral with an infinite limit, namely

$$I = \int_{-\infty}^{0} H_{0}^{(2)} \left(\frac{M}{\beta^2} \sqrt{\eta^2 + (\beta nkh)^2} \right) e^{i\eta/\beta^2}\, d\eta \tag{105}$$

Writing the exponential in real and imaginary parts and changing variables

$$I = \int_{0}^{\infty} H_{0}^{(2)} \left(\frac{M}{\beta^2} \sqrt{v^2 + (\beta nkh)^2} \right) \cos\frac{v}{\beta^2}\, dv \tag{106}$$

$$- i \int_{0}^{\infty} H_{0}^{(2)} \left(\frac{M}{\beta^2} \sqrt{v^2 + (\beta nkh)^2} \right) \sin\frac{v}{\beta^2}\, dv$$

The first integral of Equation (106) can be evaluated in closed form using the results of Infeld, Smith, and Chen [32]. Thus

$$\int_{0}^{\infty} H_{0}^{(2)} \left(\frac{M}{\beta^2} \sqrt{v^2 + (\beta nkh)^2} \right) \cos\frac{v}{\beta^2}\, dv = i\beta e^{-nkh} \tag{107}$$

The second integral of Equation (106) must be evaluated numerically. After separating the Hankel function into real and imaginary parts the resulting two real integrals were easily and accurately evaluated using the numerical quadrature method of Hurwitz and Zweifel [33].

In the evaluation of Equations (66) and (67) for zero Mach number it becomes necessary to evaluate the Sine, Cosine, and Exponential integrals. The Sine and Cosine integrals were evaluated numerically using their respective series representations given by Lebedev [34]. Trouble was encountered, however, when the series representation of the Exponential integral was used. This occurred when the wake series summation index and hence the argument of the Exponential integral became large. Following the approach of Todd [35] the Laguerre quadrature formula was used to evaluate the integral directly and the technique was found to give excellent results not only for large arguments, but for small arguments as well. Consequently, the technique was used to evaluate the Exponential integral for all values of the argument.

During the course of the numerical investigations it was found that the number of collocation points and hence the number of terms in the pressure series necessary for reliable results increased as the reduced frequency increased. For reduced frequencies between 0.0 and 0.12, three collocation points provided satisfactory results, whereas for reduced frequencies between 0.35 and 0.50, five collocation points were necessary. Since the primary interest of this research is the flutter condition for rotary wings no extensive computations were

made for reduced frequencies greater than 0.5. However, it is felt that the methods employed are good up to at least a reduced frequency of unity provided, of course, that a sufficient number of collocation points are used.

Except for low values of frequency ratio, the number of wake terms necessary to give convergence of the aerodynamic coefficients within one percent was found to be essentially independent of all parameters in the problem. For all the conditions investigated approximately forty terms were required to give satisfactory results. For low values of frequency ratio, many more terms were required. The number of terms required could possibly be reduced by using an elegant summing procedure on the wake series. For the present research, however, a simple summation of the terms was felt to be adequate.

Numerical Solution of the Two Degree of Freedom Flutter Problem

In Chapter II the characteristic equation for the two degree of freedom flutter problem was developed. This equation is a complex quadratic equation and is given by Equation (54). In this section a method is presented whereby Equation (54) can be solved for the two eigenvalues of the flutter problem; the flutter speed and the flutter frequency.

Since one of the eigenvalues, the flutter speed, does not appear explicitly in Equation (54) but is contained rather implicitly in the aerodynamic coefficients L_h, L_α, M_h, and M_α it becomes necessary to solve the characteristic equation in an indirect manner. The method to be used is that suggested by Smilg and Wasserman [29]. They suggest

letting

$$g_h = g_\alpha = g \tag{108}$$

and writing the characteristic equation in the form

$$\Lambda^2 + C_1 \Lambda + C_2 = 0 \tag{109}$$

where

$$\Lambda = \left(\frac{\omega_\alpha}{\omega}\right)^2 \left(1 + ig\right) \tag{110}$$

Following this suggestion, Equation (54) may be expanded and written as

$$B_o \Lambda^2 + B_1 \Lambda + B_2 = 0 \tag{111}$$

where

$$B_o = \mu^2 r_\alpha^2 \left(\frac{\omega_h}{\omega_\alpha}\right)^2$$

$$B_1 = -\mu \left(\frac{\omega_h}{\omega_\alpha}\right)^2 \left[\mu r_\alpha^2 + M_\alpha - \left(L_\alpha + M_h\right)\left(\frac{1}{2} + a\right) + L_h\left(\frac{1}{2} + a\right)^2\right] - \mu r_\alpha^2 \left(\mu + L_h\right)$$

$$B_2 = \left(\mu + L_h\right)\left[\mu r_\alpha^2 + M_\alpha - \left(L_\alpha + M_h\right)\left(\frac{1}{2} + a\right) + L_h\left(\frac{1}{2} + a\right)^2\right]$$

Or,

$$\Lambda^2 + C_1\Lambda + C_2 = 0 \qquad (112)$$

where

$$C_1 = B_1/B_o \qquad C_2 = B_2/B_o$$

In the present method of solution the unknowns in Equation (112) are taken as structural damping, g, and oscillatory frequency, ω. The solutions of Equation (112) are given by the quadratic formula as

$$\Lambda_{1,2} = \frac{1}{2}\left[-C_1 \pm \sqrt{C_1^2 - 4C_2}\,\right] \qquad (113)$$

Now if

$$\left.\begin{array}{l} \Lambda_1 = \Re_1 + i\,\Im_1 = \left(\dfrac{\omega_\alpha}{\omega_1}\right)^2\left(1 + ig_1\right) \\[6mm] \Lambda_2 = \Re_2 + i\,\Im_2 = \left(\dfrac{\omega_\alpha}{\omega_2}\right)^2\left(1 + ig_2\right) \end{array}\right\} \qquad (114)$$

then the unknowns g and ω are determined as

$$
\left.
\begin{array}{ll}
g_1 = \dfrac{\vartheta_1}{\Re_1} & g_2 = \dfrac{\vartheta_2}{\Re_2} \\[4ex]
\left(\dfrac{\omega_1}{\omega_\alpha}\right)^2 = \dfrac{1}{\Re_1} & \left(\dfrac{\omega_2}{\omega_\alpha}\right)^2 = \dfrac{1}{\Re_2}
\end{array}
\right\}
\qquad (115)
$$

In determining the flutter speed, the procedure is as follows. When the Mach number (M), inflow ratio (h), and frequency ratio (m) are given, the aerodynamic coefficients may be calculated by assuming a value of reduced frequency (k). Then for a given structural configuration the structural damping and oscillatory frequency for each of the two modes may be calculated as solutions of the characteristic equation, Equation (112). Finally, the nondimensional velocity for each mode is calculated using the assumed value of reduced frequency and the frequencies for each mode as calculated from Equations (115), i.e.

$$
\left(\frac{U}{b\omega_\alpha}\right)_{1,2} = \frac{1}{k}\left(\frac{\omega}{\omega_\alpha}\right)_{1,2}
\qquad (116)
$$

The flutter speed is obtained by assuming several values of reduced frequency and plotting curves of the structural damping versus nondimensional velocity for each mode. When one of the curves passes through the value of structural damping which the system actually has,

the corresponding nondimensional velocity is the flutter speed. If both the modes have a flutter speed, the flutter speed for the system is taken to be the lower of the two. Since the value of structural damping is known to be small for conventional aircraft structures, it was conservatively taken to be zero for the present research.

Discussion of the Velocity-Damping Plot

A typical plot of structural damping versus nondimensional airspeed is shown in Figure 6. As can be seen from the plot, the flutter speed occurs in the second mode at a nondimensional airspeed of approximately 3.3. From the previous discussion it is obvious that the only physically meaningful point on the plot is the point where the g_1-curve passes through zero damping since it is assumed that the system has zero structural damping. However, other points on the curve may be interpreted as follows. Since it is known that the structural damping of the system is zero, the damping indicated on the plot can be interpreted as aerodynamic damping as this is the only other damping entering the problem. For points on the curve where the airspeed is less than the flutter speed the damping is negative, indicating that the aerodynamics are taking energy out of the system and thus the motion is stable. Conversely, for airspeeds greater than the flutter speed the damping is positive and thus indicates that the aerodynamics are feeding energy into the system and the resulting motion is unstable. The flutter speed, therefore, represents the transition point between stable and unstable motion.
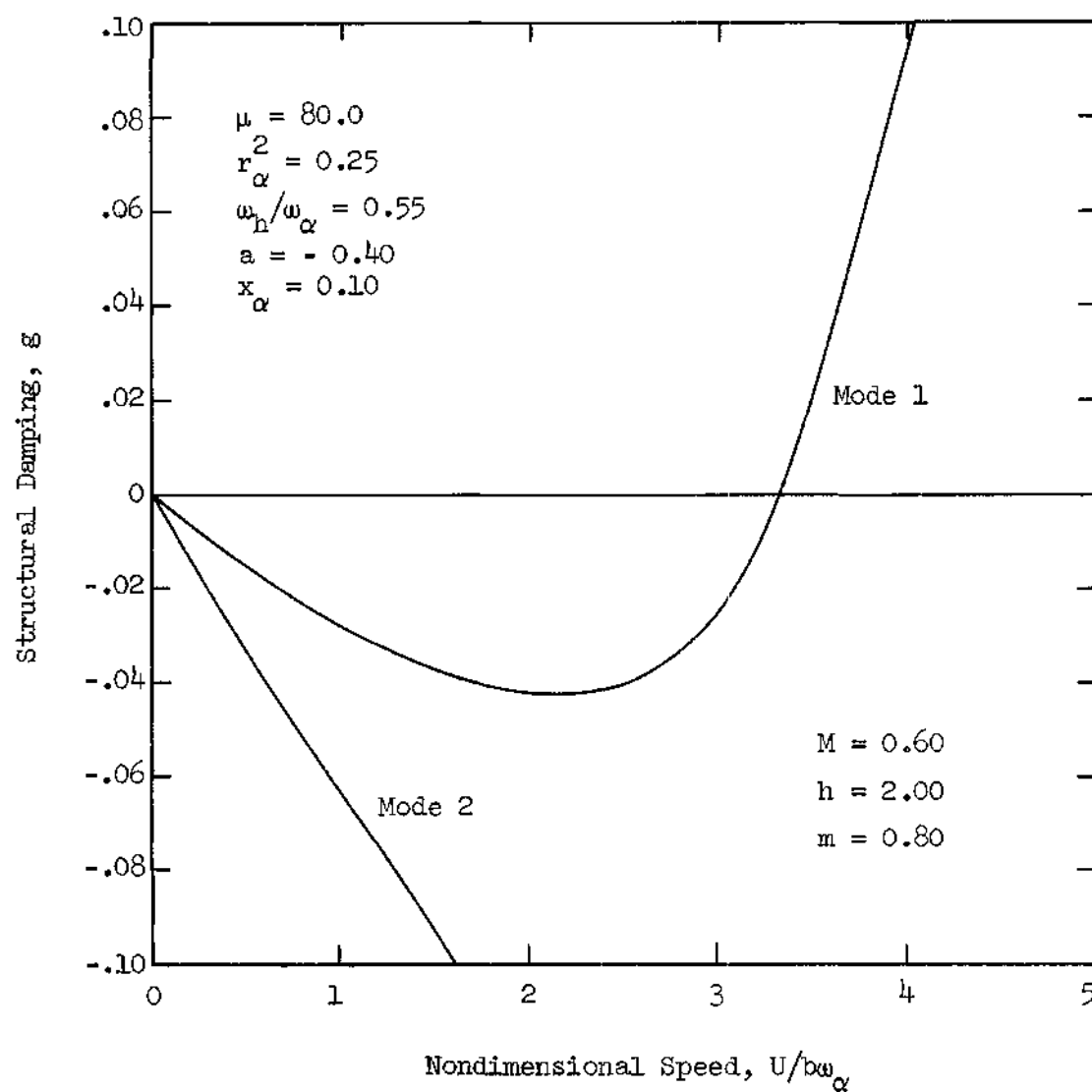
Figure 6. Typical Velocity-Damping Plot for Obtaining Flutter Speed

Static Divergence

In Chapter II is was shown that for static divergence the equations of motion become

$$\tilde{m}\,\omega_h^2\,\bar{h} = L$$

$$I_\alpha\,\omega_\alpha^2\alpha = M_{e.a.}$$

$$\tag{117}$$

where the lift and moment expressions are evaluated at zero reduced frequency. The lift and moment expressions from Equations (50) may be written as

$$L = \pi\rho_\infty U^2 b \left\{ \ell_h\,\frac{\bar{h}}{b} + \left[\ell_\alpha - \ell_h\left(\frac{1}{2} + a\right) \right]\alpha \right\}$$

$$M_{e.a.} = \pi\rho_\infty U^2 b^2 \left\{ \left[m_h - \ell_h\left(\frac{1}{2} + a\right) \right]\frac{\bar{h}}{b} \right.$$

$$\left. + \left[m_\alpha - \left(\ell_\alpha + m_\alpha\right)\left(\frac{1}{2} + a\right) + \ell_h\left(\frac{1}{2} + a\right)^2 \right]\alpha \right\}$$

$$\tag{118}$$

From Equations (77) and (93) together with Equations (84) and (89) it can be shown that only the real part of ℓ_α and the real part of m_α can have values different from zero as $k \to 0$. Further, numerical calculations show that the real part of m_α is also zero. Thus the equations of motion for static divergence become

$$\tilde{m}\,\omega_h^2\,\bar{h} = \pi\rho_\infty U_D^2 b \ell_{\alpha_0}\,\alpha$$

$$I_\alpha\,\omega_\alpha^2\alpha = \pi\rho_\infty U_D^2 b^2 \left[- \ell_{\alpha_0}\left(\frac{1}{2} + a\right) \right]\alpha$$

$$\tag{119}$$

where ℓ_{α_0} is the value of ℓ_α at $k = 0$ and is a real quantity. The static divergence speed can then be calculated from the second of Equations (119) as

$$U_D^2 = \frac{I_\alpha \omega_\alpha^2}{\pi \rho_\infty b^2 \left[- \ell_{\alpha_0} \left(\frac{1}{2} + a \right) \right]} \qquad (120)$$

The negative sign in the denominator of Equation (120) causes no problem, since it may be observed from numerical calculations that ℓ_{α_0} is always negative.

Introducing the parameters given by Equations (56) the non-dimensional divergence speed becomes

$$\frac{U_D}{b\omega_\alpha} = \sqrt{\frac{r_\alpha^2 \mu}{-\ell_{\alpha_0} \left(\frac{1}{2} + a \right)}} \qquad (121)$$

In this chapter a numerical method has been presented for solving the downwash integral equation developed in Chapter II. The method was shown to involve the use of a pressure mode assumption in conjunction with a collocation technique for determining the unknown pressure distribution on the reference airfoil section. The method for handling the singularity occurring in the downwash integral equation was presented along with a discussion of some of the compuational techniques used in the numerical solution. Finally the method for obtaining the aerodynamic coefficients from the pressure mode

assumption was presented.

The numerical method employed in solving the two degree of freedom flutter problem was also presented in this chapter. The aerodynamic coefficients from the compressible aerodynamic analysis were seen to be necessary input for the flutter analysis. Since one of the eigenvalues of the flutter problem is contained only implicitly in the aerodynamic coefficients the flutter problem was solved indirectly by taking structural damping and oscillatory frequency as unknowns. The flutter speed was finally obtained by plotting structural damping versus nondimensional airspeed and noting where the curve passed through the actual value of structural damping present in the system. The corresponding value of nondimensional airspeed was then taken as the flutter speed. The results of both the aerodynamic and the flutter analysis are presented in Chapter IV.

CHAPTER IV

DISCUSSION OF RESULTS

In the previous chapters of this thesis an unsteady compressible aerodynamic theory for rotor blades has been presented based on certain two-dimensionalizing assumptions. Also presented has been a two degree of freedom flutter analysis which made use of the previously developed aerodynamic theory. In this chapter numerical results of these analytical developments are presented together with a discussion of their overall significance.

Comparison of Aerodynamic Theories

In Chapter II analytical comparisons were made of the aerodynamic theory of the present study with the theories of Loewy [2] and Jones and Rao [24]. In that chapter it was shown that if the flow model of the present research is made to agree with the model used by Loewy and Jones and Rao then the downwash equations and hence the aerodynamic coefficients calculated using the three theories also agree. However, for realistic values of the parameters entering the aerodynamic problem the two flow models cannot be expected to be identical. For this reason, a numerical comparison of the three theories is presented in this section.

For the equivalent single bladed rotor the nth "wake airfoil" of Figure 3 leads the reference airfoil by a distance

$$D_n = 2n\pi r \qquad (122)$$

Introducing the reduced frequency and frequency ratio parameters Equation (122) may be written as

$$D_n = 2n\pi \frac{mb}{k} \qquad (123)$$

Thus from Equation (123) it can be seen that if the frequency ratio, m, is increased while all the other aerodynamic parameters are held constant, the effect of increasing the distance by which the "wake airfoils" lead the reference airfoil can be determined. This in turn allows one to determine quantitatively the effect of the two flow models on the aerodynamic coefficients.

In Appendix E it is shown that if the "wake airfoils" are made to lead the reference airfoil by an infinite distance, then the analysis of the present study is identical to that of Jones and Rao [24]. A similar result is presented in Appendix G for the case of zero Mach number and comparison with Loewy's [2] theory. Thus by increasing the frequency ratio, m, while holding the other aerodynamic parameters constant the aerodynamic theory of the present study should approach those of Loewy and Jones and Rao.

This variation of the frequency ratio was made and the results are presented in Figures 7-10. It should be noted that for convenience the aerodynamic coefficients of Reference [24] have been plotted instead of the coefficients used in the present study. In the notation of Jones and Rao the lift (positive down) and moment about the quarter-

Figure 7. Variation of the Aerodynamic Coefficients $\bar{l}_z$ and $\bar{l}_{\dot{z}}$ with Frequency Ratio (k = 0.10, h = 2.0)

Figure 8. Variation of the Aerodynamic Coefficients $\bar{l}_\alpha$ and $\bar{l}_{\dot{\alpha}}$ with Frequency Ratio (k = 0.10, h = 2.0)
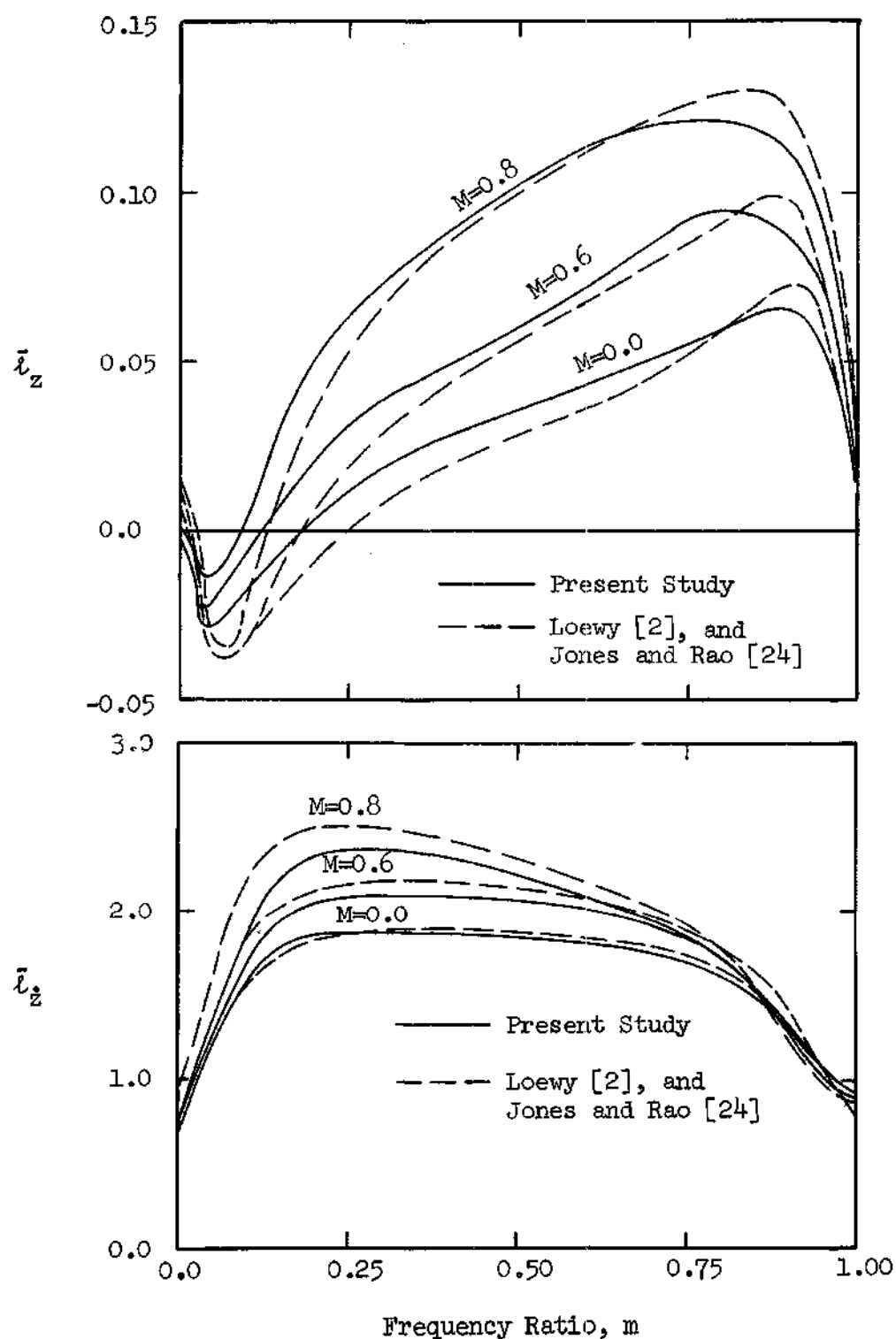
Figure 9. Variation of the Aerodynamic Coefficients $\bar{m}_z$ and $\bar{m}_{\dot{z}}$ with Frequency Ratio ($k = 0.10$, $h = 2.0$)

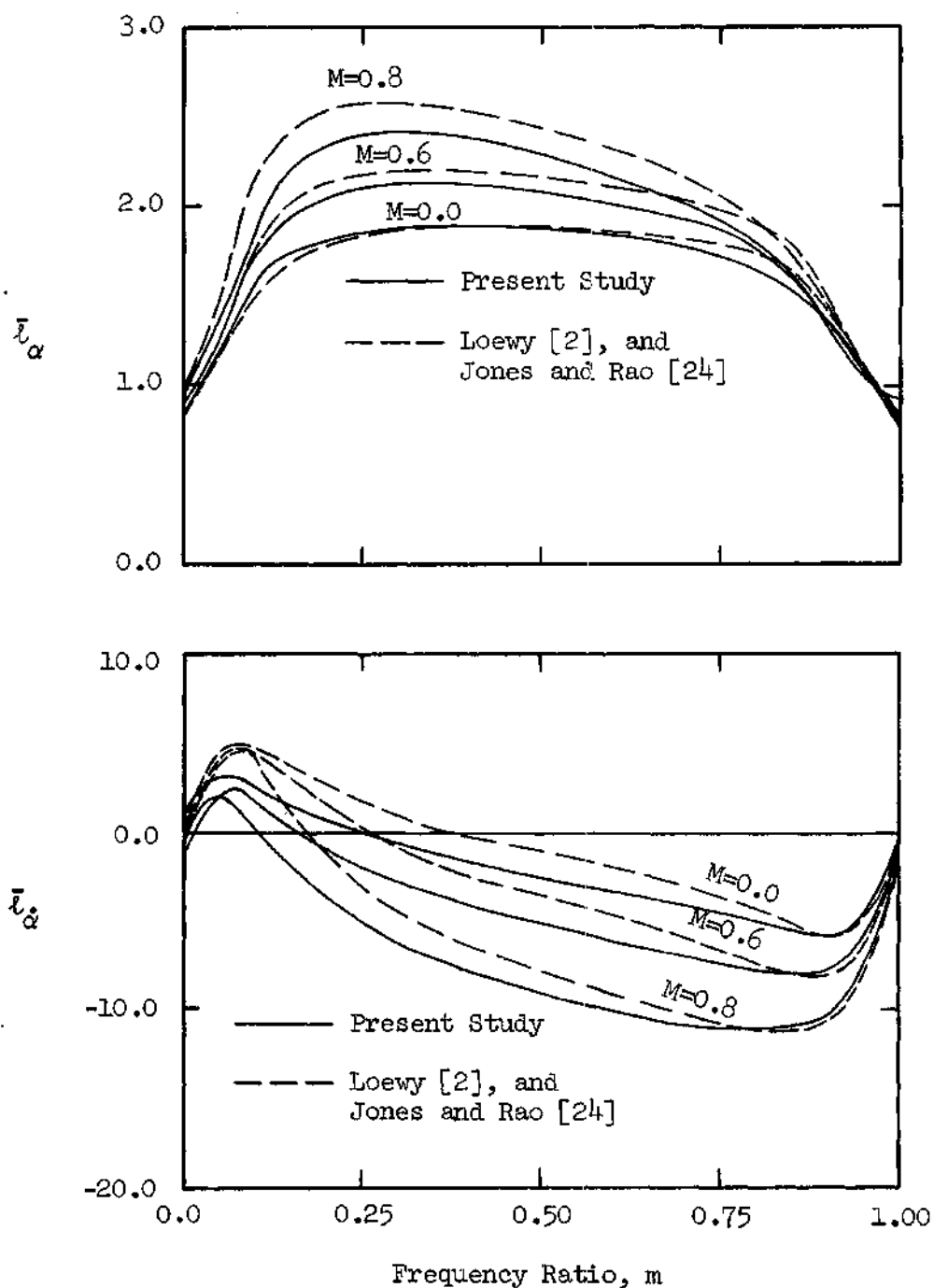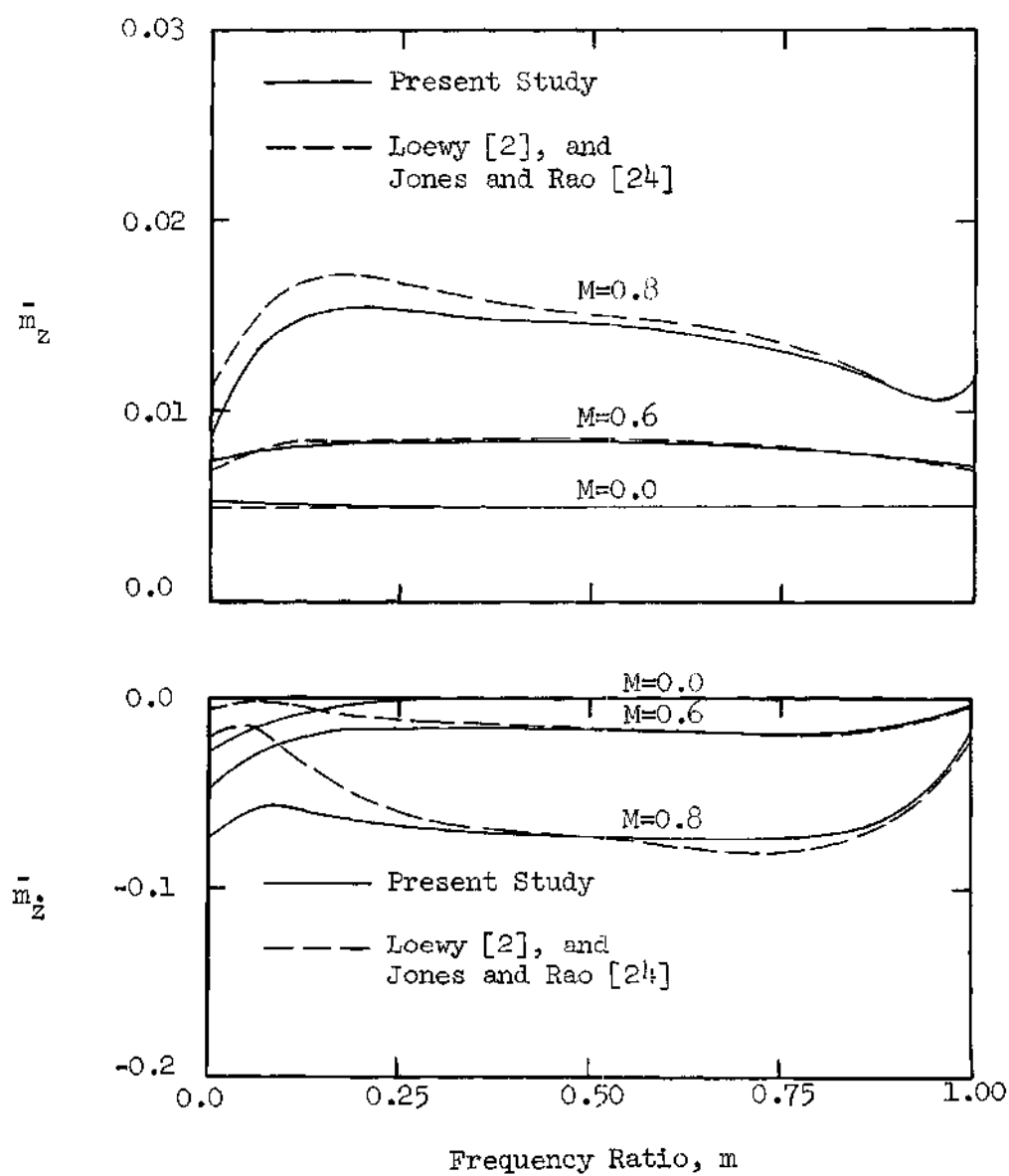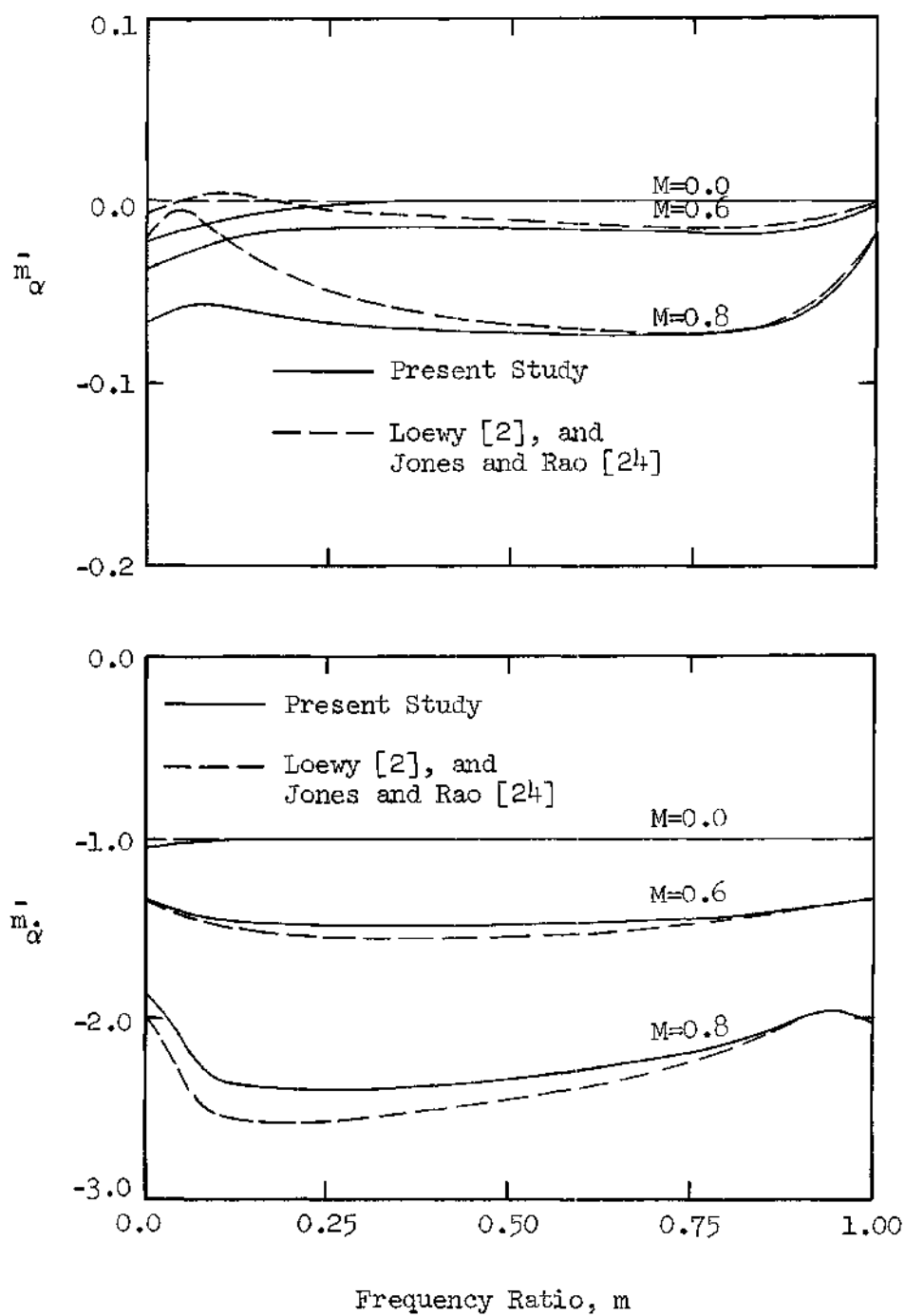Figure 10. Variation of the Aerodynamic Coefficients $\bar{m}_\alpha$ and $\bar{m}_{\dot{\alpha}}$ with Frequency Ratio (k = 0.10, h = 2.0)

chord (positive nose-up) are written as

$$
L = - \pi \rho_\infty U^2 b \left[\left(\bar{\ell}_z + ik\bar{\ell}_{\dot{z}} \right) \left(\frac{\bar{h}}{b} \right)_{c/2} + \left(\bar{\ell}_\alpha + ik\bar{\ell}_{\dot{\alpha}} \right) \alpha \right]
$$

$$
M_{c/4} = \pi \rho_\infty U^2 b^2 \left[\left(\bar{m}_z + ik\bar{m}_{\dot{z}} \right) \left(\frac{\bar{h}}{b} \right)_{c/2} + \left(\bar{m}_\alpha + ik\bar{m}_{\dot{\alpha}} \right) \alpha \right]
$$

(124)

Thus the coefficients of the present study are related to those of Equations (124) by the equations

$$
\begin{aligned}
\bar{\ell}_z &= - \Re(\ell_h) & \bar{m}_z &= \Re(m_h) \\
\bar{\ell}_{\dot{z}} &= - \frac{1}{k} \Im(\ell_h) & \bar{m}_{\dot{z}} &= \frac{1}{k} \Im(m_h) \\
\bar{\ell}_\alpha &= - \left[\Re(\ell_\alpha) - \frac{1}{2} \Re(\ell_h) \right] & \bar{m}_\alpha &= \Re(m_\alpha) - \frac{1}{2} \Re(m_h) \\
\bar{\ell}_{\dot{\alpha}} &= - \frac{1}{k} \left[\Im(\ell_\alpha) - \frac{1}{2} \Im(\ell_h) \right] & \bar{m}_{\dot{\alpha}} &= \frac{1}{k} \left[\Im(m_\alpha) - \frac{1}{2} \Im(m_h) \right]
\end{aligned}
$$

(125)

As can be seen from Figures 7 - 10 the agreement between the aerodynamic theories does indeed improve as the frequency ratio is increased. It might also be observed that some of the coefficients tend to agree better over the entire range of frequency ratios investigated than others; for instance, the $\bar{\ell}_z$ derivative appears to agree less than most of the other derivatives.

It is also of interest to point out that the aerodynamic theories of Loewy [2] and Jones and Rao [24] are cyclic in frequency ratio whereas the theory presented in the present research is not.

Thus if Figures 7 - 10 were plotted for $1 \le m \le 2$ the Loewy and Jones and Rao curves would remain exactly as shown, but the curves from the present study would change and should be in better agreement with the other two theories.

The significant point about Figures 7 - 10 is that they show the effect of the two possible mathematical representations of the two-dimensional flow over helicopter blades. As shown in the figures, the effect can be considerable at low values of frequency ratio, but tends to diminish as frequency ratio is increased.

Flutter Results

The basic goal of the present research is to determine the effect of compressibility on the flutter speed of rotary wings. To accomplish this goal a two-dimensional, compressible, unsteady aerodynamic theory has been developed for helicopter rotors and some results of that theory presented in the preceding section. However, to demonstrate the effect of compressibility on the flutter condition the aerodynamic theory must be used in conjunction with a flutter analysis. For the present study a two degree of freedom structural model was used in the flutter analysis. This model is described in detail in Chapter II. Numerical results of the analysis are presented in this section.

In ascertaining the effect of compressibility a variation of the parameters entering the flutter problem was made. When varying the aerodynamic parameters the structural parameters were held constant at a set of values typical of current blade designs. The following values

were used

$$\left.\begin{array}{r} \mu = 80.00 \\ r_\alpha^2 = 0.25 \\ \omega_h/\omega_\alpha = 0.50 \\ a = -0.40 \\ x_\alpha = 0.10 \end{array}\right\} \qquad (126)$$

When varying the structural parameters, the parameters which were not varied were held constant at their respective values given by Equations (126) and the aerodynamic parameters were held constant at the typical values

$$\left.\begin{array}{r} h = 2.00 \\ m = 0.80 \end{array}\right\} \qquad (127)$$

Three values of Mach number were investigated; 0.0, 0.6, and 0.8.

Shown in Figures 11 - 13 is the variation of nondimensional flutter speed with inflow ratio for frequency ratios of 0.2, 0.5, and 0.8 respectively. As can be seen from these curves the nondimensional flutter speed generally decreases as the Mach number is increased. Also shown on these curves is the flutter speed obtained using Loewy [2] aerodynamics. The zero Mach number data obtained using the aerodynamic theory of the present study are seen to agree better with the Loewy curves as the frequency ratio, m, is increased. This is a consequence of the two flow models being brought into closer agreement when the
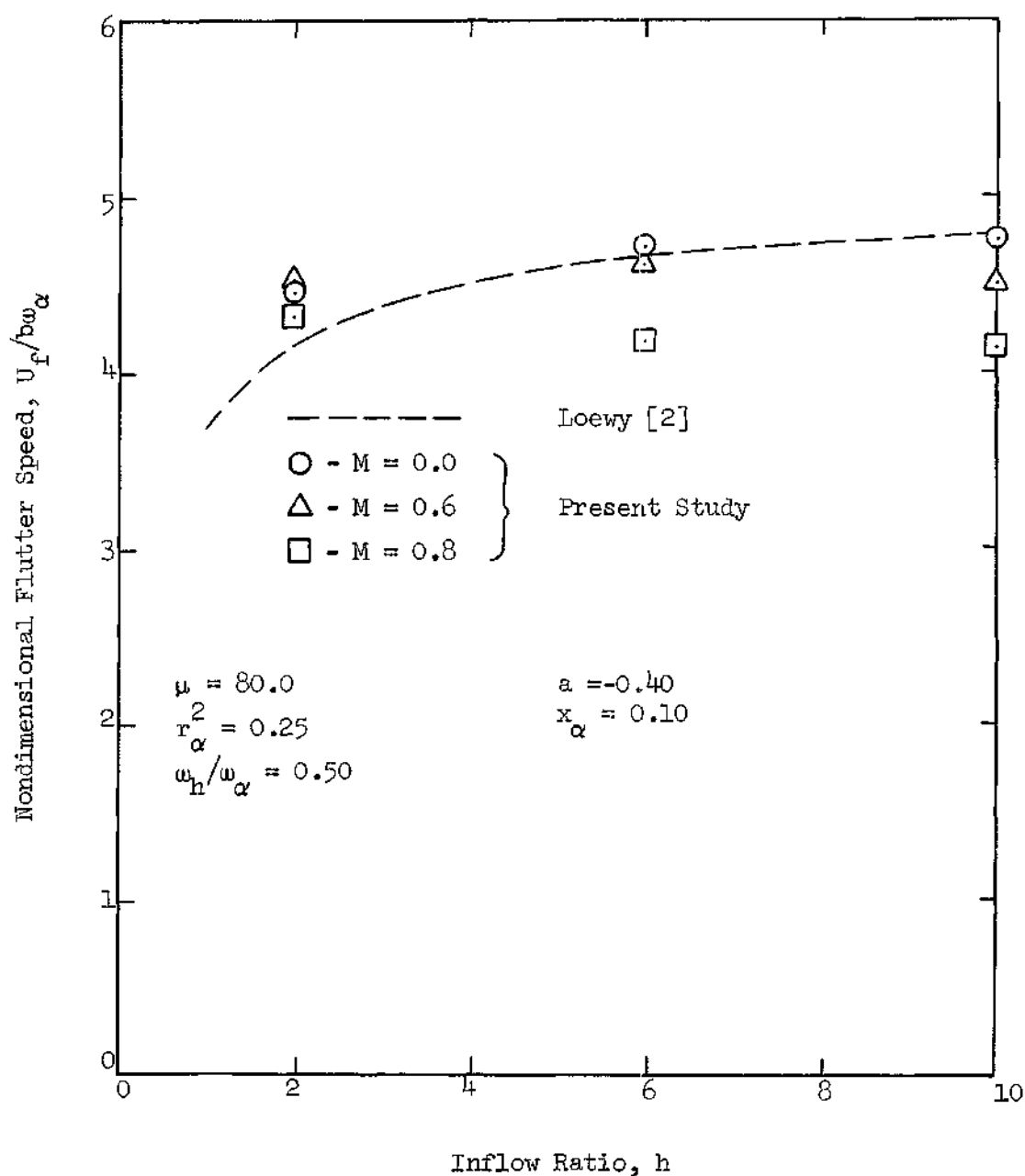
Figure 11. Variation of Flutter Speed with Inflow Ratio,
         m = 0.2
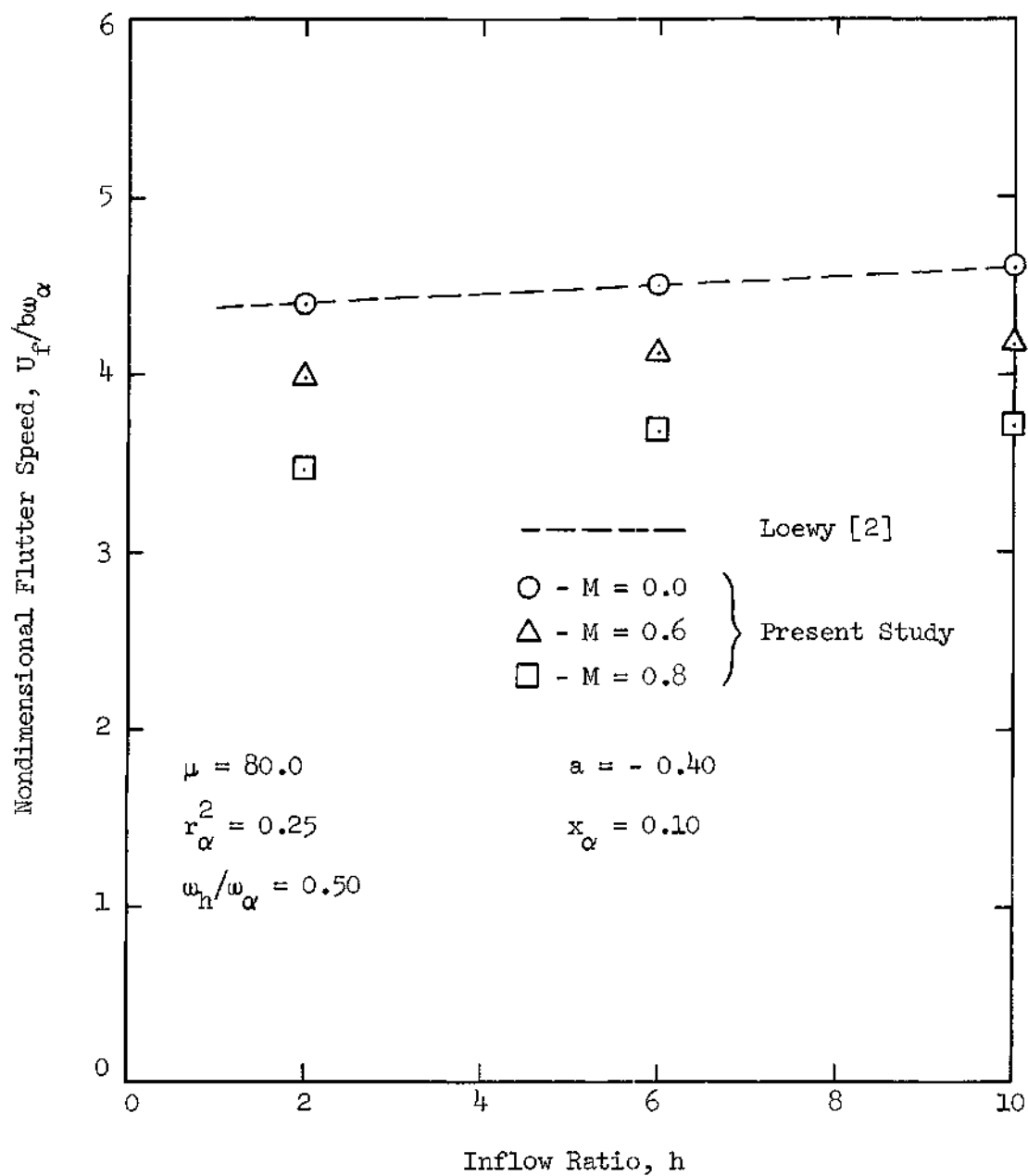
Figure 12. Variation of Flutter Speed with Inflow Ratio,
m = 0.50
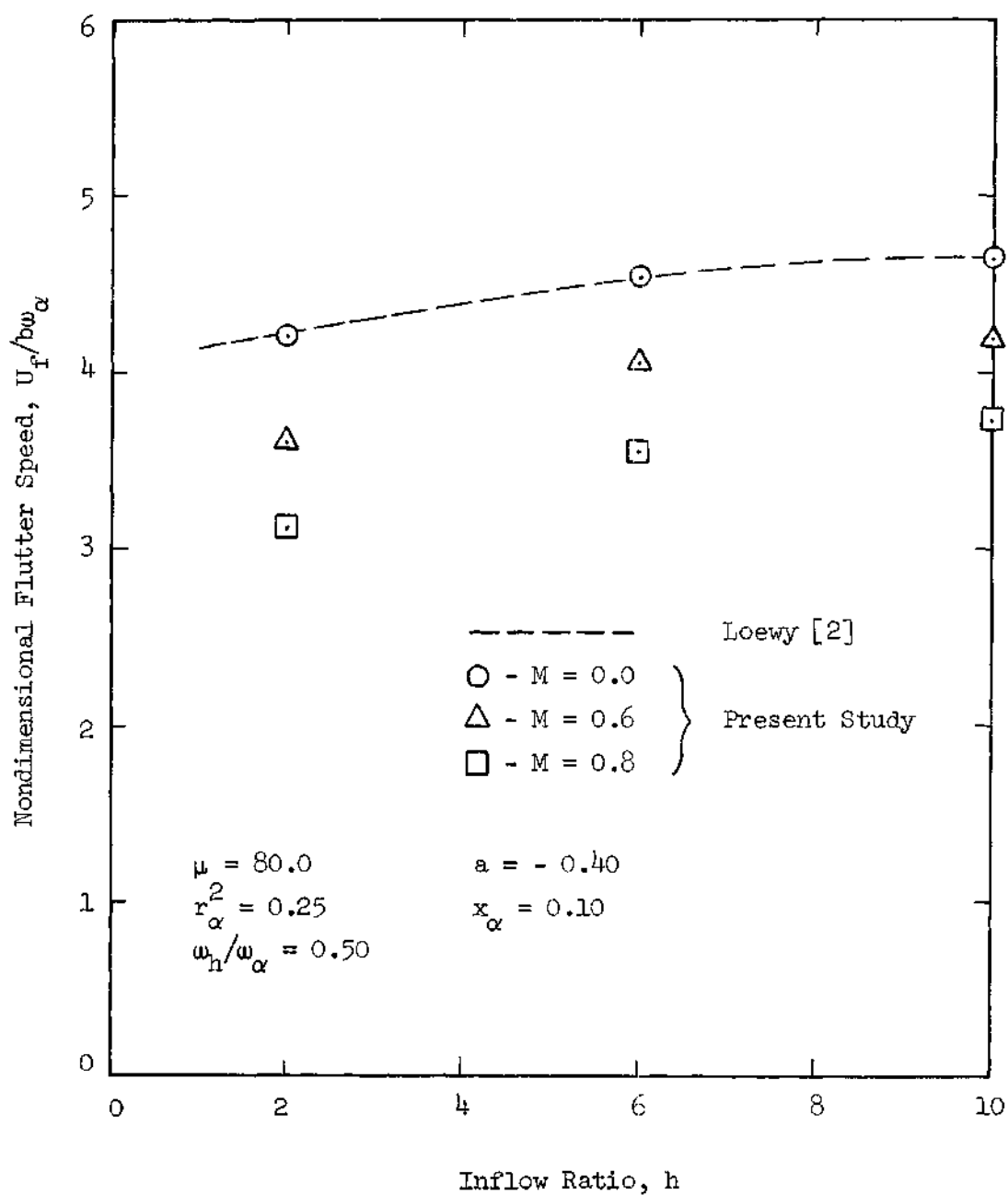
Figure 13. Variation of Flutter Speed with Inflow Ratio,
m = 0.80

frequency ratio is increased as was pointed out earlier. From Figure 11 it is apparent also that as the inflow ratio is increased the zero Mach number data come closer to the Loewy curve. This too is caused by the two flow models being brought into better agreement. For, as the inflow ratio increases, the "wake airfoils" are moved further and further from the reference airfoil and hence their influence on the aerodynamic loading of the reference airfoil becomes less and less.

It is of interest here to point out the relationship between the rotary wing flutter speed and the fixed wing flutter speed. As the inflow ratio, h, increases the vertical distance between the reference airfoil and the first "wake airfoil" increases. Thus as h becomes very large the rotary wing results should asymptotically approach the fixed wing results. In Reference [6] this was shown to indeed be true for the incompressible case when Loewy [2] aerodynamics were used. Shown in Table 1 are the nondimensional fixed wing flutter speeds for the structural parameters given by Equations (126).

Table 1. Nondimensional Fixed Wing
Flutter Speeds

Mach Number, M	Flutter Speed, $U_f/b\omega_\alpha$
0	4.75
0.6	4.36
0.8	3.82

By comparison of these data with Figures 11 - 13 it can be seen that the rotary wing data do appear to be asymptotically approaching the fixed wing data.

The increasing agreement of the zero Mach number data with the Loewy curves as frequency ratio increases is more apparent from Figures 14 - 16. On these figures the variation of flutter speed with frequency ratio is shown for inflow ratios of 2.0, 6.0, and 10.0 respectively. Again the trend is for decreasing flutter speed with increasing Mach number.

Figures 17 and 18 show the variation of nondimensional flutter speed with density ratio for nondimensional center of gravity locations of 0.0 and 0.1 respectively. In addition to the nondimensional flutter speed, the nondimensional divergence speed is also plotted on these figures. From Figure 17 it can be seen that for the larger values of density ratio the flutter speed decreases with increasing Mach number, but for lower values of μ the trend reverses. However, note that the divergence curves cross their respective flutter curves at low values of the density ratio, so that stability of the system is determined from divergence considerations rather than flutter considerations. In general then, for $x_\alpha = 0.0$ the nondimensional speed at which the system becomes unstable decreases with increasing Mach number and the stability criterion is sometimes divergence and sometimes flutter.

For $x_\alpha = 0.1$, such is not the case as can be seen from Figure 18. In this case the stability criterion is always flutter, and the flutter speed decreases with increasing Mach number. For both values of x_α, the flutter results for incompressible flow are shown to be

Figure 14. Variation of Flutter Speed with Frequency Ratio, h = 2.0

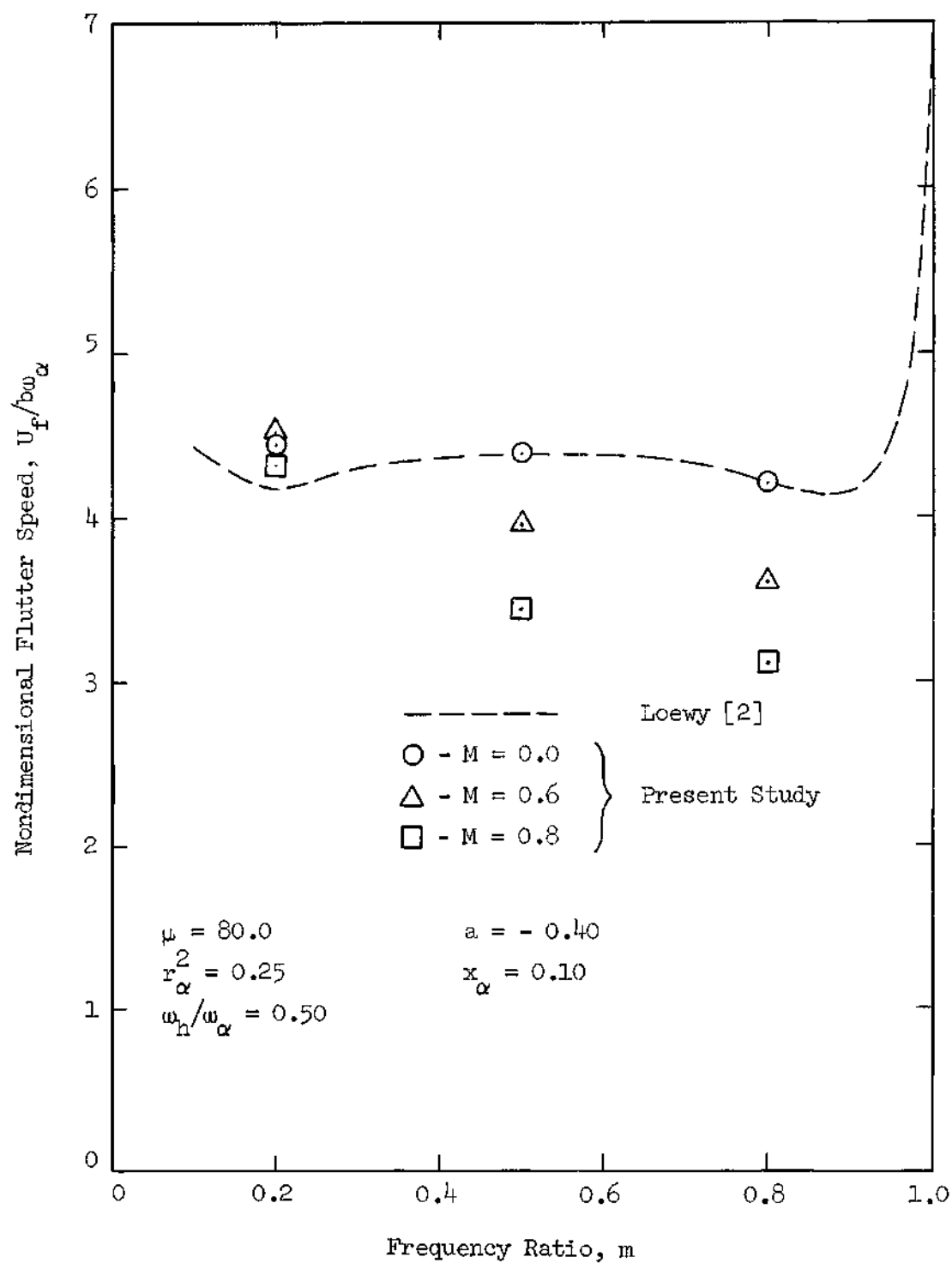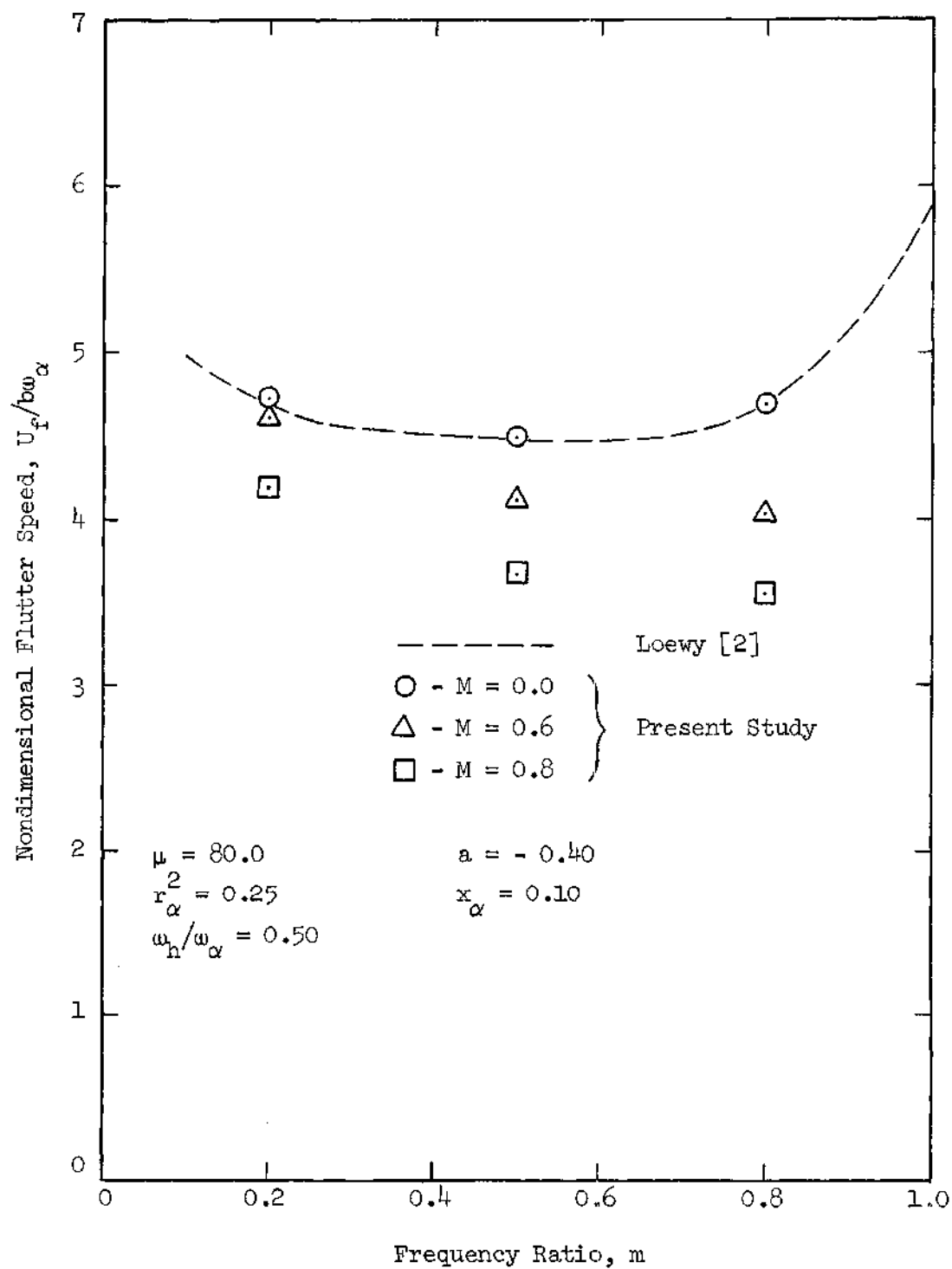Figure 15. Variation of Flutter Speed with Frequency Ratio, h = 6.0
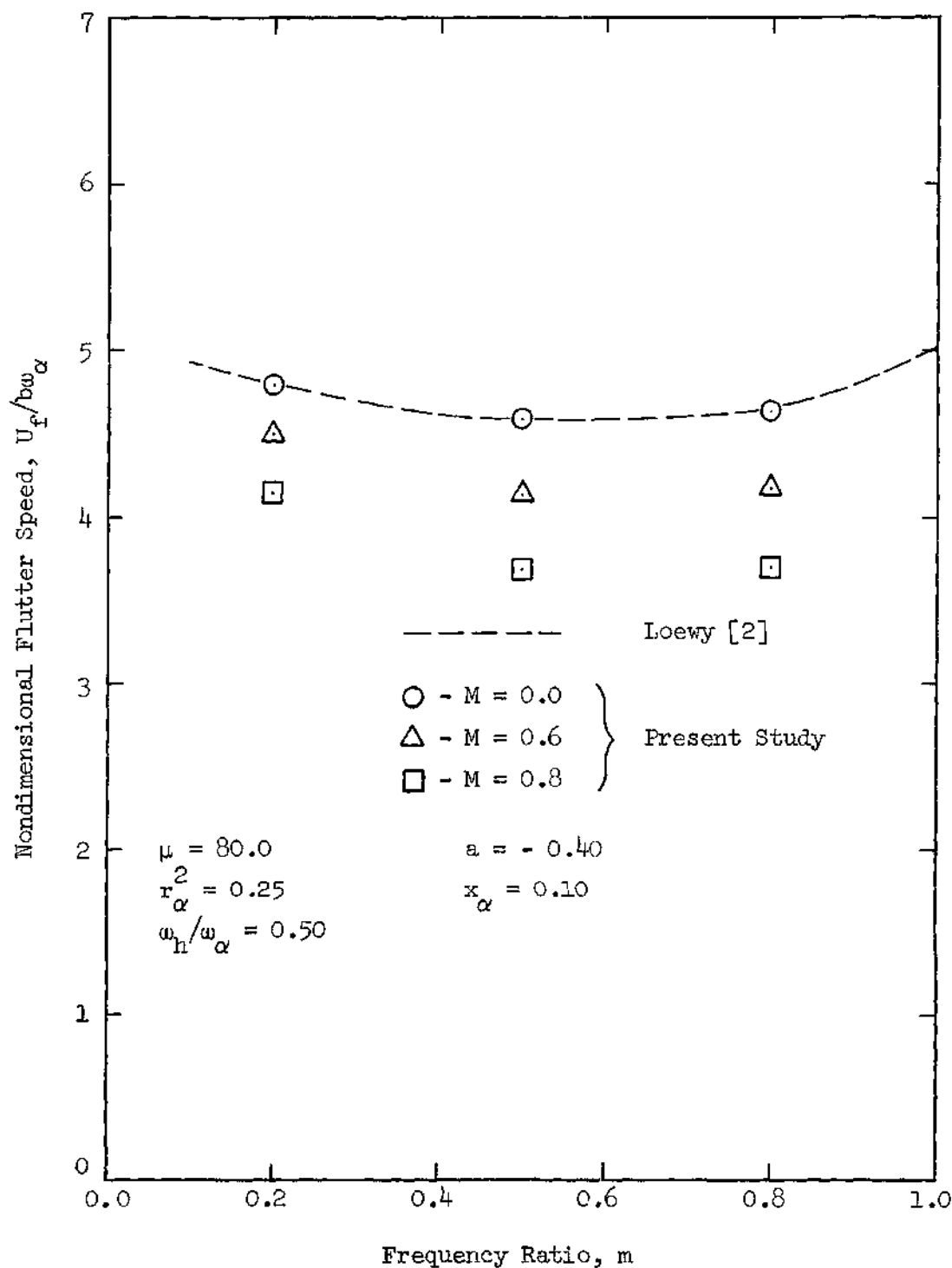
Figure 16. Variation of Flutter Speed with Frequency Ratio,
h = 10.0
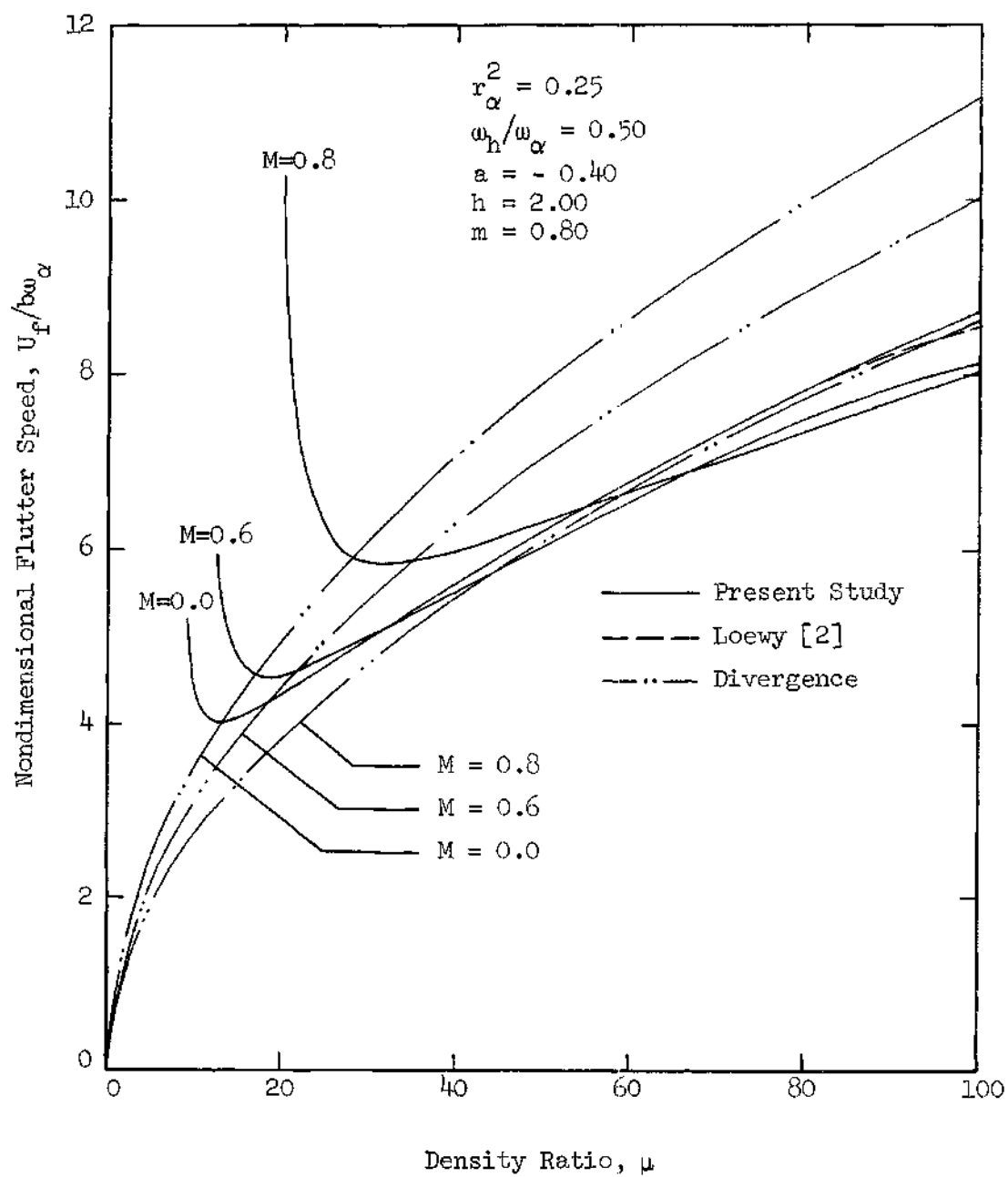
Figure 17. Variation of Flutter Speed with Density Ratio, $x_\alpha = 0.0$
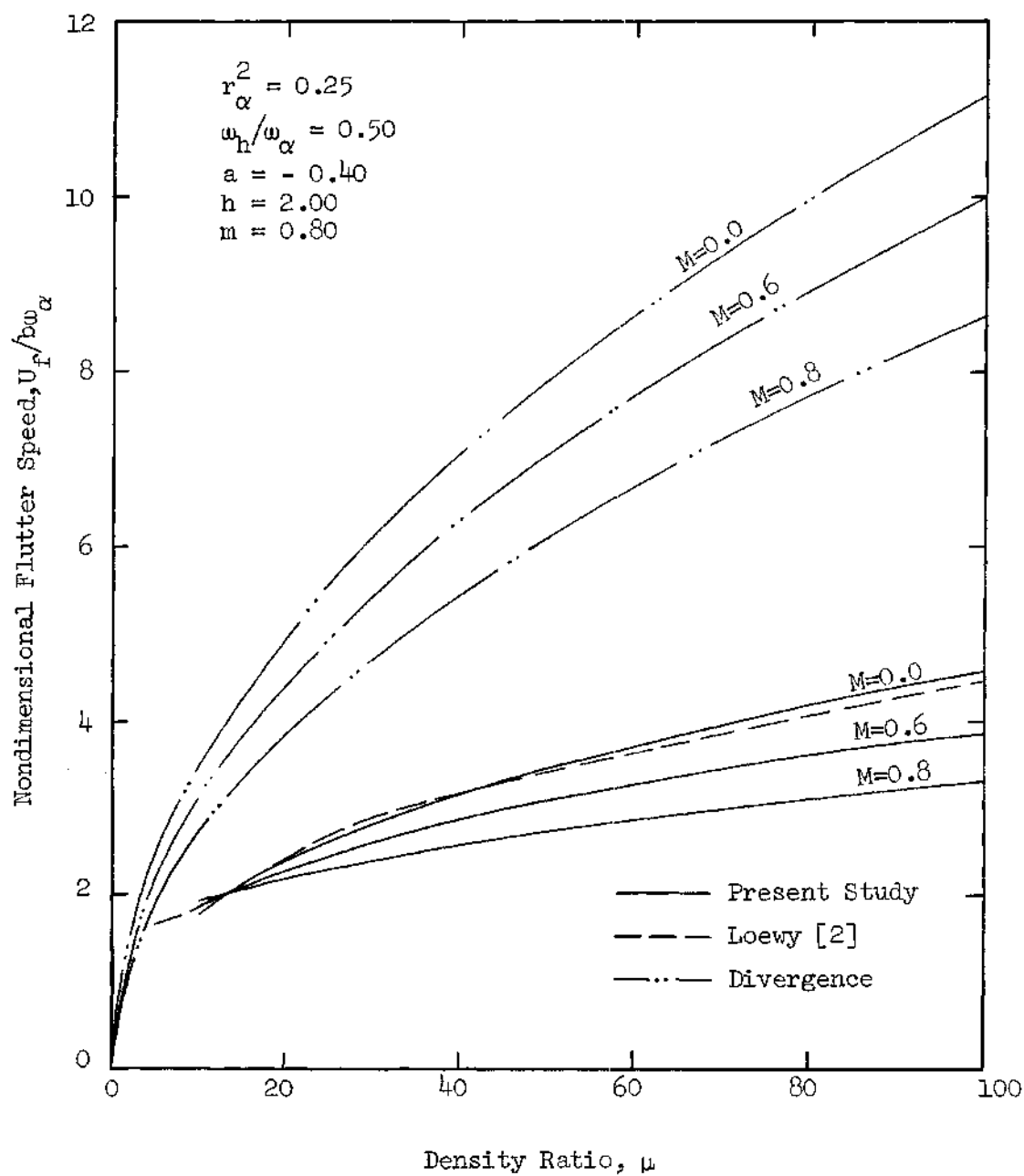
Figure 18. Variation of Flutter Speed with Density Ratio, $x_\alpha = 0.1$

almost identical with the results obtained using Loewy [2] aerodynamics.

The variation of nondimensional flutter speed with nondimensional radius of gyration is shown in Figures 19 and 20 for nondimensional center of gravity locations of 0.0 and 0.1 respectively. The trends of these curves are very much similar to the trends of Figures 17 and 18. Divergence again is an important consideration for x_α = 0.0 but is not critical for x_α = 0.1. Flutter speeds again decrease with Mach number and correlation with results using Loewy aerodynamics is excellent.

Finally, Figures 21 and 22 show the effect of bending-torsion frequency ratio on the nondimensional flutter speed for nondimensional center of gravity locations of 0.0 and 0.1 respectively. Again, divergence is important for x_α = 0.0, but not for x_α = 0.1. Note from Figure 21 that beyond a certain value of bending-torsion frequency ratio, the exact value being Mach number dependent, there is no possibility of flutter when x_α = 0.0. Beyond these values the stability of the system is based on divergence considerations. Note also that for x_α = 0.0 the flutter speed decreases with Mach number for low values of bending-torsion frequency ratio, but this trend reverses as the bending-torsion frequency ratio approaches the values where the curves turn vertical. For x_α = 0.0, the agreement of the zero Mach number data with the data obtained using Loewy aerodynamics is so close that the two curves are indistinguishable on Figure 21.

For x_α = 0.1 the variation of flutter speed with bending-torsion frequency ratio is somewhat different than when x_α = 0.0, as seen from Figure 22. In this case there is no sharp turning upward of the
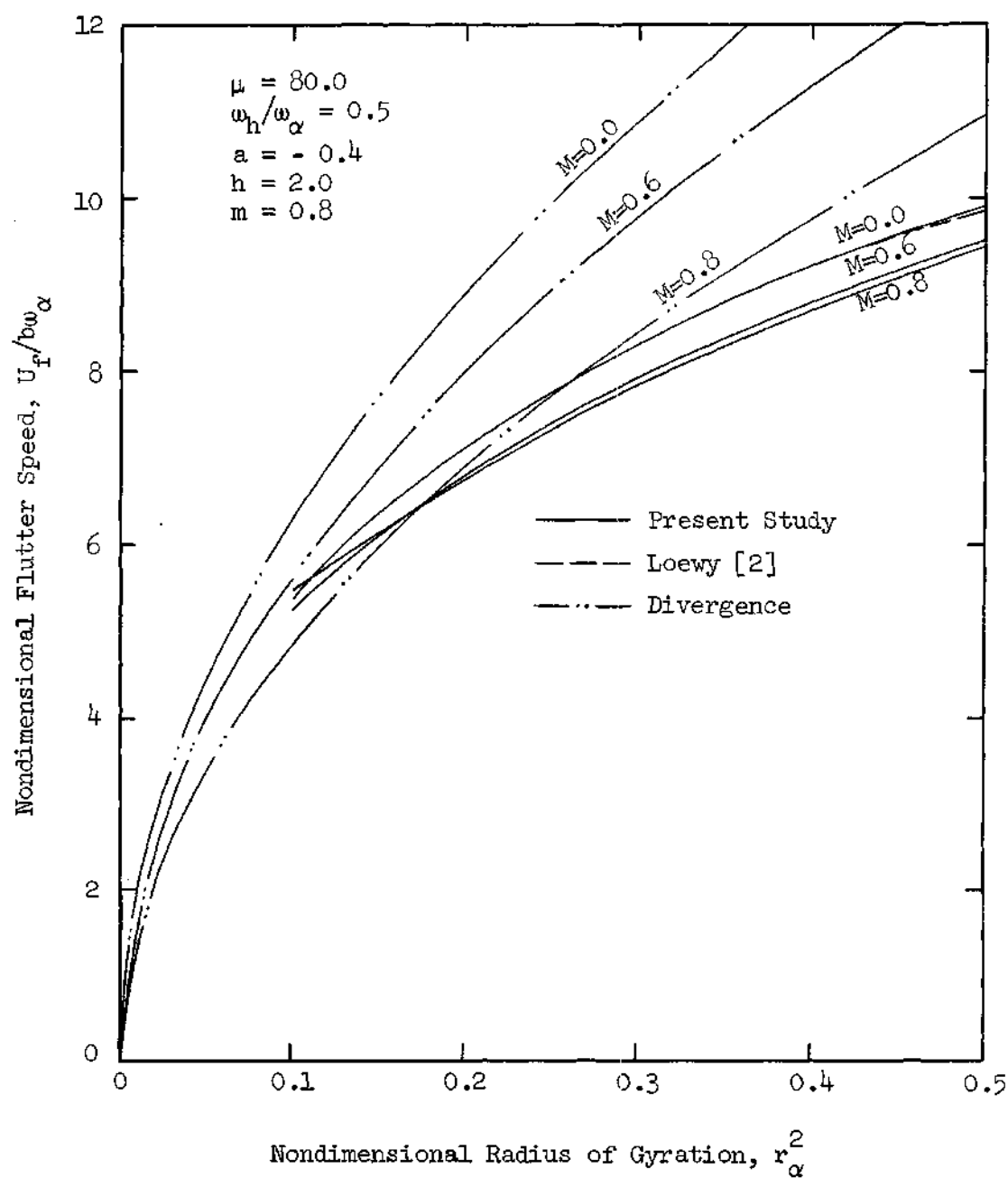
Figure 19. Variation of Flutter Speed with Nondimensional
Radius of Gyration, $x_\alpha = 0.0$
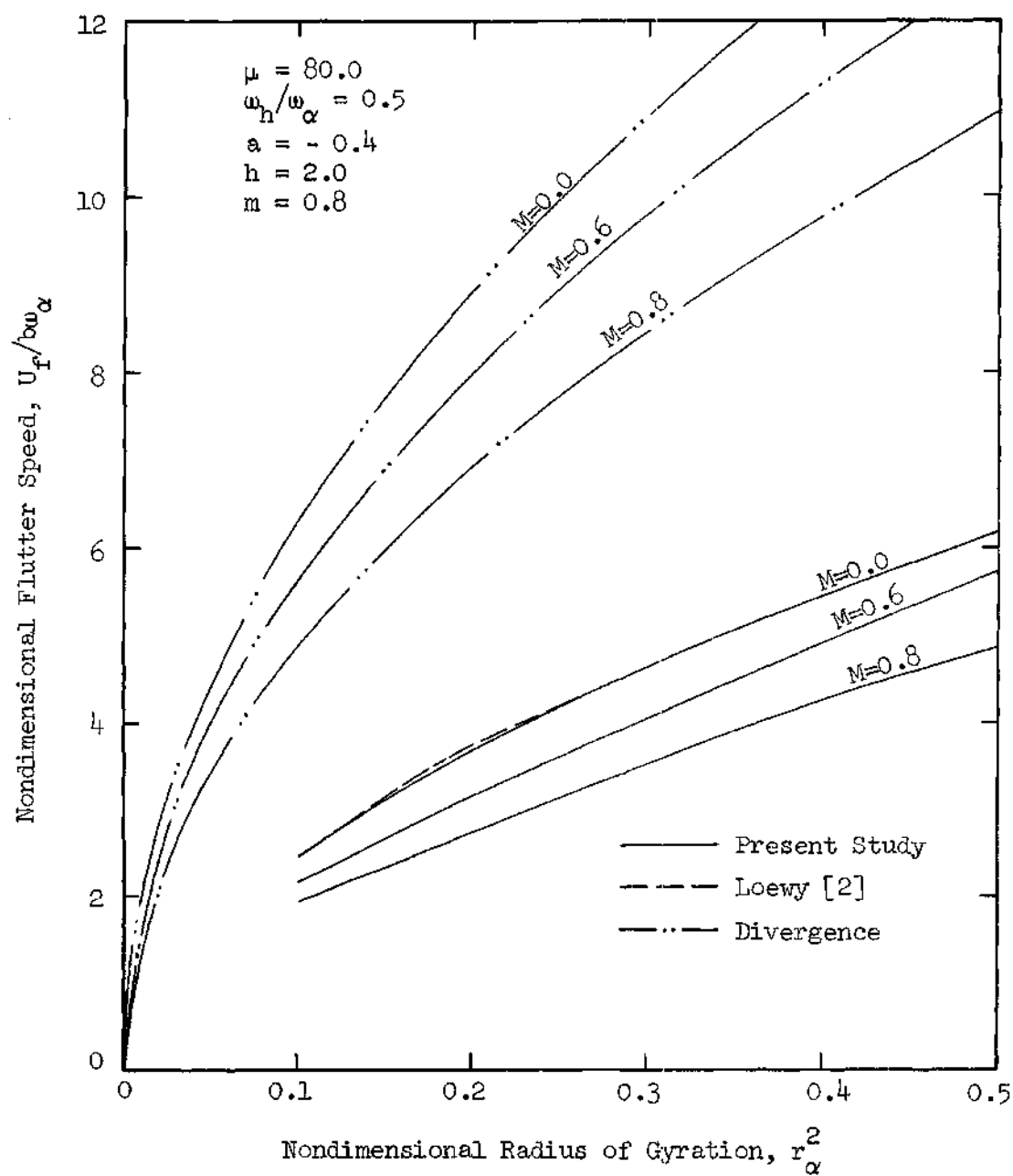
Figure 20. Variation of Flutter Speed with Nondimensional Radius of Gyration, $x_\alpha = 0.1$
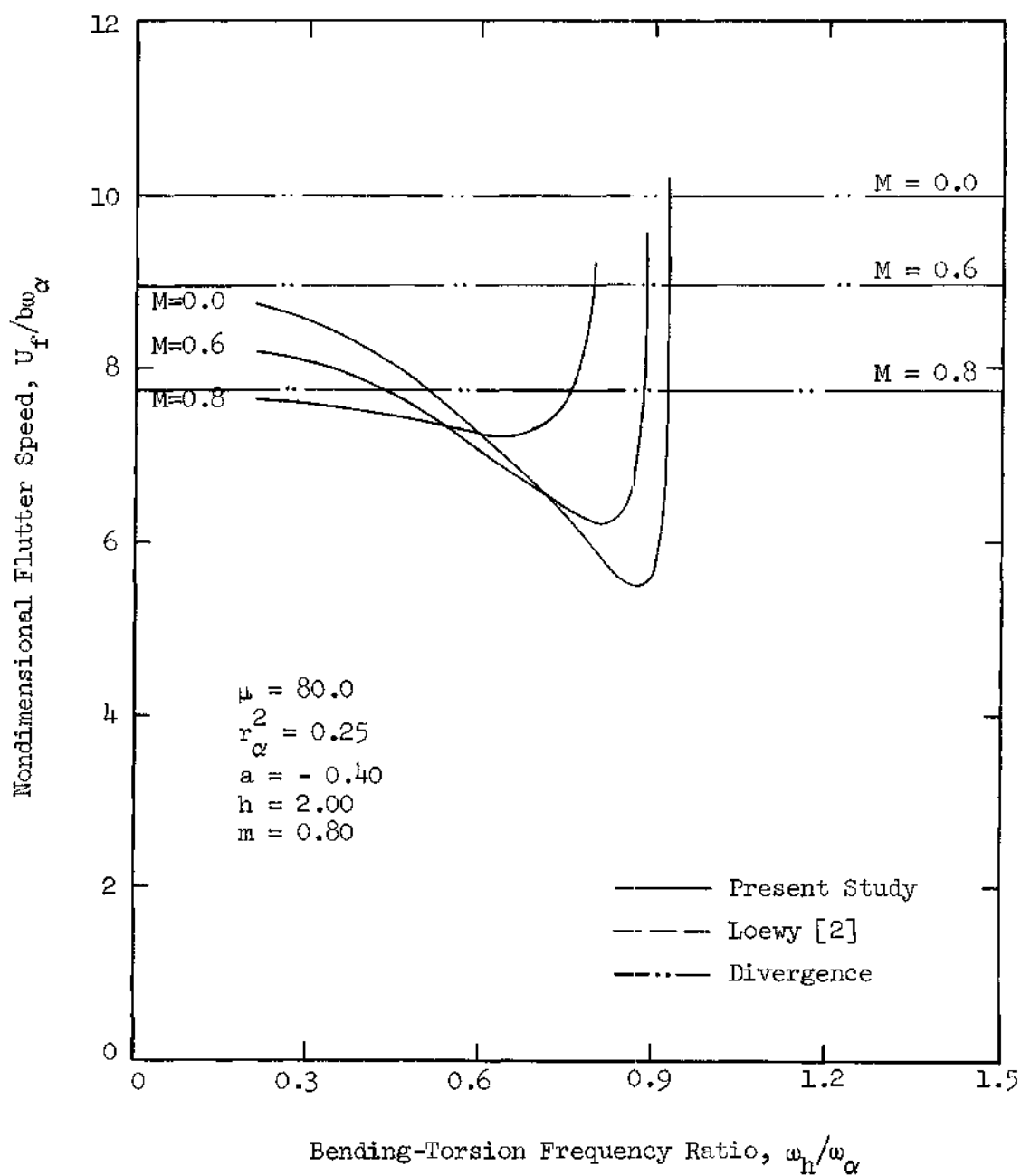
Figure 21. Variation of Flutter Speed with Bending-Torsion Frequency Ratio, $x_\alpha = 0.0$
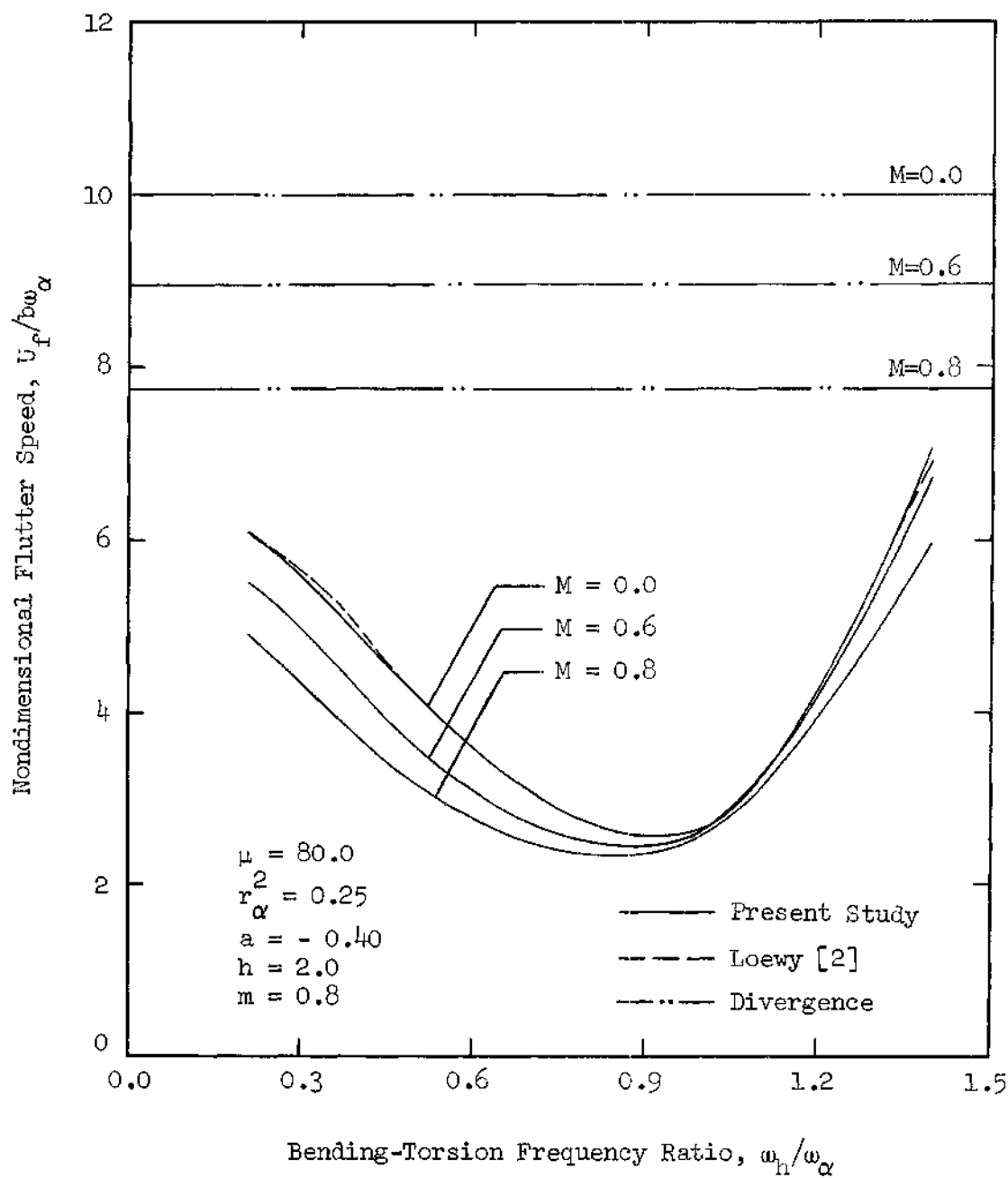
Figure 22. Variation of Flutter Speed with Bending-Torsion Frequency Ratio, $x_\alpha = 0.1$

curves as was noted from Figure 21. For this case the effect of Mach number is to decrease the flutter speed, and agreement with results obtained using Loewy aerodynamics is very close.

It will be noted that in all the preceding flutter results comparison was made with results obtained using Loewy aerodynamics but no comparisons were made with flutter results using Jones' and Rao's theory. This is because insufficient data from their theory exist at the present time. It might be noted here that the excellent agreement between the flutter results obtained using the two incompressible theories should not lead one to expect the same sort of agreement between the compressible results of the present study and those obtained using Jones' and Rao's theory. Phase lag effects which were lost in their theory could have a significant effect on flutter results. However, further study after more of their aerodynamic data become available will be necessary to substantiate this conjecture.

As a final result, it should be mentioned that for all the aerodynamic conditions considered in the preceding results the divergence of the wake series discussed in Chapter II presented no problem. For all the conditions considered, the divergence criterion, Equation (32), was satisfied for reduced frequencies substantially greater than those required for the flutter analysis.

CHAPTER V

CONCLUSIONS AND RECOMMENDATIONS

The effect of compressibility on the flutter condition of rotary wings has been investigated analytically. A two-dimensional model of the complicated three-dimensional helicopter flow field was postulated and a compressible, unsteady aerodynamic theory developed using the two-dimensional model. The governing integral equation for the two-dimensional flow with its attendant boundary condition was generated and solved numerically by collocation using a pressure mode assumption. After comparing the aerodynamic theory thus developed with other similar theories, it was used in conjunction with a two degree of freedom flutter analysis to establish the role of compressibility in helicopter rotor blade flutter. The many parameters, both aerodynamic and structural, entering the flutter problem were varied systematically so that their influence on the rotor blade flutter phenomenon under compressible flow conditions could be determined.

Conclusions

The results of the research indicate that the following conclusions can be drawn.

1. The difference in flow models used by Loewy [2] and Jones and Rao [24], and that used in the present investigation can lead to substantial differences in the aerodynamic coefficients computed for

moderate values of frequency ratio, m. For larger values of frequency ratio (in the neighborhood of unity) the agreement between the aerodynamic coefficients computed using the three theories improves.

2. The flutter results obtained using the present aerodynamic theory with zero Mach number are in excellent agreement with the results obtained using Loewy's incompressible aerodynamic theory. Aerodynamic data from Jones' and Rao's theory were not readily available and therefore no flutter calculations could be made using their results. It should be pointed out, however, that the agreement between the incompressible results should not necessarily lead one to expect the same degree of agreement between the compressible results due to the basic difference between the two types of flow.

3. The general trend is for decreasing flutter speed with increasing Mach number. Thus the effect of compressibility on the rotary wing flutter speed is the same as its effect on the fixed wing flutter speed, i.e., compressibility has a destabilizing influence on the flutter condition.

4. Static divergence is an important consideration when the elastic axis and center of gravity locations coincide. For this particular case as the Mach number increases the stability criterion changes from flutter to static divergence. For a center of gravity location one-tenth of a semi-chord aft of the elastic axis, flutter considerations always dictated the stability boundary.

5. From the limited fixed wing calculations it appears that the rotary wing flutter speeds are generally lower than the corresponding fixed wing flutter speeds for all Mach numbers. This indicates that

the use of compressible fixed wing aerodynamics in the design of rotor blades against flutter will lead to unconservative results.

Recommendations

A number of general suggestions are offered concerning the directions future studies of the rotary wing flutter problem might take.

1. First of all, since a comparison of the flutter results obtained using the present aerodynamic theory with those obtained using Loewy's [2] theory was made, a most interesting comparison could be made using the theory of Jones and Rao [24]. This study would provide results for evaluating the effect of the two different flow models under compressible flow conditions. A study of this type would substantiate or refute the conjecture made earlier that the compressible flow results might not agree as well as the incompressible results.

2. The flutter analysis used in the present study considered a rigid airfoil section free to pitch and plunge. A more realistic approach would be to consider the rotor blade as a rotating beam free to deflect and twist. This would necessitate using the aerodynamic theory of the present study in a strip theory fashion. This could be done as follows. First consider the tip Mach number fixed. This in turn specifies the Mach number at each radial station on the blade. Since the blade geometry is specified, the inflow ratio, h, could be calculated as a function of spanwise location using, for example, the combined blade element axial momentum theory. Two remaining parameters need to be determined; reduced frequency, k, and frequency ratio, m. As in all flutter analyses the three-dimensional flutter problem must

be solved by a trial and error process. The reduced frequency is always one of the trial variables. Thus if reduced frequency is specified as constant along the span then the frequency ratio can be computed as a function of span since k and m are related as

$$m = kr/b$$

With all the aerodynamic parameters thus specified as functions of radial location, the spanwise aerodynamic loading could be determined and the three-dimensional flutter analysis conducted.

3. Probably one of the greatest needs is an experimental program to corroborate the results of this and other theoretical studies of rotor blade aeroelastic phenomena. The program should definitely include the possibility of operating the rotor under compressible flow conditions, since the trend in present helicopter design is toward the high subsonic speed range.

4. An obvious extension of the present study is an unsteady three-dimensional aerodynamic theory for rotor blades which includes compressibility effects. This type of theory is desirable in order to more realistically represent the three-dimensional loading on a rotor blade.

The effect of compressibility on the flutter condition of rotory wings has been determined under two-dimensional aerodynamic conditions. More investigations, both experimental and analytical, are needed to substantiate this study and extend the results to include more of the three-dimensional effects of the physical aerodynamic and structural rotor system.

APPENDICES

APPENDIX A

DEVELOPMENT OF THE PULSATING DOUBLET SOLUTION

In this appendix a fundamental solution of the linearized acceleration potential equation is developed. This solution is called the pulsating doublet solution because it represents the acceleration potential of a doublet whose strength is allowed to vary harmonically with time. The solution will first be developed for three-dimensional flow and then reduced to that for two-dimensional flow.

Three-Dimensional Flow

In steady incompressible flow the governing equation can be taken as the linearized velocity potential equation

$$\nabla^2 \varphi = 0 \tag{A-1}$$

A familiar solution to this equation is the simple source solution given by

$$\varphi_1^s = -\frac{1}{4\pi} \frac{q_1}{\sqrt{x^2 + y^2 + z^2}} \tag{A-2}$$

where q_1 is the source strength and is constant.

In compressible subsonic flow the governing equation becomes

$$(1 - M^2) \frac{\partial^2 \varphi}{\partial x^2} + \frac{\partial^2 \varphi}{\partial y^2} + \frac{\partial^2 \varphi}{\partial z^2} = 0 \qquad (A\text{-}3)$$

where M is the free stream Mach number. The simple source solution, Equation (A-2), can be extended to this case by noting that under the transformation

$$\left. \begin{aligned} \bar{y} &= \beta \, y \\ \bar{z} &= \beta \, z \\ \beta &= \sqrt{1 - M^2} \end{aligned} \right\} \qquad (A\text{-}4)$$

Equation (A-3) becomes Laplace's equation. Thus the compressible source solution for steady subsonic flow is written

$$\varphi_c^s = - \frac{1}{4\pi} \frac{q_1}{\sqrt{x^2 + \beta^2(y^2 + z^2)}} \qquad (A\text{-}5)$$

In the case of unsteady flow the simple source solution may again be used. However, for the unsteady case the strength of the source is considered to be a function of time. For incompressible unsteady flow the governing equation is again Laplace's equation and the simple source solution is given by

$$\varphi_1^s = -\frac{1}{4\pi} \frac{q_1(t)}{\sqrt{x^2 + y^2 + z^2}} \qquad \text{(A-6)}$$

where it will be noted that the source strength, q_1, is now a function of time.

For compressible unsteady flow the linearized perturbation potential equation is given by

$$\nabla^2 \varphi - \frac{1}{a_\infty^2}\left[\frac{\partial^2 \varphi}{\partial t^2} + 2U\frac{\partial^2 \varphi}{\partial t \partial x} + U^2 \frac{\partial^2 \varphi}{\partial x^2}\right] = 0 \qquad \text{(A-7)}$$

In this case the fact that a disturbance in the flow is propagated at a finite velocity, namely the sound speed of the medium, must be taken into account. Thus the simple source solution is written

$$\varphi_c^s = -\frac{1}{4\pi} \frac{q_1(\tau)}{\sqrt{x^2 + \beta^2(y^2 + z^2)}} \qquad \text{(A-8)}$$

where τ is the time that a disturbance leaves the source.

Letting t represent the time at which the disturbance reaches the point (x,y,z), the relationship between τ and t may be developed as follows. If the source is considered to be located at the point $(0,0,0)$ as was done above, then a pressure pulse which emanates at time τ propagates outward in a spherical region while being swept downstream at a velocity U by the main flow, and reaches the point (x,y,z) at time t. The relationship between τ and t may be derived from the

geometry of the flow shown in Figure A-1. Since the flow is compressible, the disturbance propagates outward at the sound speed of the medium, a_∞. The radius of the spherical propagation front at time t may be written

$$r_f = a_\infty(t - \tau) \tag{A-9}$$

Also, from the geometry

$$r_f = \sqrt{\left[x - U(t - \tau)\right]^2 + y^2 + z^2} \tag{A-10}$$

Equating Equations (A-9) and (A-10)

$$a_\infty(t - \tau) = \sqrt{\left[x - U(t - \tau)\right]^2 + y^2 + z^2} \tag{A-11}$$

Solving for τ

$$\tau = t + \frac{1}{a_\infty\beta^2}\left[Mx \pm \sqrt{x^2 + \beta^2(y^2 + z^2)}\,\right] \tag{A-12}$$

The minus sign in Equation (A-12) is now chosen for the following reason. The radical of Equation (A-12) will produce a number which is greater than x since β^2 is less than unity. Also because M is less than unity, Mx is less than x. Therefore by choosing the minus sign the number inside the brackets of Equation (A-12) will be negative and
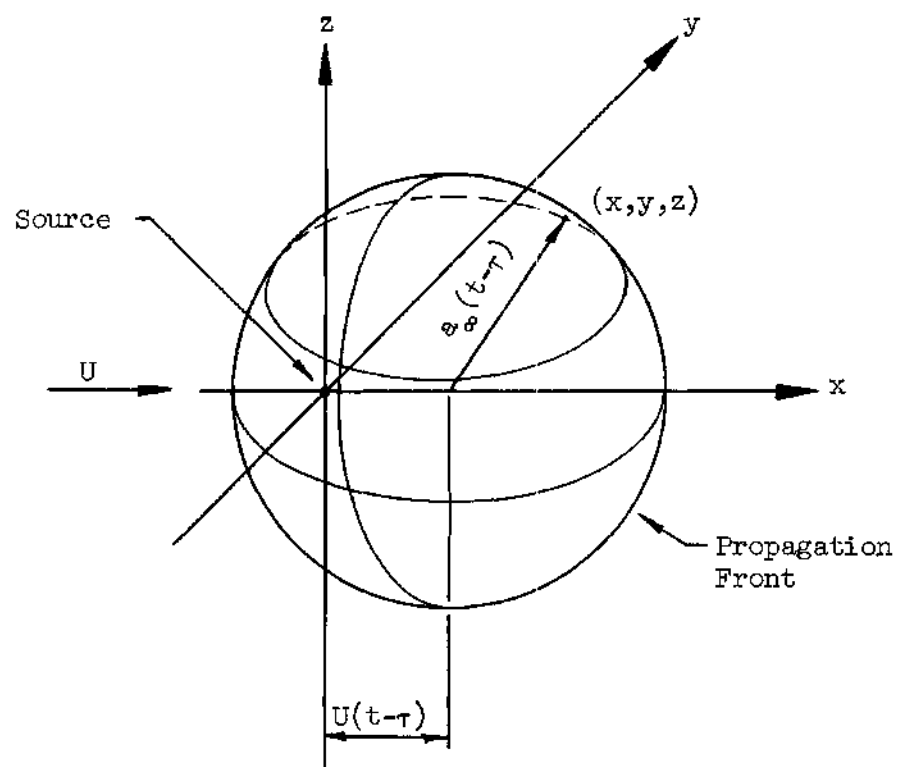
Figure A-1. The Disturbance Produced by a Subsonic Source
Pulse at the Origin at Time τ as it Reaches the
Point (x,y,z) at Time t

thus τ will be less than t which is required by the physics of the problem. The final relation between τ and t thus becomes

$$\tau = t + \frac{1}{a_\infty \beta^2} \left[Mx - \sqrt{x^2 + \beta^2(y^2 + z^2)} \right] \qquad \text{(A-13)}$$

Now the governing differential equation for the acceleration potential, Ψ, in three-dimensional flow is given by

$$\nabla^2 \Psi - \frac{1}{a_\infty^2} \left[\frac{\partial^2 \Psi}{\partial t^2} + 2U \frac{\partial^2 \Psi}{\partial t \partial x} + U^2 \frac{\partial^2 \Psi}{\partial x^2} \right] = 0 \qquad \text{(A-14)}$$

which is exactly the same as Equation (A-7). Thus any solution of Equation (A-7) will also be a solution of Equation (A-14). The acceleration potential for an unsteady source located at the origin may then be written

$$\Psi_s = - \frac{1}{4\pi} \frac{q_2(\tau)}{\sqrt{x^2 + \beta^2(y^2 + z^2)}} \qquad \text{(A-15)}$$

where τ is as given by Equation (A-13). It should be noted here that Ψ_s and φ_c^s are not identical because the boundary condition on Ψ and the boundary condition on φ are different. The relationship between Ψ and φ is

$$\Psi = \frac{\partial \varphi}{\partial t} + U \frac{\partial \varphi}{\partial x} \qquad \text{(A-16)}$$

Requiring the unsteady source strength to vary simple harmonically with time

$$q_2(\tau) = \bar{q}\, e^{i\omega\tau} \tag{A-17}$$

where $\bar{q}$ is constant, the acceleration potential for the source becomes

$$\Psi_s = -\frac{\bar{q}}{4\pi}\, \frac{e^{i\omega\tau}}{\sqrt{x^2 + \beta^2(y^2 + z^2)}} \tag{A-18}$$

Substituting the expression for τ

$$\Psi_s = -\frac{\bar{q}}{4\pi}\, \frac{e^{i\omega\left[t + \frac{Mx}{a_\infty \beta^2} - \frac{R'}{a_\infty \beta^2}\right]}}{R'} \tag{A-19}$$

where

$$R' = \sqrt{x^2 + \beta^2(y^2 + z^2)}$$

$$\Psi_s = \Psi_s(x,y,z;t)$$

Now place a sink below the x-axis and a source above the x-axis such that they are a distance ϵ apart and have equal strength. The acceleration potential for the sum of the source and the sink is given by

$$\Psi_{sink}\left(x,y,z + \frac{\epsilon}{2} \; ; \; t\right) + \Psi_{source}\left(x,y,z - \frac{\epsilon}{2} \; ; \; t\right)$$

Let

$$\Psi_{source} = - \frac{\bar{q}}{4 \pi} \bar{\Psi} \qquad \text{(A-20)}$$

then

$$\left(\Psi_{source} + \Psi_{sink}\right) = \frac{\epsilon}{4} \frac{\bar{q}}{\pi} \frac{\left[\bar{\Psi}\left(x,y,z + \frac{\epsilon}{2} \; ; \; t\right) - \bar{\Psi}\left(x,y,z - \frac{\epsilon}{2} \; ; \; t\right)\right]}{\epsilon} \qquad \text{(A-21)}$$

The transformation to the doublet is made by shrinking the distance between the source and the sink ($\epsilon \to 0$) in such a way that the quantity $\frac{\epsilon \bar{q}}{4\pi}$ remains constant, say A. Thus

$$\Psi_{doublet} = \lim_{\epsilon \to 0} \left(\frac{\epsilon \bar{q}}{4\pi}\right) \frac{\bar{\Psi}\left(x,y,z + \frac{\epsilon}{2} \; ; \; t\right) - \bar{\Psi}\left(x,y,z - \frac{\epsilon}{2} \; ; \; t\right)}{\epsilon} \qquad \text{(A-22)}$$

But the limit of the second factor is just the partial derivative with respect to z, so that

$$\Psi_{doublet} = A \frac{\partial}{\partial z} \bar{\Psi}\left(x,y,z; \; t\right) \qquad \text{(A-23)}$$

or

$$\Psi_{\text{doublet}} = A \frac{\partial}{\partial z} \frac{e^{i\omega\left[t + \frac{Mx}{a_\infty\beta^2} - \frac{R'}{a_\infty\beta^2}\right]}}{R'}$$

$$R' = \sqrt{x^2 + \beta^2(y^2 + z^2)}$$

(A-24)

Equations (A-24) represent the acceleration potential of a doublet located at the point $(0,0,0)$. The acceleration potential for a doublet at the point (ξ,η,ζ) is obtained from Equations (A-24) by replacing x with $(x - \xi)$, y with $(y - \eta)$ and z with $(z - \zeta)$. The acceleration potential for a harmonically pulsating doublet at the general point (ξ,η,ζ) in three-dimensional flow is thus given by

$$\Psi_D = A \frac{\partial}{\partial z} \frac{e^{i\omega\left[t + \frac{M(x-\xi)}{a_\infty\beta^2} - \frac{R}{a_\infty\beta^2}\right]}}{R}$$

$$R = \sqrt{(x - \xi)^2 + \beta^2\left[(y - \eta)^2 + (z - \zeta)^2\right]}$$

A = Magnitude of doublet strength

(A-25)

Two-Dimensional Flow

The reduction of the pulsating doublet acceleration potential for two-dimensional flow is obtained by first returning to the pulsating source acceleration potential, Equation (A-15) and integrating out the spanwise or y-dependence. Thus for two-dimensional flow the acceleration potential for the pulsating source becomes

$$
\left.
\begin{aligned}
\Psi_s(x,z;t) &= -\frac{1}{4\pi} \int_{-\infty}^{\infty} \frac{q_2\Big(\tau(y)\Big)\, dy}{\sqrt{x^2 + \beta^2(y^2 + z^2)}} \\[2em]
\Psi_s(x,z;t) &= -\frac{1}{2\pi} \int_{-\infty}^{0} \frac{q_2\Big(\tau(y)\Big)\, dy}{\sqrt{x^2 + \beta^2(y^2 + z^2)}}
\end{aligned}
\right\} \quad \text{(A-26)}
$$

Now from Equation (A-13)

$$
d\tau = -\frac{y}{a_\infty} \frac{dy}{\sqrt{x^2 + \beta^2(y^2 + z^2)}} \quad \text{(A-27)}
$$

and

$$
y = \sqrt{a_\infty^2(t-\tau)^2 - \left[x - U(t-\tau)\right]^2 - z^2} \quad \text{(A-28)}
$$

so that Equation (A-26) becomes

$$\Psi_s(x,z;t) = - \frac{a_\infty}{2\pi} \int_{-\infty}^{\tau_o} \frac{q_2(\tau)\ d\tau}{\sqrt{a_\infty^2(t-\tau)^2 - [x - U(t-\tau)]^2 - z^2}} \tag{A-29}$$

where

$$\tau_o = t + \frac{1}{a_\infty\beta^2}\left[Mx - \sqrt{x^2 + \beta^2 z^2}\ \right] \tag{A-30}$$

and τ_o represents the time at which the last disturbance arriving at the point (x,z) at time t left the source.

If the source is considered to be pulsating harmonically, then

$$q_2(\tau) = \bar{q}\ e^{i\omega\tau} \tag{A-31}$$

and

$$\Psi_s(x,z;t) = - \frac{a_\infty\bar{q}}{2\pi} \int_{-\infty}^{\tau_o} \frac{e^{i\omega\tau}\ d\tau}{\sqrt{a_\infty^2(t-\tau)^2 - [x - U(t-\tau)]^2 - z^2}} \tag{A-32}$$

In order to simplify the above integral let

$$\nu = \frac{a_\infty\beta^2(t-\tau) + Mx}{\sqrt{x^2 + \beta^2 z^2}} \tag{A-33}$$

Equation (A-32) then becomes

$$\Psi_s(x,z;t) = -\frac{\bar{q}}{2\pi\beta}\, e^{i\omega\,[t + (M^2 x/\beta^2 U)]} \int_1^\infty \frac{e^{-i\zeta\nu}}{\sqrt{\nu^2 - 1}}\, d\nu$$

$$\zeta = \frac{\omega M}{U\,\beta^2}\sqrt{x^2 + \beta^2\, z^2} \qquad\qquad (A\text{-}34)$$

But the integral in Equation (A-34) is a known representation of the Hankel function $H_o^{(2)}(\zeta)$, i.e.

$$\int_1^\infty \frac{e^{-i\zeta\nu}}{\sqrt{\nu^2 - 1}}\, d\nu = -\frac{i\pi}{2}\, H_o^{(2)}(\zeta) \qquad\qquad (A\text{-}35)$$

so that Equation (A-34) becomes

$$\Psi_s(x,z;t) = \frac{i\bar{q}}{4\beta}\, e^{i\omega\,[t + (M^2 x/\beta^2 U)]}\, H_o^{(2)}\!\left(\frac{\omega M}{U\beta^2}\sqrt{x^2 + \beta^2\, z^2}\right) \qquad (A\text{-}36)$$

The transformation to a doublet is now made as before by placing a sink above the x-axis, a source below the x-axis and letting the distance between the two approach zero while holding the resultant strength constant. The acceleration potential for the pulsating doublet

is thus given by

$$\Psi_D(x,z;t) = \lim_{\epsilon \to 0} \left[\Psi_{sink}(x,z - \tfrac{\epsilon}{2};t) + \Psi_{source}(x,z + \tfrac{\epsilon}{2}; t) \right]$$

$$\Psi_D(x,z;t) = \lim_{\epsilon \to 0} \left(\epsilon \bar{q} \right) \frac{\bar{\Psi}_s(x,z + \tfrac{\epsilon}{2}; t) - \bar{\Psi}_s(x,z - \tfrac{\epsilon}{2}; t)}{\epsilon}$$

$$\Biggr\} \quad (A\text{-}37)$$

where

$$\bar{\Psi}_s(x,z;t) = \frac{i}{4\beta} e^{i\omega \left(t + \frac{M^2}{\beta^2} \frac{x}{U} \right)} H_o^{(2)} \left(\frac{\omega M}{U\beta^2} \sqrt{x^2 + \beta^2 z^2} \right) \qquad (A\text{-}38)$$

Letting $U\mu_D$ represent the magnitude of the doublet strength the acceleration potential for a pulsating doublet at the origin of a two-dimensional flow field is given by

$$\Psi_D(x,z;t) = U\mu_D \frac{\partial \bar{\Psi}_s}{\partial z} \qquad (A\text{-}39)$$

The transformation to a doublet located at the general point (ξ,ζ) is then made as before to give

$$\Psi_D(x,z;t) = U\mu_D \frac{\partial}{\partial z} \left\{ \frac{i}{4\beta} e^{i\omega \left[t + \frac{M}{\beta^2} \frac{(x-\xi)}{U} \right]} H_o^{(2)} \left(\frac{\omega M}{U\beta^2} \sqrt{(x-\xi)^2 + \beta^2 (z-\zeta)^2} \right) \right\}$$

$$(A\text{-}40)$$

The acceleration potential has thus been developed for a harmonically pulsating doublet in both a three-dimensional and a two-dimensional uniform compressible stream. These basic solutions of the linearized acceleration potential equation provide the starting point for many unsteady compressible flow analyses.

APPENDIX B

RELATIONSHIP BETWEEN THE DOUBLET DISTRIBUTION
AND THE PRESSURE DISTRIBUTION

In this appendix the relationship between the strength of the pulsating doublet distributions on the reference airfoil and the "wake airfoils" shown in Figure 3 and the pressure distribution on the reference airfoil is developed. This relationship is desirable since it is ultimately the pressure distribution on the reference airfoil which is used to determine the lift and moment on the airfoil.

Introducing the quantities defined by Equation (8) the acceleration potential may be written as

$$\Psi(x,z;t) = \frac{iU}{4\beta} e^{i\omega t} \left\{ \int_{-b}^{b} \mu_D(\xi) e^{ikM^2(x-\xi)/\beta^2 b} \right. \tag{B-1}$$

$$\cdot \frac{\partial}{\partial z} H_0^{(2)} \left(\frac{kM}{\beta^2} \sqrt{\left(\frac{x-\xi}{b}\right)^2 + \beta^2 \left(\frac{z}{b}\right)^2} \right) d\xi$$

$$+ \sum_{n=o}^{\infty} \sum_{q=1}^{Q-1} e^{i\Psi_q + i[2\pi m M^2(nQ + q)/\beta^2 Q]} \int_{-b}^{b} \mu_D(\xi) e^{ikM^2(x-\xi)/\beta^2 b}$$

$$\cdot \frac{\partial}{\partial z} H_o^{(2)} \left(\frac{M}{\beta^2} \sqrt{\left[\frac{k(x-\xi)}{b} + \frac{2\pi m}{Q}(nQ+q) \right]^2 + \beta^2 \left[\frac{kz}{b} + (nQ+q) kh \right]^2} \; \right) d\xi$$

$$+ \sum_{n=1}^{\infty} e^{i2n\pi m M^2/\beta^2} \int_{-b}^{b} \mu_D(\xi) \; e^{ikM^2(x-\xi)/\beta^2 b}$$

$$\cdot \frac{\partial}{\partial z} H_o^{(2)} \left(\frac{M}{\beta^2} \sqrt{\left[\frac{k(x-\xi)}{b} + 2n\pi m \right]^2 + \beta^2 \left[\frac{kz}{b} + nQkh \right]^2} \; \right) d\xi \Bigg\}$$

Let

$$w' = \frac{kM}{\beta^2} \sqrt{\left(\frac{x-\xi}{b} \right)^2 + \beta^2 \left(\frac{z}{b} \right)^2} \qquad (B-2)$$

then

$$\frac{\partial H_o^{(2)}(w')}{\partial z} = \frac{d H_o^{(2)}(w')}{dw'} \; \frac{\partial w'}{\partial z} \qquad (B-3)$$

The Hankel function satisfies a recurrence relation given by Lebedev [34] as

$$\frac{d}{dz} H_\nu^{(p)}(z) - \frac{\nu}{z} H_\nu^{(p)}(z) = - H_{\nu+1}^{(p)}(z) \qquad (B-4)$$

so that finally

$$\frac{\partial H_o^{(2)}(w')}{\partial z} = - \frac{\omega^2 M^2}{U^2 \beta^2} \frac{z}{w'} H_1^{(2)}(w') \tag{B-5}$$

Similarily by letting

$$w'' = \frac{M}{\beta^2} \sqrt{\left[\frac{k(x-\xi)}{b} + \frac{2\pi m}{Q}(nQ + q)\right]^2 + \beta^2 \left[\frac{kz}{b} + (nQ + q)\, kh\right]^2}$$

$$w''' = \frac{M}{\beta^2} \sqrt{\left[\frac{k(x-\xi)}{b} + 2n\pi m\right]^2 + \beta^2 \left[\frac{kz}{b} + nQkh\right]^2}$$
$$\left.\right\} \tag{B-6}$$

the other partial derivatives appearing in Equation (B-1) may be evaluated as

$$\frac{\partial H_o^{(2)}(w'')}{\partial z} = - \frac{\omega M^2}{U\beta^2} \frac{\left[\frac{kz}{b} + (nQ + q)kh\right]}{w''} H_1^{(2)}(w'')$$

$$\frac{\partial H_o^{(2)}(w''')}{\partial z} = - \frac{\omega M^2}{U\beta^2} \frac{\left[\frac{kz}{b} + nQkh\right]}{w'''} H_1^{(2)}(w''')$$
$$\left.\right\} \tag{B-7}$$

Using these results the total acceleration potential becomes

$$
\Psi(x,z;t) = \frac{iU}{4\beta}\, e^{i\omega t} \left\{ -\frac{\omega^2 M^2}{U^2 \beta^2}\, z \int_{-b}^{b} \mu_D(\xi)\, e^{ikM^2(x-\xi)/\beta^2 b}\, \frac{H_1^{(2)}(w')}{w'}\, d\xi \right. \tag{B-8}
$$

$$
-\frac{\omega M^2}{U\beta^2} \sum_{n=o}^{\infty} \sum_{q=1}^{Q-1} e^{i\Psi_q + i[2\pi m M^2(nQ + q)/\beta^2 Q]} \left[\frac{kz}{b} + (nQ + q)\, kh \right]
$$

$$
\cdot \int_{-b}^{b} \mu_D(\xi)\, e^{ikM^2(x-\xi)/\beta^2 b}\, \frac{H_1^{(2)}(w'')}{w''}\, d\xi
$$

$$
-\frac{\omega M^2}{U\beta^2} \sum_{n=1}^{\infty} e^{i2n\pi m M^2/\beta^2} \left[\frac{kz}{b} + nQkh \right]
$$

$$
\left. \cdot \int_{-b}^{b} \mu_D(\xi)\, e^{ikM^2(x-\xi)/\beta^2 b}\, \frac{H_1^{(2)}(w''')}{w'''}\, d\xi \right\}
$$

Now as z approaches zero from either the upper half plane or the lower half plane the integrands of the second and third terms are well behaved and these terms remain finite. The first term, however, approaches zero except at the point $\xi=x$ where the integrand becomes infinite. This condition will now be investigated in detail. Let

$$I = z \int_{-b}^{b} \mu_D(\xi) \, e^{ikM^2(x-\xi)/\beta^2 b} \, \frac{H_1^{(2)}(w')}{w'} \, d\xi \qquad (B-9)$$

When z is allowed to approach zero isolate the point $\xi = x$ with a strip of length 2ϵ sufficiently small so that the continuous functions $\mu_D(\xi)$ and $e^{ikM^2(x-\xi)/\beta^2 b}$ can be replaced by their values at the center of the interval, i.e.

$$\lim_{z \to 0} I = \lim_{z \to 0} \left\{ z \int_{-b}^{x-\epsilon} \mu_D(\xi) \, e^{ikM^2(x-\xi)/\beta^2 b} \, \frac{H_1^{(2)}(w')}{w'} \, d\xi \right. \qquad (B-10)$$

$$+ z \, \mu_D(x) \int_{x-\epsilon}^{x+\epsilon} \frac{H_1^{(2)}(w')}{w'} \, d\xi$$

$$\left. + z \int_{x+\epsilon}^{b} \mu_D(\xi) \, e^{ikM^2(x-\xi)/\beta^2 b} \, \frac{H_1^{(2)}(w')}{w'} \, d\xi \right\}$$

The limit of the first and third term of Equation (B-10) is zero and the value of w' in the second term is very small throughout the integration range so that the Hankel function can be replaced by its asymptotic representation given by Lebedev [34] as

$$H_1^{(2)}(w') \cong \frac{2i}{\pi w'} \quad \text{when} \quad w' \to 0 \qquad (B-11)$$

When z is allowed to approach zero from the upper half plane let

$$
\left.
\begin{aligned}
I_U &= \lim_{z \to 0^+} I \\[2mm]
I_U &= \mu_D(x) \lim_{z \to 0^+} \left\{ z \int_{x-\epsilon}^{x+\epsilon} \frac{H_1^{(2)}(w')}{w'} \, d\xi \right\}
\end{aligned}
\right\}
\qquad \text{(B-12)}
$$

Substituting the asymptotic representation of the Hankel function

$$
I_U = \mu_D(x) \lim_{z \to 0^+} \left\{ \frac{2iz}{\pi} \int_{x-\epsilon}^{x+\epsilon} \frac{d\xi}{\dfrac{k^2 M^2}{\beta^4} \left[\left(\dfrac{x-\xi}{b}\right)^2 + \beta^2 \left(\dfrac{z}{b}\right)^2 \right]} \right\} \qquad \text{(B-13)}
$$

This integral can be evaluated to give

$$
I_U = \frac{2i\beta^3 b^2}{\pi k^2 M^2} \mu_D(x) \lim_{z \to 0^+} \left\{ \tan^{-1}\left(\frac{\epsilon}{\beta z}\right) - \tan^{-1}\left(\frac{-\epsilon}{\beta z}\right) \right\} \qquad \text{(B-14)}
$$

or

$$
I_U = \frac{2i\beta^3 b^2}{k^2 M^2} \mu_D(x) \qquad \text{(B-15)}
$$

Similarily when z is allowed to approach zero from the lower half plane let

$$I_L = \lim_{z \to 0^-} I \tag{B-16}$$

then

$$I_L = \frac{2i\beta^3 b^2}{\pi k M^2} \mu_D(x) \lim_{z \to 0^-} \left\{ \tan^{-1}\left(\frac{\epsilon}{\beta z}\right) - \tan^{-1}\left(\frac{-\epsilon}{\beta z}\right) \right\} \tag{B-17}$$

and

$$I_L = - \frac{2i\beta^3 b^2}{k^2 M^2} \mu_D(x) \tag{B-18}$$

The acceleration potential, $\Psi(x,0^+;t)$, on the upper surface of the reference airfoil may now be written as

$$\Psi(x,0^+;t) = \frac{iU}{4\beta} e^{i\omega t} \left\{ - \frac{\omega^2 M^2}{U^2 \beta^2} \left[\frac{2i\beta^3 b^2}{k^2 M^2} \right] \mu_D(x) \right. \tag{B-19}$$

$$- \frac{\omega M^2}{U\beta^2} \sum_{n=0}^{\infty} \sum_{q=1}^{Q-1} e^{i\Psi_q + i[2\pi m M^2(nQ+q)/\beta^2 Q]} \left[\left(nQ + q \right) kh \right]$$

$$
\cdot \int_{-b}^{b} \mu_D(\xi) \; e^{ikM^2(x-\xi)/\beta^2 b} \; \frac{H_1^{(2)}(\bar{w}'')}{\bar{w}''} \; d\xi
$$

$$
- \frac{\omega M^2}{U\beta^2} \sum_{n=1}^{\infty} e^{i2n\pi mM^2/\beta^2} (nQkh) \int_{-b}^{b} \mu_D(\xi) \; e^{ikM^2(x-\xi)/\beta^2 b} \frac{H_1^{(2)}(\bar{w}''')}{\bar{w}'''} \; d\xi \; \Big\}
$$

where

$$
\left.
\begin{aligned}
\bar{w}'' &= \lim_{z \to o} w'' = \frac{M}{\beta^2} \sqrt{\left[\frac{k(x-\xi)}{b} + \frac{2\pi m}{Q}(nQ + q)\right]^2 + \beta^2\left[(nQ + q) \, kh\right]^2} \\[2em]
\bar{w}''' &= \lim_{z \to o} w''' = \frac{M}{\beta^2} \sqrt{\left[\frac{k(x-\xi)}{b} + 2n\pi m\right]^2 + \beta^2\left(nQkh\right)^2}
\end{aligned}
\right\} \quad \text{(B-20)}
$$

Similarily the acceleration potential, $\Psi(x,0^-;t)$, on the lower surface of the reference airfoil is given by

$$
\Psi(x,0^-;t) = \frac{iU}{4\beta} e^{i\omega t} \left\{ - \frac{\omega^2 M^2}{U^2\beta^2} \left[- \frac{2i\beta^3 b^2}{k^2 M^2} \right] \mu_D(x) \right. \qquad \text{(B-21)}
$$

$$
- \frac{\omega M^2}{U\beta^2} \sum_{n=o}^{\infty} \sum_{q=1}^{Q-1} e^{i\Psi_q + i[2\pi mM^2(nQ+q)/\beta^2 Q]} \left[\left(nQ + q\right)kh\right]
$$

$$\cdot \int_{-b}^{b} \mu_D(\xi)\ e^{ikM^2(x-\xi)/\beta^2 b}\ \frac{H_1^{(2)}(\bar{w}'')}{\bar{w}''}\ d\xi$$

$$-\frac{\omega M^2}{U\beta^2} \sum_{n=1}^{\infty} e^{i2n\pi mM^2/\beta^2}\ (nQkh) \int_{-b}^{b} \mu_D(\xi)\ e^{ikM^2(x-\xi)/\beta^2 b}\ \frac{H_1^{(2)}(\bar{w}''')}{\bar{w}'''}\ d\xi \ \Bigg\}$$

The pressure on the reference airfoil is finally obtained by using the relation between pressure and the acceleration potential, Equation (3). For the upper surface of the reference airfoil

$$p_U(x;t) - p_\infty = -\rho_\infty \Psi(x,0^+;t) \qquad (\text{B-22})$$

and for the lower surface

$$p_L(x;t) - p_\infty = -\rho_\infty \Psi(x,0^-;t) \qquad (\text{B-23})$$

The pressure differential across the reference airfoil will be denoted by

$$\left. \begin{aligned} \Delta p_a(x;t) &= p_U(x;t) - p_L(x;t) \\[2mm] \Delta p_a(x;t) &= -\rho_\infty \left[\Psi(x,0^+;t) - \Psi(x,0^-;t) \right] \end{aligned} \right\} \qquad (\text{B-24})$$

Substituting the acceleration potential expressions

$$\Delta p_a(x;t) = - \rho_\infty \left[\frac{iU}{4\beta} e^{i\omega t} \left(- \frac{\omega^2 M^2}{U^2 \beta^2} \right) \left(\frac{2i\beta^3 b^2}{k^2 M^2} \right) \mu_D(x) \right.$$

$$\left. - \frac{iU}{4\beta} e^{i\omega t} \left(- \frac{\omega^2 M^2}{U^2 \beta^2} \right) \left(- \frac{2i\beta^3 b^2}{k^2 M^2} \right) \mu_D(x) \right]$$

(B-25)

Then collecting terms

$$\Delta p_a(x;t) = - \rho_\infty U \mu_D(x) e^{i\omega t}$$

(B-26)

Since the pressure oscillates simple harmonically

$$\Delta p_a(x;t) = \Delta \bar{p}_a(x) e^{i\omega t}$$

(B-27)

then

$$\Delta \bar{p}_a(x) = - \rho_\infty U \mu_D(x)$$

(B-28)

or

$$\mu_D(x) = - \frac{\Delta \bar{p}_a(x)}{\rho_\infty U}$$

(B-29)

The relationship is thus established between the strength of the pulsating doublet distributions on the reference airfoil and the "wake airfoils" of Figure 3 and the pressure differential across the reference airfoil.

APPENDIX C

EVALUATION OF THE INTEGRAL LEADING TO THE KERNEL
OF THE DOWNWASH INTEGRAL EQUATION

The three interior integrals of Equation (18) may be evaluated
to produce the kernel of the downwash integral equation, Equation (22).
A generalized integral which encompasses all three of these integrals
will be evaluated in this appendix.

Consider the integral

$$
I_g = \int_{-\infty}^{x} e^{ik(\xi'-\xi)/\beta^2 b} \frac{\partial^2}{\partial z^2} H_o^{(2)} \left(\frac{M}{\beta^2} \sqrt{\left[\frac{k(\xi'-\xi)}{b} + A \right]^2 + \beta^2 \left[\frac{kz}{b} + B \right]^2} \right) d\xi
$$

$$(C-1)$$

where A and B are constants with respect to the integration. A
critical step in the evaluation of this integral is the use of a
partial differential equation which has been used by other investigators
(see e.g. References [15,36]) to determine the airloads on a two-
dimensional fixed-wing airfoil oscillating in a compressible medium.
This equation is derived in Appendix D where it is shown that

$$
\beta^2 \frac{\partial^2 H_o^{(2)}(\zeta)}{\partial \bar{\xi}^2} + \frac{\partial^2 H_o^{(2)}(\zeta)}{\partial \bar{z}^2} + \frac{\omega^2}{\beta^2 a_\infty^2} H_o^{(2)}(\zeta) = 0 \qquad (C-2)
$$

and

$$\zeta = \frac{M}{\beta^2}\sqrt{\left[\frac{k(\bar{\xi}-\xi)}{b}\right]^2 + \beta^2\left[\frac{k\bar{z}}{b}\right]^2}$$

Change variables in Equation (C-1) by letting

$$\left.\begin{aligned}\frac{k(\bar{\xi}-\xi)}{b} &= \frac{k(\xi'-\xi)}{b} + A\\[2em]\frac{k\bar{z}}{b} &= \frac{kz}{b} + B\end{aligned}\right\} \quad\text{(C-3)}$$

Equation (C-1) then becomes

$$I_g = e^{-iA/\beta^2}\int_{-\infty}^{x+(bA/k)} e^{ik(\bar{\xi}-\xi)/\beta^2 b}\ \frac{\partial^2}{\partial\bar{z}^2}H_o^{(2)}\left(\frac{M}{\beta^2}\sqrt{\left[\frac{k(\bar{\xi}-\xi)}{b}\right]^2 + \beta^2\left[\frac{k\bar{z}}{b}\right]^2}\right)d\bar{\xi}$$

$$\text{(C-4)}$$

The differential Equation (C-2) may now be substituted to yield

$$I_g = -e^{-iA/\beta^2}\left\{\beta^2\int_{-\infty}^{x+(bA/k)} e^{ik(\bar{\xi}-\xi)/\beta^2 b}\ \frac{\partial^2 H_o^{(2)}(\zeta)}{\partial\bar{\xi}^2}\,d\bar{\xi}\right. \quad\text{(C-5)}$$

$$\left.+ \frac{\omega^2}{\beta^2 a_\infty^2}\int_{-\infty}^{x+(bA/k)} e^{ik(\bar{\xi}-\xi)/\beta^2 b}\ H_o^{(2)}(\zeta)\,d\bar{\xi}\right\}$$

Letting

$$\xi_o = \bar{\xi} - \xi \tag{C-6}$$

the equation becomes

$$I_g = - e^{-iA/\beta^2} \left\{ \beta^2 \int_{-\infty}^{(x-\xi) + (bA/k)} e^{ik\xi_o/\beta^2 b} \frac{\partial^2 H_o^{(2)}(\bar{\zeta})}{d\xi_o^2} d\xi_o \right.$$

$$\left. + \frac{\omega^2}{\beta^2 a^2} \int_{-\infty}^{(x-\xi) + (bA/k)} e^{ik\xi_o/\beta^2 b} H_o^{(2)}(\bar{\zeta}) d\xi_o \right\} \tag{C-7}$$

where

$$\bar{\zeta} = \frac{M}{\beta^2} \sqrt{\left[\frac{k\xi_o}{b}\right]^2 + \beta^2 \left[\frac{k\bar{z}}{b}\right]^2}$$

A pair of integrations by parts on the first integral of Equation (C-7) yields the result that

$$I_g = - e^{-iA/\beta^2} \left\{ \beta^2 \left[e^{ik\xi_o/\beta^2 b} \frac{\partial H_o^{(2)}(\bar{\zeta})}{\partial \xi_o} \right. \right. \tag{C-8}$$

$$-\frac{ik}{\beta^2 b} e^{ik\xi_0/\beta^2 b} \left. H_0^{(2)}(\bar{\zeta}) \right]_{\xi_0 = -\infty}^{\xi_0 = (x-\xi) + (bA/k)}$$

$$-\frac{\omega^2}{U^2} \int_{-\infty}^{(x-\xi) + (bA/k)} e^{ik\xi_0/\beta^2 b} H_0^{(2)}(\bar{\zeta}) \, d\xi_0 \Big\}$$

The limits of the first term in Equation (C-8) can be evaluated using the properties of Hankel functions given by Lebedev [34] so that

$$I_g = \frac{kM}{\beta^2} \left\{ \left[\frac{k(x-\xi)}{b} + A \right] \Big/ \sqrt{\left[\frac{k(x-\xi)}{b} + A \right]^2 + \beta^2 \left[\frac{k\bar{z}}{b} \right]^2} \right\} \qquad (C-9)$$

$$\cdot\, e^{ik(x-\xi)/\beta^2 b} \; H_1^{(2)} \left(\frac{M}{\beta^2} \sqrt{\left[\frac{k(x-\xi)}{b} + A \right]^2 + \beta^2 \left(\frac{k\bar{z}}{b} \right)^2} \right)$$

$$+\frac{ik}{b} e^{ik(x-\xi)/\beta^2 b} \; H_0^{(2)} \left(\frac{M}{\beta^2} \sqrt{\left[\frac{k(x-\xi)}{b} + A \right]^2 + \beta^2 \left[\frac{k\bar{z}}{b} \right]^2} \right)$$

$$+\frac{\omega^2}{U^2} e^{-iA/\beta^2} \int_{-\infty}^{(x-\xi) + (bA/k)} e^{ik\xi_0/\beta^2 b} \; H_0^{(2)} \left(\frac{M}{\beta^2} \sqrt{\left[\frac{k\xi_0}{b} \right]^2 + \beta^2 \left[\frac{k\bar{z}}{b} \right]^2} \right) d\xi_0$$

The final desired result is obtained by returning to the original variables and letting

$$\eta = \frac{k}{b}\, \xi_o$$

in the integral of Equation (C-9). Thus

$$I_g = \frac{\omega M}{U} \left\{ \left[\frac{k(x-\xi)}{b} + A \right] \bigg/ \sqrt{\left[\frac{k(x-\xi)}{b} + A \right]^2 + \beta^2 \left[\frac{kz}{b} + B \right]^2} \right\} \quad (C\text{-}10)$$

$$\cdot\, e^{\,ik(x-\xi)/\beta^2 b}\; H_1^{(2)} \left(\frac{M}{\beta^2} \sqrt{\left[\frac{k(x-\xi)}{b} + A \right]^2 + \beta^2 \left[\frac{kz}{b} + B \right]^2} \right)$$

$$+\, \frac{i\omega}{U}\, e^{\,ik(x-\xi)/\beta^2 b}\; H_0^{(2)} \left(\frac{M}{\beta^2} \sqrt{\left[\frac{k(x-\xi)}{b} + A \right]^2 + \beta^2 \left[\frac{kz}{b} + B \right]^2} \right)$$

$$+\, \frac{\omega}{U}\, e^{\,-iA/\beta^2} \int_{-\infty}^{[k(x-\xi)/b]\,+\,A} e^{\,i\eta/\beta^2}\, H_0^{(2)} \left(\frac{M}{\beta^2} \sqrt{\eta^2 + \beta^2 \left[\frac{kz}{b} + B \right]^2} \right) d\eta$$

APPENDIX D

DEVELOPMENT OF A USEFUL PARTIAL DIFFERENTIAL EQUATION

In this appendix a partial differential equation is developed which proves useful in reducing the kernel of the downwash integral equation for two-dimensional airfoils oscillating in a compressible stream. The equation was first used by investigators (see e.g. References [15,36]) considering oscillating fixed wing type airfoils, but as shown in Appendix C the equation is equally useful when considering oscillating rotary wing airfoils.

The governing linearized equation for the acceleration potential in two-dimensional, unsteady, compressible flow may be written as

$$\frac{1}{a_\infty^2} \frac{\partial^2 \psi}{\partial t^2} + \frac{2M}{a_\infty} \frac{\partial^2 \psi}{\partial x \partial t} - \beta^2 \frac{\partial^2 \psi}{\partial x^2} = \frac{\partial^2 \psi}{\partial z^2} \tag{D-1}$$

If the transformation

$$\left. \begin{aligned} \tau &= t + \frac{M}{\beta^2 a_\infty} x \\[2mm] \zeta &= \frac{x}{\beta^2 a_\infty} \\[2mm] \eta &= \frac{z}{\beta \, a_\infty} \end{aligned} \right\} \tag{D-2}$$

is made Equation (D-2) becomes

$$\frac{\partial^2 \Psi}{\partial \tau^2} - \frac{\partial^2 \Psi}{\partial \zeta^2} = \frac{\partial^2 \Psi}{\partial \eta^2} \qquad \text{(D-3)}$$

Now introduce the polar coordinates

$$\left.\begin{array}{l} \zeta = \bar{r} \cos \theta \\[2ex] \eta = \bar{r} \sin \theta \\[2ex] \bar{r} = \sqrt{\zeta^2 + \eta^2} = \dfrac{1}{\beta^2 a_\infty} \sqrt{x^2 + \beta^2 z^2} \\[2ex] \theta = \tan^{-1}\left(\dfrac{\eta}{\zeta}\right) = \tan^{-1}\left(\dfrac{\beta z}{x}\right) \end{array}\right\} \qquad \text{(D-4)}$$

Equation (D-3) then becomes

$$\frac{\partial^2 \Psi}{\partial \tau^2} = \frac{\partial^2 \Psi}{\partial \bar{r}^2} + \frac{1}{\bar{r}^2} \frac{\partial^2 \Psi}{\partial \theta^2} + \frac{1}{\bar{r}} \frac{\partial \Psi}{\partial \bar{r}} \qquad \text{(D-5)}$$

Assuming a solution of the form

$$\Psi(\bar{r}, \theta, \tau) = e^{i\omega\tau} e^{in\theta} R(\bar{r}) \qquad \text{(D-6)}$$

and substituting in Equation (D-5) it is found that $R(\bar{r})$ satisfies the equation

$$\frac{d^2R}{dr^2} + \frac{1}{r}\frac{dR}{dr} + \left(\omega^2 - \frac{n^2}{r^2}\right)R = 0 \qquad (D\text{-}7)$$

which is Bessel's differential equation of order n. Taking the Hankel functions of the first and second kinds and order n $\left(H_n^{(1)}(\omega\bar{r})\text{ and } H_n^{(2)}(\omega\bar{r})\text{ respectively}\right)$ as the fundamental solutions of Equation (D-7), the general solution of Equation (D-5) becomes

$$\Psi(\bar{r},\theta,\tau) = e^{i\omega\tau}\sum_{n=o}^{\infty} e^{in\theta}\left[A_n H_n^{(1)}(\omega\bar{r}) + B_n H_n^{(2)}(\omega\bar{r})\right] \qquad (D\text{-}8)$$

Thus a particular solution of Equation (D-5) would be

$$\Psi_o(\bar{r},\theta,\tau) = H_o^{(2)}(\omega\bar{r})\,e^{i\omega\tau} \qquad (D\text{-}9)$$

But this is also a particular solution of Equation (D-3) so that

$$\frac{\partial^2}{\partial\tau^2}\left[H_o^{(2)}(\omega\bar{r})\,e^{i\omega\tau}\right] = \frac{\partial^2}{\partial\zeta^2}\left[H_o^{(2)}(\omega\bar{r})\,e^{i\omega\tau}\right] + \frac{\partial^2}{\partial\eta^2}\left[H_o^{(2)}(\omega\bar{r})\,e^{i\omega\tau}\right] \qquad (D\text{-}10)$$

or

$$-\omega^2 H_o^{(2)}(\omega\bar{r}) = \frac{\partial^2}{\partial\zeta^2}\left[H_o^{(2)}(\omega\bar{r})\right] + \frac{\partial^2}{\partial\eta^2}\left[H_o^{(2)}(\omega\bar{r})\right] \qquad (D\text{-}11)$$

Returning to the original coordinates

$$\beta^2 \frac{\partial^2}{\partial x^2} H_o^{(2)} \left(\frac{\omega}{\beta^2 a_\infty} \sqrt{x^2 + \beta^2 z^2} \right) + \frac{\partial^2}{\partial z^2} H_o^{(2)} \left(\frac{\omega}{\beta^2 a_\infty} \sqrt{x^2 + \beta^2 z^2} \right)$$

$$\text{(D-12)}$$

$$+ \frac{\omega}{\beta^2 a_\infty^2} H_o^{(2)} \left(\frac{\omega}{\beta^2 a_\infty} \sqrt{x^2 + \beta^2 z^2} \right) = 0$$

Introducing the reduced frequency parameter

$$k = \frac{b\omega}{U}$$

Equation (D-12) becomes

$$\beta^2 \frac{\partial^2}{\partial x^2} H_o^{(2)} \left(\frac{kM}{\beta^2} \sqrt{\left(\frac{x}{b}\right)^2 + \beta^2 \left(\frac{z}{b}\right)^2} \right) + \frac{\partial^2}{\partial z^2} H_o^{(2)} \left(\frac{kM}{\beta^2} \sqrt{\left(\frac{x}{b}\right)^2 + \beta^2 \left(\frac{z}{b}\right)^2} \right)$$

$$\text{(D-13)}$$

$$+ \frac{\omega^2}{\beta^2 a_\infty^2} H_o^{(2)} \left(\frac{kM}{\beta^2} \sqrt{\left(\frac{x}{b}\right)^2 + \beta^2 \left(\frac{z}{b}\right)^2} \right) = 0$$

If the change of variables

$$\bar{\xi} = x + \xi \qquad \text{(D-14)}$$

is made and ξ is considered to be constant then Equation (D-14) becomes

$$\beta^2 \; \frac{\partial^2}{\partial \bar{\xi}^2} \; H_o^{(2)} \left(\frac{kM}{\beta^2} \sqrt{\left(\frac{\bar{\xi}-\xi}{b}\right)^2 + \beta^2 \left(\frac{z}{b}\right)^2} \right) \tag{D-15}$$

$$+ \frac{\partial^2}{\partial z^2} H_o^{(2)} \left(\frac{kM}{\beta^2} \sqrt{\left(\frac{\bar{\xi}-\xi}{b}\right)^2 + \beta^2 \left(\frac{z}{b}\right)^2} \right)$$

$$+ \frac{\omega^2}{\beta^2 a_\infty^2} H_o^{(2)} \left(\frac{kM}{\beta^2} \sqrt{\left(\frac{\bar{\xi}-\xi}{b}\right)^2 + \beta^2 \left(\frac{z}{b}\right)^2} \right) = 0$$

which is the desired result.

APPENDIX E

ANALYTICAL COMPARISON WITH THE RESULTS OF JONES AND RAO

Since Jones and Rao [24] have presented an analysis of essentially the same aerodynamic problem considered in the present research but incorporating a different mathematical model and approach to the problem, it is desirable to make a comparison of their downwash equation and Equation (18). This comparison is made in the present appendix by manipulating Equation (18) and reducing it to such a form that it can be readily identified with the downwash equation given in Reference [24].

In the inner integrals of Equation (18) make the change of variables

$$\xi_o = x - \xi' + \xi \qquad (E\text{-}1)$$

and then reverse the order of integration. The downwash then becomes

$$\bar{w}(x,z) = - \frac{ie^{-ikx/b}}{4\rho_\infty U\beta} \left[\int_{-b}^{b} e^{ik(x-\xi_o)/\beta^2 b} \frac{\partial^2}{\partial z^2} H_o^{(2)}\left(\frac{kM}{\beta^2}\sqrt{\left(\frac{x-\xi_o}{b}\right)^2 + \beta^2\left(\frac{z}{b}\right)^2}\right) \right.$$

$$\left. \cdot \int_{-b}^{\xi_o} \Delta\bar{p}_a(\xi) e^{ik\xi/b} \, d\xi \, d\xi_o \right.$$

$$(E\text{-}2)$$

$$+ \int_b^\infty e^{ik(x-\xi_o)/\beta^2 b} \frac{\partial^2}{\partial z^2} H_o^{(2)} \left(\frac{kM}{\beta^2} \sqrt{\left(\frac{x-\xi_o}{b}\right)^2 + \beta^2 \left(\frac{z}{b}\right)^2} \right)$$

$$\cdot \int_{-b}^b \Delta \bar{p}_a(\xi) \, e^{ik\xi/b} \, d\xi \, d\xi_o$$

$$+ \sum_{n=o}^\infty \sum_{q=1}^{Q-1} e^{i\Psi_q + i[2\pi m M^2 (nQ+q)/\beta^2 Q]} \left\{ \int_{-b}^b e^{ik(x-\xi_o)/\beta^2 b} \right.$$

$$\cdot \frac{\partial^2}{\partial z^2} H_o^{(2)} \left(\frac{M}{\beta^2} \sqrt{\left[\frac{k(x-\xi_o)}{b} + \frac{2\pi m}{Q}(nQ+q)\right]^2 + \beta^2 \left[\frac{kz}{b} + (nQ+q)\, kh\right]^2} \right)$$

$$\cdot \int_{-b}^{\xi_o} \Delta \bar{p}_a(\xi) \, e^{ik\xi/b} \, d\xi \, d\xi_o$$

$$+ \int_b^\infty e^{ik(x-\xi_o)/b} \frac{\partial^2}{\partial z^2} H_o^{(2)} \left(\frac{M}{\beta^2} \sqrt{\left[\frac{k(x-\xi_o)}{b} + \frac{2\pi m}{Q}(nQ+q)\right]^2 + \beta^2 \left[\frac{kz}{b} + (nQ+q)kh\right]^2} \right)$$

$$\left. \cdot \int_{-b}^b \Delta \bar{p}_a(\xi) \, e^{ik\xi/b} \, d\xi \, d\xi_o \right\}$$

$$+ \sum_{n=1}^{\infty} e^{i2n\pi m M^2/\beta^2} \left\{ \int_{-b}^{b} e^{ik(x-\xi_0)/\beta^2 b} \right.$$

$$\cdot \frac{\partial^2}{\partial z^2} H_o^{(2)} \left(\frac{M}{\beta^2} \sqrt{\left[\frac{k(x-\xi_0)}{b} + 2n\pi m \right]^2 + \beta^2 \left[\frac{kz}{b} + nQkh \right]^2 } \right)$$

$$\cdot \int_{-b}^{\xi_0} \Delta \bar{p}_a(\xi) e^{ik\xi/b} \, d\xi \, d\xi_0$$

$$+ \int_{b}^{\infty} e^{ik(x-\xi_0)/\beta^2 b} \frac{\partial^2}{\partial z^2} H_o^{(2)} \left(\frac{M}{\beta^2} \sqrt{\left[\frac{k(x-\xi_0)}{b} + 2n\pi m \right]^2 + \beta^2 \left[\frac{kz}{b} + nQkh \right]^2 } \right)$$

$$\left. \cdot \int_{-b}^{b} \Delta \bar{p}_a(\xi) e^{ik\xi/b} \, d\xi \, d\xi_0 \right\} \Bigg]$$

Now Jones and Rao introduce a distribution function $K(x)$ which is related to $\Delta \bar{p}_a(x)$ as shown below

$$K(x) = \begin{cases} - \dfrac{1}{\rho_\infty U b} e^{-ikx/\beta^2 b} \displaystyle\int_{-b}^{x} \Delta \bar{p}_a(\xi) e^{ik\xi/b} \, d\xi & \text{for } x \le b \\[2em] - \dfrac{1}{\rho_\infty U b} e^{-ikx/\beta^2 b} \displaystyle\int_{-b}^{b} \Delta \bar{p}_a(\xi) e^{ik\xi/b} \, d\xi & \text{for } x > b \end{cases} \qquad (E\text{-}3)$$

Using this distribution function the downwash equation becomes

$$\bar{w}(x,z) = \frac{ib}{4\beta} \, e^{ikM^2 x/\beta^2 b} \left\{ \int_{-b}^{\infty} K(\xi_o) \right. \tag{E-4}$$

$$\cdot \frac{\partial^2}{\partial z^2} H_o^{(2)}\!\left(\frac{kM}{\beta^2} \sqrt{\left(\frac{x - \xi_o}{b}\right)^2 + \beta^2 \left(\frac{z}{b}\right)^2} \right) d\xi_o$$

$$+ \sum_{n=o}^{\infty} \sum_{q=1}^{Q-1} e^{i\Psi_q + i[2\pi m M^2(nQ+q)/\beta^2 Q]} \int_{-b}^{\infty} K(\xi_o)$$

$$\cdot \frac{\partial^2}{\partial z^2} H_o^{(2)}\!\left(\frac{M}{\beta^2} \sqrt{\left[\frac{k(x-\xi_o)}{b} + \frac{2\pi m}{Q}(nQ+q)\right]^2 + \beta^2 \left[\frac{kz}{b} + (nQ+q)kh\right]^2} \right) d\xi_o$$

$$+ \sum_{n=1}^{\infty} e^{i2n\pi m M^2/\beta^2} \int_{-b}^{\infty} K(\xi_o)$$

$$\cdot \frac{\partial^2}{\partial z^2} H_o^{(2)} \left(\frac{M}{\beta^2} \sqrt{\left[\frac{k(x - \xi_o)}{b} + 2n\pi m\right]^2 + \beta^2 \left[\frac{kz}{b} + nQkh\right]^2} \right) d\xi_o \left. \right\}$$

This is exactly the downwash equation one would obtain by setting up Jones and Rao's approach using the model of Figure 3. However to see how the equation can be reduced to downwash equation of Reference [24] it is necessary to return to the form of Equation (E-2). First note that Jones and Rao introduce more notation for $K(x)$ in the wake by defining

$$K_{oo}(x) = -\frac{1}{\rho_\infty Ub} e^{-ikx/\beta^2 b} \int_{-b}^{b} \Delta\bar{p}_a(\xi) e^{ik\xi/b} d\xi \qquad (E-5)$$

Now define the parameters

$$\left.\begin{array}{l} D_{nq} = \left(\frac{2\pi q}{Q} + 2n\pi\right)r \\[3mm] D_n = 2n\pi r \end{array}\right\} \qquad (E-6)$$

which characterize the distance by which the "wake airfoils" representing previous passages of blades other than the reference blade and previous passages of the reference blade respectively lead the reference airfoil. By introducing these parameters and making the appropriate changes of variables Equation (E-2) may be written as follows

$$\bar{w}(x,z) \approx \frac{ib}{4\beta} e^{ikM^2 x/\beta^2 b} \left\{ \int_{-b}^{\infty} K(\xi_0) \right. \tag{E-7}$$

$$\cdot \frac{\partial^2}{\partial z^2} H_o^{(2)} \left(\frac{kM}{\beta^2} \sqrt{\left(\frac{x-\xi_0}{b}\right)^2 + \beta^2 \left(\frac{z}{b}\right)^2} \right) d\xi_0$$

$$+ bK_{oo}(x) \sum_{n=o}^{\infty} \sum_{q=1}^{Q-1} e^{i\Psi_q - i[2\pi m(nQ+q)/Q]} \int_{-[(x-b)/b] - (D_{nq}/b)}^{\infty} e^{-ik\xi/\beta^2}$$

$$\cdot \frac{\partial^2}{\partial z^2} H_o^{(2)} \left(\frac{kM}{\beta^2} \sqrt{\xi^2 + \beta^2 \left[\frac{z}{b} + (nQ+q)h\right]^2} \right) d\xi$$

$$+ bK_{oo}(x) \sum_{n=1}^{\infty} e^{-i2n\pi m} \int_{-[(x-b)/b] - (D_n/b)}^{\infty} e^{-ik\xi/\beta^2}$$

$$\cdot \frac{\partial^2}{\partial z^2} H_o^{(2)} \left(\frac{kM}{\beta^2} \sqrt{\xi^2 + \beta^2 \left[\frac{z}{b} + nQh\right]^2} \right) d\xi \left. \right\}$$

$$+ \frac{ibe^{-ikx/b}}{4\rho_\infty U\beta} \sum_{n=o}^{\infty} \sum_{q=1}^{Q-1} e^{i\Psi_q - i[2\pi m(nQ+q)/Q]} \int_{[(x+b)/b] + (D_{nq}/b)}^{[(x-b)/b] + (D_{nq}/b)} e^{ik\eta/\beta^2}$$

$$\cdot \frac{\partial^2}{\partial z^2} H_o^{(2)} \left(\frac{kM}{\beta^2} \sqrt{\eta^2 + \beta^2 \left[\frac{z}{b} + (nQ+q)h \right]^2} \right) \int_{-b}^{x-b\eta+D_{nq}} \Delta\bar{p}_a(\xi) \, e^{ik\xi/b} \, d\xi \, d\eta$$

$$+ \frac{ibe^{-ikx/b}}{4\rho_\infty U\beta} \sum_{n=1}^{\infty} e^{-i2n\pi m} \int_{[(x+b)/b] + (D_n/b)}^{[(x-b)/b] + (D_n/b)} e^{ik\eta/\beta^2}$$

$$\cdot \frac{\partial^2}{\partial z^2} H_o^{(2)} \left(\frac{kM}{\beta^2} \sqrt{\eta^2 + \beta^2 \left[\frac{z}{b} + nQh \right]^2} \right) \int_{-b}^{x-b\eta+D_n} \Delta\bar{p}_a(\xi) \, e^{ik\xi/b} \, d\xi \, d\eta$$

Now if all the "wake airfoils" of Figure 3 are allowed to lead the reference airfoil by an infinite distance, i.e. if

$$\left. \begin{array}{c} D_{nq} \to \infty \\[12pt] D_n \to \infty \end{array} \right\} \qquad (E\text{-}8)$$

then the mathematical model used in the present study would agree with the model used by Jones and Rao and hence the downwash equations from both approaches should agree. Letting D_{nq} and D_n approach infinity Equation (E-7) becomes

$$\bar{w}(x,z) = \frac{ib}{4\beta} e^{ikM^2 x/\beta^2 b} \left\{ \int_{-b}^{\infty} K(\xi_o) \right. \tag{E-9}$$

$$\cdot \frac{\partial^2}{\partial z^2} H_o^{(2)} \left(\frac{kM}{\beta^2} \sqrt{\left(\frac{x-\xi_o}{b}\right)^2 + \beta^2 \left(\frac{z}{b}\right)^2} \right) d\xi_o$$

$$+ bK_{oo}(x) \sum_{n=o}^{\infty} \sum_{q=1}^{Q-1} e^{i\Psi_q - i[2\pi m(nQ+q)/Q]} \int_{-\infty}^{\infty} e^{-ik\xi/\beta^2}$$

$$\cdot \frac{\partial^2}{\partial z^2} H_o^{(2)} \left(\frac{kM}{\beta^2} \sqrt{\xi^2 + \beta^2 \left[\frac{z}{b} + (nQ+q)h\right]^2} \right) d\xi$$

$$+ bK_{oo}(x) \sum_{n=1}^{\infty} e^{-i2n\pi m} \int_{-\infty}^{\infty} e^{-ik\xi/\beta^2}$$

$$\cdot \frac{\partial^2}{\partial z^2} H_o^{(2)} \left(\frac{kM}{\beta^2} \sqrt{\xi^2 + \beta^2 \left[\frac{z}{b} + nQh\right]^2} \right) d\xi \left. \right\}$$

Introducing the nondimensional notation of Reference [24]

$$X = \frac{x}{b} \qquad Z = \frac{\beta z}{b}$$

$$W(X,Z) = \frac{1}{\beta} \, \bar{w} \, (X,Z) \, e^{-ikM^2 X/\beta^2} \Bigg\} \qquad (E\text{-}10)$$

Equation (E-9) may be written

$$2\pi \left[W(X,Z) - W_i(X,Z) \right] = \int_{-1}^{\infty} K(\Xi) \frac{\partial^2}{\partial Z^2} \left[\frac{i\pi}{2} H_o^{(2)} \left(\frac{kM}{\beta^2} \sqrt{\left(X - \Xi\right)^2 + Z^2} \right) \right] d\Xi$$

$$(E\text{-}11)$$

where

$$2\pi \, W_i(X,Z) = K_{oo}(X) \sum_{n=1}^{\infty} e^{-i2n\pi m} \int_{-\infty}^{\infty} e^{-ik(\Xi - X)/\beta^2} \qquad (E\text{-}12)$$

$$\cdot \frac{\partial^2}{\partial Z^2} \left[\frac{i\pi}{2} H_o^{(2)} \left(\frac{kM}{\beta^2} \sqrt{(\Xi - X)^2 + (Z + nQ\beta h)^2} \right) \right] d\Xi$$

$$+ K_{oo}(X) \sum_{n=o}^{\infty} \sum_{q=1}^{Q-1} e^{i\Psi_q -i[2\pi m(nQ+q)/Q]} \int_{-\infty}^{\infty} e^{-ik(\Xi - X)/\beta^2}$$

$$\cdot \frac{\partial^2}{\partial Z^2} \left[\frac{i\pi}{2} H_o^{(2)} \left(\frac{kM}{\beta^2} \sqrt{(\Xi - X)^2 + [Z + (nQ+q)\beta h]^2} \right) \right] d\Xi$$

Except for the sign this is precisely the downwash equation given by Jones and Rao. The difference in sign is accounted for by the fact that their z-axis is opposite to that used here, and thus their downwash should be opposite in sign to that of Equation (E-12).

Therefore if the mathematical model used in the present study is modified to agree with that of Jones and Rao then the downwash equation is the same for both cases and hence the loads calculated must be the same for both cases. However the difference in models can cause considerable differences in loads for those cases where the flow parameters dictate that the "wake airfoils" of Figure 3 lead the reference airfoil by a relatively short distance. A discussion of this situation is presented in Chapter IV along with a numerical comparison of the two methods.

APPENDIX F

REDUCTION OF THE KERNEL FOR ZERO MACH NUMBER

The downwash integral equation developed in Chapter II is for compressible flow over the model shown in Figure 3. As in most compressible flow analyses, it is convenient in the present study to reduce the analysis for the case of zero Mach number in order to facilitate comparison with known incompressible results and thus obtain a partial check of the analysis. In the present research this is accomplished by reducing the kernel of the downwash integral equation presented in Chapter II for zero Mach number and comparing the resulting incompressible downwash integral equation with the downwash equation given by Loewy [2]. The reduction of the compressible flow kernel for zero Mach number is presented in this appendix.

The kernel of the compressible downwash integral equation is given by Equation (21) of Chapter II and is repeated here for completeness

$$K\left[M, \frac{k(x-\xi)}{b}, \frac{kz}{b}\right] = \frac{iM}{4\beta} \left\{ \left[\frac{k(x-\xi)}{b}\right] \Big/ \sqrt{\left[\frac{k(x-\xi)}{b}\right]^2 + \beta^2 \left[\frac{kz}{b}\right]^2} \right\}$$

(F-1)

$$\cdot H_1^{(2)}\left(\frac{M}{\beta^2}\sqrt{\left[\frac{k(x-\xi)}{b}\right]^2 + \beta^2\left[\frac{kz}{b}\right]^2}\right) e^{ikM^2(x-\xi)/\beta^2 b}$$

$$-\frac{1}{4\beta} e^{ikM^2(x-\xi)/\beta^2 b} H_o^{(2)} \left(\frac{M}{\beta^2}\sqrt{\left[\frac{k(x-\xi)}{b}\right]^2 + \beta^2 \left[\frac{kz}{b}\right]^2}\right)$$

$$+\frac{i}{4\beta} e^{-ik(x-\xi)/b} \int_{-\infty}^{k(x-\xi)/b} e^{i\eta/\beta^2} H_o^{(2)} \left(\frac{M}{\beta^2}\sqrt{\eta^2 + \beta^2 \left[\frac{kz}{b}\right]^2}\right) d\eta$$

First consider the integral appearing in Equation (F-1). For small arguments the Hankel function of the second kind and order zero can be represented by its asymptotic value given by Lebedev [34] as

$$H_o^{(2)}(\nu) \sim \frac{2i}{\pi} \ln \frac{2}{\nu} \quad \text{as} \quad \nu \to 0 \tag{F-2}$$

Making this substitution the integral becomes

$$\lim_{M \to o} I = \lim_{M \to o} \left\{ \frac{2i}{\pi} \int_{-\infty}^{k(x-\xi)/b} e^{i\eta/\beta^2} \ln \frac{2}{\frac{M}{\beta^2}\sqrt{\eta^2 + \beta^2 \left[\frac{kz}{b}\right]^2}} \, d\eta \right\} \tag{F-3}$$

Integrating by parts

$$\lim_{M \to o} I = \lim_{M \to o} \left\{ \frac{2\beta^2}{\pi} e^{ik(x-\xi)/\beta^2 b} \ln \frac{2}{\frac{M}{\beta^2}\sqrt{\left[\frac{k(x-\xi)}{b}\right]^2 + \beta^2 \left[\frac{kz}{b}\right]^2}} \right. \tag{F-4}$$

$$+ \frac{2\beta^2}{\pi} \int_{-\infty}^{k(x-\xi)/b} \frac{\eta\, e^{i\eta/\beta^2}}{\eta^2 + \beta^2 \left(\frac{kz}{b}\right)^2}\, d\eta \Big\}$$

Now the Hankel function of the second kind and order one has the asymptotic representation given by Lebedev [34] as

$$H_1^{(2)}(\nu) \sim \frac{2i}{\pi\nu} \quad \text{as} \quad \nu \to 0 \tag{F-5}$$

Making this substitution along with Equations (F-2) and (F-4), Equation (F-1) becomes for small M

$$\lim_{M \to 0} K\left[M, \frac{k(x-\xi)}{b}, \frac{kz}{b}\right] = \lim_{M \to 0}\Bigg\{ - \frac{\beta}{2\pi}\, \frac{\left[\frac{k(x-\xi)}{b}\right] e^{ikM^2(x-\xi)/\beta^2 b}}{\left[\frac{k(x-\xi)}{b}\right]^2 + \beta^2 \left[\frac{kz}{b}\right]^2}$$

$$\tag{F-6}$$

$$- \frac{i}{2\pi\beta}\, e^{ikM^2(x-\xi)/\beta^2 b} \ln \frac{2}{\frac{M}{\beta^2}\sqrt{\left[\frac{k(x-\xi)}{b}\right]^2 + \beta^2 \left[\frac{kz}{b}\right]^2}}$$

$$+ \frac{i\beta}{2\pi}\, e^{ikM^2(x-\xi)/\beta^2 b} \ln \frac{2}{\frac{M}{\beta^2}\sqrt{\left[\frac{k(x-\xi)}{b}\right]^2 + \beta^2 \left[\frac{kz}{b}\right]^2}}$$

$$+ \frac{i\beta}{2\pi} e^{-ik(x-\xi)/b} \int_{-\infty}^{k(x-\xi)/b} \frac{\eta \, e^{i\eta/\beta^2}}{\eta^2 + \beta^2 \left(\frac{kz}{b}\right)^2} \, d\eta \; \Big\}$$

Thus in the limit as $M \to 0$, $\beta \to 1$ and the kernel becomes

$$K\left[0, \frac{k(x-\xi)}{b}, \frac{kz}{b}\right] = -\frac{1}{2\pi} \frac{\frac{k(x-\xi)}{b}}{\left[\frac{k(x-\xi)}{b}\right]^2 + \left[\frac{kz}{b}\right]^2} \qquad (F-7)$$

$$+ \frac{i}{2\pi} e^{-ik(x-\xi)/b} \int_{-\infty}^{k(x-\xi)/b} \frac{\eta \, e^{i\eta}}{\eta^2 + \left(\frac{kz}{b}\right)^2} \, d\eta$$

The form of the zero Mach number kernel given by Equation (F-7) is the form which is useful when comparison is made with Loewy's [2] results. However, the integral which appears in Equation (F-7) can be evaluated in terms of known transcendental functions. This is accomplished as follows. First split the integral into two parts

$$I = \int_{-\infty}^{0} \frac{\eta \, e^{i\eta/\beta^2}}{\eta^2 + \left(\frac{kz}{b}\right)^2} \, d\eta + \int_{0}^{k(x-\xi)/b} \frac{\eta \, e^{i\eta}}{\eta^2 + \left(\frac{kz}{b}\right)^2} \, d\eta \qquad (F-8)$$

Making an appropriate change of variables the first integral of Equation (F-8) may be written

$$I_1 = - \int_0^\infty \frac{v \cos v}{v^2 + \left(\frac{kz}{b}\right)^2} \, dv + i \int_0^\infty \frac{v \sin v}{v^2 + \left(\frac{kz}{b}\right)^2} \, dv \qquad \text{(F-9)}$$

Now from Erdélyi, et al. [37]

$$\int_0^\infty \frac{t \cos xt}{a^2 + t^2} \, dt = \frac{1}{2} \left[e^{ax} E_1(ax) - e^{-ax} E^*(ax) \right] \qquad \text{(F-10)}$$

where $E_1(x)$ and $E^*(x)$ are the exponential and modified exponential integrals respectively. Then from Dwight [38]

$$\int_0^\infty \frac{x \sin mx}{a^2 + x^2} \, dx = \frac{\pi}{2} e^{-ma} \qquad \text{(F-11)}$$

Using these results Equation (F-9) becomes

$$I_1 = - \frac{1}{2} \left[e^{kz/b} E_1 \left(\frac{kz}{b}\right) - e^{-kz/b} E^* \left(\frac{kz}{b}\right) \right] + \frac{i\pi}{2} e^{-kz/b} \qquad \text{(F-12)}$$

Turning now to the second integral of Equation (F-8) let

$$I_2 = \int_0^{k(x-\xi)/b} \frac{\eta \, e^{i\eta}}{\eta^2 + \left(\frac{kz}{b}\right)^2} \, d\eta \qquad \text{(F-13)}$$

From Abramowitz and Stegun [39]

$$\int \frac{x \, e^{ix}}{a^2 + x^2} \, dx = -\frac{1}{2} \left[e^{-a} \, E_1(-a -ix) + e^{a} \, E_1(a -ix) \right] + \text{constant} \qquad \text{(F-14)}$$

so that

$$I_2 = -\frac{1}{2} \left[e^{-\frac{kz}{b}} E_1\left(-\frac{kz}{b} - i\eta \right) + e^{\frac{kz}{b}} E_1\left(\frac{kz}{b} - i\eta \right) \right] \Bigg|_{\eta=0}^{\eta = \frac{k(x-\xi)}{b}}$$

$$\text{(F-15)}$$

Evaluating at the limits and using the fact that

$$E_1(-x - i0) = -E^*(x) + i\pi \qquad \text{(F-16)}$$

from Abramowitz and Stegun [39], Equation (F-15) becomes

$$I_2 = -\frac{1}{2} \left\{ e^{-kz/b} E_1\left[-\frac{kz}{b} - i\frac{k(x-\xi)}{b} \right] + e^{kz/b} E_1\left[\frac{kz}{b} - i\frac{k(x-\xi)}{b} \right] \right\}$$

$$\text{(F-17)}$$

$$+ \frac{1}{2} e^{-kz/b} \left[-E^*\left(\frac{kz}{b} \right) + i\pi \right] + \frac{1}{2} e^{kz/b} E_1\left(\frac{kz}{b} \right)$$

Using the above results the integral of Equation (F-8) becomes

$$I = i\pi \, e^{-kz/b} - \frac{1}{2} \left\{ e^{-kz/b} E_1\left[-\frac{kz}{b} - i\frac{k(x-\xi)}{b} \right] \right. \qquad \text{(F-18)}$$

$$\left. + e^{kz/b} E_1\left[\frac{kz}{b} - i\frac{k(x-\xi)}{b} \right] \right\}$$

and finally the kernel given by Equation (F-7) becomes

$$K\left[0, \frac{k(x-\xi)}{b}, \frac{kz}{b}\right] = \frac{1}{2\pi} \frac{\frac{k(x-\xi)}{b}}{\left[\frac{k(x-\xi)}{b}\right]^2 + \left[\frac{kz}{b}\right]^2} - \frac{1}{2} e^{-(kz/b)-i[k(x-\xi)/b]}$$

(F-19)

$$- \frac{i}{4\pi} e^{-(kz/b) - i[k(x-\xi)/b]} E_1\left[-\frac{kz}{b} - i\frac{k(x-\xi)}{b}\right]$$

$$- \frac{i}{4\pi} e^{(kz/b) - i[k(x-\xi)/b]} E_1\left[\frac{kz}{b} - i\frac{k(x-\xi)}{b}\right]$$

The case where $z = 0$ is also of interest because it is this case which gives the kernel for the integral representing the downwash caused by the reference airfoil itself. Furthermore, this is the entire kernel of the downwash integral equation for a two-dimensional fixed wing airfoil. If z is set equal to zero in Equation (F-7) the kernel becomes

$$K\left[0, \frac{k(x-\xi)}{b}, 0\right] = -\frac{1}{2\pi}\left[k(x-\xi)/b\right]^{-1} + \frac{i}{2\pi} e^{-k(x-\xi)/b} \int_{-\infty}^{k(x-\xi)/b} \frac{e^{i\eta}}{\eta} d\eta$$

(F-20)

The integral appearing in this kernel may be written as

$$I = \int_{-\infty}^{k(x-\xi)/b} \frac{\cos \eta}{\eta} d\eta + i \int_{-\infty}^{k(x-\xi)/b} \frac{\sin \eta}{\eta} d\eta$$

(F-21)

Now the sine and cosine integrals are defined respectively by Lebedev [34] as

$$\left.\begin{array}{l} Si(z) = \int_0^z \frac{\sin t}{t}\, dt \qquad \text{for all } z \\[3em] Ci(z) = \int_\infty^z \frac{\cos t}{t}\, dt \qquad \begin{array}{l}\text{for } z \geq 0 \\ (\text{undefined for } z < 0)\end{array} \end{array}\right\} \qquad (F\text{-}22)$$

The second integral of Equation (F-21) may be written as

$$I_2 = \int_0^\infty \frac{\sin u}{u}\, du + \int_0^{k(x-\xi)/b} \frac{\sin \eta}{\eta}\, d\eta \qquad (F\text{-}23)$$

so that

$$\left.\begin{array}{l} I_2 = Si(\infty) + Si\left[\frac{k(x-\xi)}{b}\right] \\[3em] I_2 = \frac{\pi}{2} + Si\left[\frac{k(x-\xi)}{b}\right] \end{array}\right\} \qquad (F\text{-}24)$$

By changing variables the first integral of Equation (F-21) may be written in the following forms

$$I_1 = \int_\infty^{-k(x-\xi)/b} \frac{\cos \zeta}{\zeta}\, d\zeta \qquad (F\text{-}25)$$

$$I_1 = \int_{-\infty}^{k(x-\xi)/b} \frac{\cos \zeta}{\zeta} \, d\zeta + \int_{k(x-\xi)/b}^{-k(x-\xi)/b} \frac{\cos \zeta}{\zeta} \, d\zeta \qquad (F\text{-}26)$$

The second integral of Equation (F-26) is seen to be zero because it is the integral of an odd function over an even interval. Now if $\frac{k(x-\xi)}{b}$ is negative then from Equation (F-25)

$$I_1 = Ci \left[\left| \frac{k(x-\xi)}{b} \right| \right] \qquad (F\text{-}27)$$

and if $\frac{k(x-\xi)}{b}$ is positive the value of I_1 is given by Equation (F-26) as

$$I_1 = Ci \left[\frac{k(x-\xi)}{b} \right] \qquad (F\text{-}28)$$

Thus for all values of $\frac{k(x-\xi)}{b}$ the integral may be written as

$$I_1 = Ci \left[\left| \frac{k(x-\xi)}{b} \right| \right] \qquad (F\text{-}29)$$

Using the above evaluations of the integrals appearing in Equation (F-21) the kernel given in Equation (F-20) becomes

$$K \left[0, \frac{k(x-\xi)}{b}, 0 \right] = -\frac{1}{2\pi} \frac{1}{\frac{k(x-\xi)}{b}} + \frac{i}{2\pi} e^{-k(x-\xi)/b} \left\{ Ci \left[\left| \frac{k(x-\xi)}{b} \right| \right] \right.$$

$$\left. + i \frac{\pi}{2} + i \, Si \left[\frac{k(x-\xi)}{b} \right] \right\} \qquad (F\text{-}30)$$

The reduction for zero Mach number of the kernel given by
Equation (21) of Chapter II for the compressible flow downwash integral
equation is thus completed. By using this reduced kernel, the
compressible downwash integral equation developed for the flow model
of Figure 3 becomes the downwash equation for incompressible flow over
the model of Figure 3. This reduction then permits comparison with
Loewy's incompressible results and hence a partial check of the
compressible flow analysis.

APPENDIX G

ANALYTICAL COMPARISON WITH LOEWY'S RESULTS

In most compressible flow analyses it is beneficial at some point to make the reduction to zero Mach number so that a comparison can be made with known incompressible results. In this appendix the downwash integral equation developed in Chapter II for two-dimensional rotary wings in compressible flow is reduced for zero Mach number to a form which can readily be compared with the downwash expression given by Loewy [2] for incompressible flow. This comparison indicates analytically the effect of the different flow models used in the two analyses.

Using the kernel developed in Appendix F for zero Mach number the downwash integral equation developed in Chapter II becomes for incompressible flow

$$\bar{w}_a(x) = \frac{\omega}{2\pi\rho_\infty U^2} \left\{ \int_{-b}^{b} \Delta\bar{p}_a(\xi) \left\{ \left[k(x-\xi)/b \right]^{-1} \right. \right. \tag{G-1}$$

$$\left. \left. - ie^{-ik(x-\xi)/b} \int_{-\infty}^{k(x-\xi)/b} \frac{1}{\eta} e^{i\eta} \, d\eta \right\} d\xi \right.$$

$$+ \sum_{n=o}^{\infty} \sum_{q=1}^{Q-1} e^{i\Psi_q} \int_{-b}^{b} \Delta\bar{p}_a(\xi) \left\{ \frac{\frac{k(x-\xi)}{b} + 2\pi(nQ+q)\frac{m}{Q}}{\left[\frac{k(x-\xi)}{b} + 2\pi(nQ+q)\frac{m}{Q}\right]^2 + \left[(nQ+q)kh\right]^2} \right.$$

$$- ie^{-i\{[k(x-\xi)/b] + [2\pi m(nQ+q)/Q]\}} \int_{-\infty}^{\{[k(x-\xi)/b] + 2\pi m(nQ+q)/Q\}} \frac{\eta\, e^{i\eta}}{\eta^2 + [(nQ+q)kh]^2} d\eta \left.\right\} d\xi$$

$$+ \sum_{n=1}^{\infty} \int_{-b}^{b} \Delta\bar{p}_a(\xi) \left\{ \frac{\frac{k(x-\xi)}{b} + 2n\pi m}{\left[\frac{k(x-\xi)}{b} + 2n\pi m\right]^2 + \left[nQkh\right]^2} \right.$$

$$- ie^{-i\{[k(x-\xi)/b] + 2n\pi m\}} \int_{-\infty}^{\{[k(x-\xi)/b] + 2n\pi m\}} \frac{\eta\, e^{i\eta}}{\eta^2 + (nQkh)^2} d\eta \left.\right\} d\xi \left.\right]\!\left.\right)$$

In reducing Equation (G-1) to a form which can be compared directly with the downwash equation given by Loewy a generalized form of the three chordwise integrals appearing in Equation (G-1) is first considered. The generalized chordwise integral is given by

$$I = \int_{-b}^{b} \frac{\Delta\bar{p}_a(\xi)}{\rho_\infty U} \left\{ \frac{\frac{k(x-\xi)}{b} + A}{\left[\frac{k(x-\xi)}{b} + A\right]^2 + B^2} \right. \tag{G-2}$$

$$- ie^{-i\{[k(x-\xi)/b] + A\}} \int_{-\infty}^{[k(x-\xi)/b] + A} \frac{\eta \, e^{i\eta}}{\eta^2 + B^2} \, d\eta \, \Big\} \, d\xi$$

where A and B are constants with respect to the integrations.

For incompressible flow the pressure differential across the reference airfoil, $\Delta \bar{p}_a(x)$, is related to the vorticity distribution, $\bar{\gamma}_a(x)$, used by Loewy through the following equation given by Bisplinghoff, Ashley, and Halfman [36]

$$\frac{\Delta \bar{p}_a(x)}{\rho_\infty U} = - \bar{\gamma}_a(x) - \frac{i\omega}{U} \int_{-b}^{x} \bar{\gamma}_a(\xi) \, d\xi \qquad (G-3)$$

Substituting Equation (G-3) into Equation (G-2)

$$I = - \int_{-b}^{b} \frac{\left[\frac{k(x-\xi)}{b} + A \right] \bar{\gamma}_a(\xi)}{\left[\frac{k(x-\xi)}{b} + A \right]^2 + B^2} \, d\xi \qquad (G-4)$$

$$- \frac{i\omega}{U} \int_{-b}^{b} \frac{\left[\frac{k(x-\xi)}{b} + A \right]}{\left[\frac{k(x-\xi)}{b} + A \right]^2 + B^2} \int_{-b}^{\xi} \bar{\gamma}_a(\zeta) \, d\zeta \, d\xi$$

$$+ i \int_{-b}^{b} e^{-i\{[k(x-\xi)/b] + A\}} \bar{\gamma}_a(\xi) \int_{-\infty}^{[k(x-\xi)/b] + A} \frac{\eta \, e^{i\eta}}{\eta^2 + B^2} \, d\eta \, d\xi$$

$$- \frac{\omega}{U} \int_{-b}^{b} e^{-i\{[k(x-\xi)/b] + A\}} \int_{-b}^{\xi} \bar{\gamma}_a(\zeta) \, d\zeta \int_{-\infty}^{[k(x-\xi)/b] + A} \frac{\eta \, e^{i\eta}}{\eta^2 + B^2} \, d\eta \, d\xi$$

If the triple integral appearing in Equation (G-4) is integrated by parts once then Equation (G-4) reduces to

$$I = - \int_{-b}^{b} \frac{\frac{k(x-\xi)}{b} + A}{\left[\frac{k(x-\xi)}{b} + A\right]^2 + B^2} \, \bar{\gamma}_a(\xi) \, d\xi \tag{G-5}$$

$$+ \, ie^{-i\{[k(x-b)/b] + A\}} \left[\int_{-b}^{b} \bar{\gamma}_a(\zeta) d\zeta \right] \int_{-\infty}^{[k(x-b)/b] + A} \frac{\eta \, e^{i\eta}}{\eta^2 + B^2} \, d\eta$$

or changing variables

$$I = - \int_{-(bA/k)-b}^{-(bA/k)+b} \frac{\frac{k(x-\zeta)}{b}}{\left[\frac{k(x-\zeta)}{b}\right]^2 + B^2} \, \bar{\gamma}_a(\zeta) \, d\zeta \tag{G-6}$$

$$+ \frac{ik}{b} e^{ik -iA} \left[\int_{-b}^{b} \bar{\gamma}_a(\zeta) \, d\zeta \right] \int_{-(bA/k)+b}^{\infty} \frac{\frac{k(x-\xi)}{b} e^{-ik\xi/b}}{\left[\frac{k(x-\xi)}{b}\right]^2 + B^2} \, d\xi$$

Defining the total circulation given by Loewy as

$$\bar{\Gamma} = \frac{1}{b} e^{ik} \int_{-b}^{b} \bar{\gamma}_a(\zeta) \, d\zeta \qquad (G-7)$$

Equation (G-6) becomes

$$I = - \int_{-(bA/k)-b}^{-(bA/k)+b} \frac{\frac{k(x-\zeta)}{b}}{\left[\frac{k(x-\zeta)}{b}\right]^2 + B^2} \bar{\gamma}_a(\zeta) \, d\zeta \qquad (G-8)$$

$$+ ik \, \bar{\Gamma} e^{-iA} \int_{-(bA/k)+b}^{\infty} \frac{\frac{k(x-\xi)}{b} e^{-ik\xi/b}}{\left[\frac{k(x-\xi)}{b}\right]^2 + B^2} \, d\xi$$

Before applying the result of Equation (G-8) to the downwash equation, Equation (G-1), the distance by which each "wake airfoil" leads the reference airfoil will be defined. For the airfoils representing previous passages of blades other than the reference blade the distance is given by

$$D_{nq} = 2\pi(nQ+q) \frac{r}{Q} \qquad (G-9)$$

where n is the revolution index and q is the blade index. For the airfoils representing previous passages of the reference blade the distance is given by

$$D_n = 2n\pi r \qquad\qquad (G\text{-}10)$$

Using the definitions given by Equations (G-9) and (G-10) together with the result given by Equation (G-8) with the proper choices for the constants A and B the downwash equation, Equation (G-1), may be written as follows

$$\bar{w}_a(x) = -\frac{1}{2\pi}\left\{ \int_{-b}^{b} \frac{\bar{\gamma}_a(\xi)\,d\xi}{(x-\xi)} - ik\bar{\Gamma}\int_{b}^{\infty} \frac{e^{-ik\xi/b}}{(x-\xi)}\,d\xi \right. \qquad (G\text{-}11)$$

$$+ \sum_{n=0}^{\infty}\sum_{q=1}^{Q-1} e^{i\Psi_q}\left\{ \int_{-D_{nq}-b}^{-D_{nq}+b} \frac{(x-\xi)\,\bar{\gamma}_a(\xi)}{(x-\xi)^2 + [(nQ+q)bh]^2}\,d\xi \right.$$

$$\left. - ik\bar{\Gamma}\,e^{-i2\pi m(nQ+q)/Q}\int_{-D_{nq}+b}^{\infty} \frac{(x-\xi)\,e^{-ik\xi/b}}{(x-\xi)^2 + [(nQ+q)bh]^2}\,d\xi \right\}$$

$$+ \sum_{n=1}^{\infty}\left\{ \int_{-D_n-b}^{-D_n+b} \frac{(x-\xi)\,\bar{\gamma}_a(\xi)}{(x-\xi)^2 + (nQbh)^2}\,d\xi \right.$$

$$\left.\left. - ik\bar{\Gamma}\,e^{-i2n\pi m}\int_{-D_n+b}^{\infty} \frac{(x-\xi)\,e^{-ik\xi/b}}{(x-\xi)^2 + (nQbh)^2}\,d\xi \right\}\right\}$$

From Equation (G-11) the difference between the flow model used by Loewy and the flow model used in the present research becomes apparent. The most obvious dissimilarities between this equation and the downwash equation given by Loewy are the first integrals in each of the summations of Equation (G-11). These integrals represent the downwash associated with the bound vorticity of each of the wake airfoils and hence the terms do not appear in Loewy's downwash equation. In Loewy's flow model the wake layers are made up of shed vorticity from the reference blade and from other blades of the rotor. Since these wake layers are allowed by Loewy to extend from minus infinity to plus infinity the summation terms which appear in Loewy's downwash equation are shed vorticity terms only and are similar to the second terms appearing in each of the summations of Equation (G-11).

The flow model being used in the present research, shown in Figure 3, can be made to agree with that used by Loewy, shown in Figure 2, by forcing each of the "wake airfoils" of Figure 3 to lead the reference airfoil by an infinite distance. If this is done then

$$\left. \begin{array}{c} D_{nq} \to \infty \\[2em] D_n \to \infty \end{array} \right\} \qquad (G-12)$$

and Equation (G-11) becomes

$$\bar{w}_a(x) = - \frac{1}{2\pi} \left\{ \int_{-b}^{b} \frac{\bar{\gamma}_a(\xi)}{(x-\xi)} \, d\xi - i k \bar{\Gamma} \int_{b}^{\infty} \frac{e^{-ik\xi/b}}{(x-\xi)} \, d\xi \right. \qquad (G-13)$$

$$- ik\bar{\Gamma} \sum_{n=0}^{\infty} \sum_{q=1}^{Q-1} e^{i\Psi_q - i[2\pi m(nQ+q)/Q]} \int_{-\infty}^{\infty} \frac{(x-\xi)\, e^{-ik\xi/b}}{(x-\xi)^2 + [(nQ+q)bh]^2}\, d\xi$$

$$- ik\bar{\Gamma} \sum_{n=1}^{\infty} e^{-i2n\pi m} \int_{-\infty}^{\infty} \frac{(x-\xi)\, e^{-ik\xi/b}}{(x-\xi)^2 + (nQbh)^2}\, d\xi \Big\}$$

which is exactly the downwash equation obtained by Loewy.

It has thus been shown that if the flow model used by Loewy and the flow model used in the present dissertation are made to agree, then the downwash equation obtained from the present approach for zero Mach number agrees with that given by Loewy. This agreement of the downwash equations then implies agreement of the unsteady aerodynamic loading on the reference airfoil obtained from the two different approaches. If the flow models are not made to agree then the differences between the two downwash equations are explained in terms of the bound vorticity associated with the "wake airfoils" of Figure 3. The numerical significance of these differences is presented in Chapter IV.

APPENDIX H

CONVERGENCE OF THE WAKE SERIES

The integral equation for the downwash at the reference airfoil section of a helicopter rotor blade is developed in terms of the pressure differential across that section in Chapter II. This integral equation is shown to contain an infinite series which must be truncated in the numerical evaluation of the integral equation. Consequently the question of convergence of this series is of utmost importance. In this appendix the convergence of the series is investigated and it is shown that the series converges except for a certain combination of the aerodynamic parameters.

In Chapter II it is shown that the downwash integral equation for the pressure distribution on the reference airfoil of an equivalent single bladed rotor can be written as

$$\bar{w}(x) = - \frac{\omega}{\rho_\infty U^2} \left\{ \int_{-b}^{b} \Delta \bar{p}_a(\xi) \, K\left[M, \frac{k(x-\xi)}{b}, 0\right] d\xi \right. \tag{H-1}$$

$$\left. + \sum_{n=1}^{\infty} \int_{-b}^{b} \Delta \bar{p}_a(\xi) \, K\left[M, \frac{k(x-\xi)}{b} + 2n\pi m, \, nkh\right] d\xi \right\}$$

where the kernels of the above integrals are given by Equation (21).

If the integration and summation operations in the second term

of Equation (H-1) are reversed then Equation (H-1) may be written as

$$\bar{w}(x) = - \frac{\omega}{\rho_\infty U^2} \left\{ \int_{-b}^{b} \Delta\bar{p}_a(\xi) \, K\left[M, \frac{k(x-\xi)}{b}, 0\right] d\xi \right.$$ (H-2)

$$\left. + \int_{-b}^{b} \Delta\bar{p}_a(\xi) \, \bar{K}_h\left[M, \frac{k(x-\xi)}{b} + 2n\pi m, \, nkh\right] d\xi \right\}$$

where

$$\bar{K}_h = \frac{1}{4\beta} e^{ikM^2(x-\xi)/\beta^2 b} \left[iMS_1 - S_2 + ie^{-ik(x-\xi)/\beta^2 b} S_3\right]$$ (H-3)

and

$$S_1 = \sum_{n=1}^{\infty} \left\{ \left[\frac{k(x-\xi)}{b} + 2n\pi m\right] \middle/ \sqrt{\left[\frac{k(x-\xi)}{b} + 2n\pi m\right]^2 + \left(\beta nkh\right)^2} \right\}$$ (H-4)

$$\cdot H_1^{(2)}\left(\frac{M}{\beta^2} \sqrt{\left[\frac{k(x-\xi)}{b} + 2n\pi m\right]^2 + \left(\beta nkh\right)^2}\right) e^{i2n\pi m M^2/\beta^2}$$

$$S_2 = \sum_{n=1}^{\infty} H_0^{(2)}\left(\frac{M}{\beta^2} \sqrt{\left[\frac{k(x-\xi)}{b} + 2n\pi m\right]^2 + \left(\beta nkh\right)^2}\right) e^{i2n\pi m M^2/\beta^2}$$ (H-5)

$$S_3 = \sum_{n=1}^{\infty} e^{-i2n\pi m} \int_{-\infty}^{\infty} e^{[k(x-\xi)/b] + 2n\pi m} H_o^{(2)} \left(\frac{M}{\beta^2} \sqrt{\eta^2 + \left(\beta n k h\right)^2} \right) e^{i\eta/\beta^2} d\eta$$

(H-6)

It should be noted here that the justification for reversing the order of integration and summation accomplished above lies in the fact that Equation (H-1) can be developed with the summation either inside or outside the integral, depending on the approach taken. In the present study Equation (H-1) was developed with the summation outside the integral, while in a similar study by Carta [26] the equation was developed with the summation inside the integral.

The series given by Equations (H-4), (H-5), and (H-6) will now be investigated in detail to determine under what conditions the series converge. The approach taken parallels that used by Carta [26], since these series are similar to the ones which he encountered. The approach is to look at the terms in the series as the summation index becomes large and apply the results of the theorem appearing in Appendix I. First consider the series S_1. Define the parameter

$$P = \frac{M}{\beta^2} \sqrt{\left[\frac{k(x-\xi)}{b} + 2n\pi m\right]^2 + \left(\beta n k h\right)^2}$$

(H-7)

Then if the following are defined

$$2\pi\zeta = \frac{M}{\beta^2} \sqrt{\left(2\pi m\right)^2 + \left(\beta k h\right)^2}$$

(H-8)

$$D_1 = \frac{4\pi m \left(\frac{M}{\beta 2}\right)^2 \left[\frac{k(x-\xi)}{b}\right]}{\left(2\pi\zeta\right)^2} \qquad (H-9)$$

$$D_2 = \frac{\left(\frac{M}{\beta 2}\right)^2 \left[\frac{k(x-\xi)}{b}\right]^2}{\left(2\pi\zeta\right)^2} \qquad (H-10)$$

Equation (H-7) may be written as

$$P = 2\pi\zeta n \sqrt{1 + \frac{1}{n}\left(D_1 + \frac{1}{n}D_2\right)} \qquad (H-11)$$

For large values of n the radical in Equation (H-11) can be expanded using the binomial theorem. Retaining only the first two terms

$$P \cong 2\pi\zeta n \left[1 + \frac{1}{2n}\left(D_1 + \frac{1}{n}D_2\right)\right] \qquad (H-12)$$

If S_{1n} represents the nth term of Equation (H-4), then for large values of n

$$S_{1n} \sim \frac{2\pi m \left[\frac{2D_2}{D_1} + n\right]}{\left(\frac{\beta^2}{M}\right) 2\pi\zeta n \left[1 + \frac{1}{2n}\left(D_1 + \frac{1}{n}D_2\right)\right]} e^{i2n\pi m M^2/\beta^2} \qquad (H-13)$$

$$\cdot H_1^{(2)}\left(2\pi\zeta n \left[1 + \frac{1}{2n}\left(D_1 + \frac{1}{n}D_2\right)\right]\right)$$

For large values of the argument the Hankel function can be expanded in a series given by Lebedev [34] as

$$H_1^{(2)}(z) \cong \sqrt{\frac{2}{\pi z}} \, e^{-i[z-(3\pi/4)]} \left\{ 1 - \frac{3i}{8z} + \frac{15}{128z^2} - \cdots \right\} \qquad \text{(H-14)}$$

Substituting this expansion into Equation (H-13) and retaining only the first two terms

$$S_{1n} \sim \left[\frac{mM e^{i3\pi/4}}{\pi\beta^2 \zeta^{3/2}} \right] \frac{\left[n + \frac{2D_2}{D_1} \right] e^{-i\left\{ 2\pi\zeta n + 2\pi\zeta D_1 + (\pi\zeta D_2/n) - (2\pi m M^2/\beta^2) \right\}}}{\left\{ n \left[1 + \frac{1}{2n} \left(D_1 + \frac{1}{n} D_2 \right) \right] \right\}^{3/2}}$$

$$\text{(H-15)}$$

$$\cdot \left\{ 1 - \frac{3i}{16\pi\zeta n \left[1 + \frac{1}{2n} \left(D_1 + \frac{1}{n} D_2 \right) \right]} \right\}$$

Since n is assumed to be large, $\frac{1}{n} D_2$ is negligible compared to D_1 and $\frac{1}{2n} \left(D_1 + \frac{1}{n} D_2 \right)$ is negligible compared to unity so that

$$S_{1n} \sim \left[\frac{mM e^{i3\pi/4}}{\pi\beta^2 \zeta^{3/2}} \right] e^{-i\pi\zeta D_1} \left\{ e^{i2\pi n[(mM^2/\beta^2) - \zeta]} \right. \qquad \text{(H-16)}$$

$$\left. \cdot \left[\frac{1}{n^{1/2}} + \frac{(2D_2/D_1)}{n^{3/2}} - \frac{3i}{(16\pi\zeta)n^{3/2}} - \frac{3i(2D_2/D_1)}{(16\pi\zeta)n^{5/2}} \right] \right\}$$

Now the series containing the last three terms of Equation (H-16) can be shown to have absolute convergence because the power of n in the denominator is greater than unity in each case. The convergence of the series containing the first term, however, must be determined by applying the following theorem which is proved in Appendix I.

Consider the series

$$S = \sum_{n=1}^{\infty} a_n \, e^{id_n}$$

If a_n is a positive decreasing sequence approaching zero monotonically as n increases indefinitely and if d_n monotonically approaches nd where d is a constant and is not equal to any integral multiple of 2π, the series converges. If d_n monotonically approaches nd where d is constant and is equal to any integral multiple of 2π, or if d_n is a constant or asymptotically approaches a constant, the convergence or divergence of the series depends on the behavior of the series

$$S' = \sum_{n=1}^{\infty} a_n$$

Applying this theorem, the series containing the first term of Equation (H-16) will converge if

$$\frac{mM^2}{\beta^2} - \zeta \neq \delta \qquad \delta = 0, 1, 2, \ldots \qquad (H-17)$$

and the series diverges if equality holds. Thus the original series S_1 will converge unless

$$\frac{mM^2}{\beta^2} - \frac{M}{2\pi\beta^2} \sqrt{(2\pi m)^2 + (\beta kh)^2} = \delta \qquad \delta = 0, 1, 2, \ldots \qquad (H-18)$$

Now deal with the series S_2 given by Equation (H-5). Using the notation given earlier, the nth term of the series, S_{2n}, becomes for large values of n

$$S_{2n} \sim H_0^{(2)}\left(2\pi\zeta n \left[1 + \frac{1}{n}\left(D_1 + \frac{1}{n} D_2\right)\right]\right) e^{i2\pi m M^2/\beta^2} \qquad (H-19)$$

For large values of the argument, the Hankel function can be approximated as follows

$$H_0^{(2)}(z) \cong \sqrt{\frac{2}{\pi z}} \ e^{-i[z-(\pi/4)]}\left(1 + \frac{i}{8z} + \ldots\right) \qquad (H-20)$$

Retaining only the first two terms of the expansion

$$S_{2n} \sim \frac{e^{i\pi/4}}{\pi \ \zeta^{1/2}} \ \frac{e^{i\{2\pi n(mM^2/\beta^2) - 2\pi n\zeta - \pi\zeta[D_1 + (D_2/n)]\}}}{\sqrt{n\left[1 + \frac{1}{2n}\left(D_1 + \frac{1}{n} D_2\right)\right]}} \qquad (H-21)$$

$$\cdot \left\{1 + \frac{i}{16\pi\zeta n\left[1 + \frac{1}{2n}\left(D_1 + \frac{1}{n} D_2\right)\right]}\right\}$$

Since n is assumed to be large, $\frac{1}{n} D_2$ is negligible compared to D_1 and $\frac{1}{2n}(D_1 + \frac{1}{n}D_2)$ is negligible compared to unity so that

$$S_{2n} \sim \frac{e^{i[(\pi/4) - \pi\zeta D_1]}}{\pi \zeta^{1/2}} \ e^{i2\pi n[(mM^2/\beta^2) - \zeta]} \left[\frac{1}{n^{1/2}} + \frac{i}{16\pi\zeta n^{3/2}} \right] \quad \text{(H-22)}$$

The series containing the second term of the above equation can be shown to have absolute convergence because of the power of n in the denominator. The convergence of the series containing the first term of Equation (H-22) is determined using the theorem appearing in Appendix I. Applying the theorem, the series will converge except when the relation

$$\frac{mM^2}{\beta^2} - \zeta = \delta \qquad \delta = 0, 1, 2, \ldots \quad \text{(H-23)}$$

is satisfied. Thus the series S_2 will converge unless

$$\frac{mM^2}{\beta^2} - \frac{M}{2\pi\beta^2} \sqrt{(2\pi m)^2 + (\beta k h)^2} = \delta \qquad \delta = 0, 1, 2, \ldots \quad \text{(H-24)}$$

which is the same as the divergence criterion found for the series S_1.

Turning to the third series, S_3, given by Equation (H-6), the nth term of the series is given by

$$S_{3n} = e^{-i2n\pi m} \int_{-\infty}^{[k(x-\xi)/b]+2n\pi m} H_o^{(2)}\left(\frac{M}{\beta^2}\sqrt{\eta^2 + (\beta nkh)^2}\right) e^{i\eta/\beta^2} d\eta$$

(H-25)

For large values of the index, n

$$S_{3n} \sim e^{-i2n\pi m} \int_{-\infty}^{\infty} H_o^{(2)}\left(\frac{M}{\beta^2}\sqrt{\eta^2 + (\beta nkh)^2}\right) e^{i\eta/\beta^2} d\eta$$

(H-26)

The integral appearing in Equation (H-26) can be evaluated as

$$\int_{-\infty}^{\infty} H_o^{(2)}\left(\frac{M}{\beta^2}\sqrt{\eta^2 + (\beta nkh)^2}\right) e^{i\eta/\beta^2} d\eta = 2i\beta e^{-nkh}$$

(H-27)

Thus

$$S_{3n} \sim 2i\beta e^{-nkh} e^{-i2n\pi m}$$

(H-28)

Applying the theorem appearing in Appendix I, the series S_3 is seen to converge for all values of the parameters.

Thus the series occurring in the downwash integral equation are shown to converge except for those values of the parameters for which the relation

$$\frac{mM^2}{\beta^2} - \frac{M}{2\pi\beta^2}\sqrt{(2\pi m)^2 + (\beta kh)^2} = \delta \qquad \delta = 0, 1, 2, \ldots$$

(H-29)

is satisfied.

A condition similar to Equation (H-29) was encountered by Carta [26] when studying the compressible unsteady flow over an infinite cascade of airfoils. In Carta's study the cascade airfoils represented compressor blades which are present in the physical flow field of a turbine engine. Fanti and Carta [40] were subsequently able to show that their condition similar to Equation (H-29) corresponded physically to an acoustic resonance condition. However, in the present study the "wake airfoils" of Figure 3 are not present in the physical helicopter flow field and thus Equation (H-29) should be interpreted as only a mathematical instability associated with the flow model.

It should be noted here that the technique used in determining the convergence of the series denoted by S_1, S_2, and S_3 is not applicable in a general sense. Consider the series

$$\sum_{n=1}^{\infty} a_n$$

and denote by $\hat{a}_n$ an asymptotic approximation for the a_n valid for large n, say $n > \bar{N}-1$. Suppose that $\hat{a}_n$ has the form

$$\hat{a}_n = \frac{(-1)^n}{n^{1/2}} + \frac{(-1)^n}{n^{3/2}} + \frac{1}{n} + o(\frac{1}{n})$$

Then even though the series

$$\sum_{n=N}^{\infty} \left[\frac{(-1)^n}{n^{1/2}} + \frac{(-1)^n}{n^{3/2}} \right]$$

converges, the original series will not converge because if one takes the third term of the asymptotic expansion the series

$$\sum_{n=N}^{\infty} \left[\frac{(-1)^n}{n^{1/2}} + \frac{(-1)^n}{n^{3/2}} + \frac{1}{n} \right]$$

diverges.

This dilema does not arise, however, with the particular examples investigated in this appendix. For the series denoted by S_1, S_2, and S_3 the asymptotic representations for the a_n are either of the form

$$e^{-i2\pi n d} \, \hat{a}_n = \frac{A}{n^{1/2}} + \frac{B}{n^{3/2}} + o\left(\frac{1}{n^{3/2}}\right)$$

where

$$d = \frac{mM^2}{\beta^2} - \zeta$$

and A and B are constants, or

$$\hat{a}_n = 2i\beta \, e^{-nkh} \, e^{-i2n\pi m}$$

Now by applying the theorem given in Appendix I series of the form

$$\sum_{n=\bar{N}}^{\infty} \frac{e^{i2\pi nd}}{n^{s+(1/2)}} \qquad s \geq 0$$

will converge provided d is not an integer. If d is an integer the series diverges for $s = 0$ and converges for all $s > 0$. Further, series of the form

$$\sum_{n=\bar{N}}^{\infty} e^{-nkh} \, e^{i2n\pi m}$$

clearly converge so that the original series denoted by S_1 and S_2 converge whenever

$$\frac{mM^2}{\beta^2} - \zeta \neq \delta \qquad \delta = 0,1,2,3, \ldots$$

and the series denoted by S_3 converges for all values of the parameters. Finally, it should be pointed out that throughout this entire argument it is implied that since the a_n are bounded the sum

$$\sum_{n=1}^{\bar{N}-1} a_n$$

can only produce a finite sum and hence cannot affect convergence or divergence of the infinite series.

APPENDIX I

A THEOREM ON THE CONVERGENCE OF
A CERTAIN INFINITE SERIES

In this appendix a mathematical theorem and its proof are presented which establish the convergence of a particular type of infinite series. Both the theorem and its proof are due to Dr. E. N. Nilson of Pratt and Whitney Aircraft, East Hartford, Connecticut.

THEOREM: If a_k is a positive decreasing sequence approaching zero monotonically as $k \to \infty$ and if

$$d_k = kd + \epsilon_k$$

where d is not an integral multiple of 2π and either $\epsilon_k = 0$ for all k, or ϵ_k is positive and decreasing monotonically to zero as $k \to \infty$, or ϵ_k is negative and increasing monotonically to zero as $k \to \infty$, then the series

$$\sum_{k=1}^{\infty} a_k e^{id_k} \tag{I-1}$$

converges. If d is an integral multiple of 2π and $\epsilon_k = 0$ for all k then the convergence of the series given by Equation (I-1) depends on the convergence of the series

$$\sum_{k=1}^{\infty} a_k$$

PROOF: The following Lemma is needed in the proof of the theorem and covers the case where $e_k = 0$ for all k.

Lemma: The series $\sum_{k=1}^{\infty} a_k e^{ikd}$ converges.

Proof of Lemma: Abel's transformation

$$\sum_{k=m}^{n} u_k v_k = \sum_{k=m}^{n-1} \bar{U}_k(v_k - v_{k+1}) - \ddot{U}_{m-1} v_m + \bar{U}_n v_n \qquad 0 \le m \le n$$

$$\ddot{U}_k = u_1 + u_2 + \ldots + u_k \qquad \bar{U}_o = 0$$

is used as follows. Set

$$u_k = e^{ikd} \qquad v_k = a_k$$

Then if d is not an integral multiple of 2π

$$\ddot{U}_k = e^{id} + e^{i2d} + \ldots + e^{ikd}$$

$$\bar{U}_k = \frac{e^{i(k+1)d} - e^{id}}{e^{id} - 1}$$

$$\bar{U}_k = e^{i(k+1)d/2} \frac{\sin(kd/2)}{\sin(d/2)}$$

Then from this last relation

$$|\bar{U}_k| = \left|\frac{\sin(kd/2)}{\sin(d/2)}\right| \leq \frac{1}{|\sin(d/2)|}$$

Further, if a_k is positive and decreasing monotonically to zero as $k \to \infty$ then

$$a_1 = a_1 - a_2 + a_2 - a_3 + a_3 - a_4 + a_4 - \ldots$$

$$a_1 = |a_1 - a_2| + |a_2 - a_3| + |a_3 - a_4| + \ldots$$

Since

$$\sum_{k=1}^{\infty} |a_k - a_{k+1}| = \sum_{k=1}^{\infty} |v_k - v_{k+1}|$$

converges (to a_1, as a matter of fact) the Cauchy criterion for convergence implies that (for arbitrary $\epsilon > 0$)

$$\sum_{k=m}^{n-1} |v_k - v_{k+1}| < \epsilon$$

provided m is sufficiently large (n ≥ m of course). Hence by the Abel transformation

$$\left| \sum_{k=m}^{n} a_k e^{ikd} \right| = \left| \sum_{k=m}^{n-1} \bar{U}_k (v_k - v_{k+1}) - \bar{U}_{m-1} v_m + \bar{U}_n v_n \right|$$

$$\leq \sum_{k=m}^{n-1} |\bar{U}_k| \, |v_k - v_{k+1}| + |\bar{U}_{m-1}| \, |v_m| + |\bar{U}_n| \, |v_n|$$

$$\leq \frac{1}{|\sin(d/2)|} \left(\sum_{k=m}^{n-1} |v_k - v_{k+1}| + |v_m| + |v_n| \right)$$

$$< \frac{1}{|\sin(d/2)|} \left(\varepsilon + |v_m| + |v_n| \right)$$

Now $\left| \sum_{k=m}^{n} a_k e^{ikd} \right|$ can be made as small as desired simply by making m sufficiently large ($v_m \to 0$, $|v_n| < |v_m|$). Therefore, by the Cauchy test for convergence, the series

$$\sum_{k=1}^{\infty} e^{ikd}$$

converges. This completes the proof of the lemma.

To prove the theorem, it will be shown that the difference of the two series

$$\sum_{k=1}^{\infty} a_k \left(e^{id_k} - e^{ikd} \right)$$

converges. Then the convergence of the series given by Equation (I-1) follows from the convergence of the series

$$\sum_{k=1}^{\infty} a_k e^{ikd}$$

The method employed in the proof of the lemma will again be used. In this case let

$$u_k = \left(e^{i\epsilon_k} - 1 \right) e^{ikd}$$

$$v_k = a_k$$

If it can be shown that

$$\left| \bar{U}_k \right| \leq \bar{M} \quad \text{for some } \bar{M} \quad k = 1, 2, \ldots$$

then

$$\left| \sum_{k=m}^{n} a_k \left(e^{i\epsilon_k} - 1 \right) e^{ikd} \right| = \left| \sum_{k=m}^{n-1} \bar{U}_k (v_k - v_{k+1}) - \bar{U}_{m-1} v_m + \bar{U}_n v_n \right|$$

$$\left| \sum_{k=m}^{n} a_k \left(e^{i\varepsilon_k} - 1 \right) e^{ikd} \right| \leq \sum_{k=m}^{n-1} |\bar{U}_k| |v_k - v_{k+1}| + |\bar{U}_{m-1}| |v_m| + |\bar{U}_n| |v_n|$$

$$\leq \bar{M} \left(\sum_{k=m}^{n-1} |v_k - v_{k+1}| + |v_m| + |v_n| \right)$$

$$< \bar{M} \left(\varepsilon + |v_m| + |v_n| \right)$$

and the absolute value of the sum can be made as small as desired by making m sufficiently large. Again the Cauchy criterion gives convergence.

It must be shown then, that

$$|\bar{U}_k| = \left| \sum_{j=1}^{k} \left(e^{i\varepsilon_j} - 1 \right) e^{ijd} \right| \leq \bar{M} \qquad (I\text{-}2)$$

for some $\bar{M}$ and all k. Again employ the Abel transformation. Set

$$u_j^* = e^{ijd} \qquad v_j^* = e^{i\varepsilon_j} - 1$$

so that

$$\bar{U}_j^* = u_1^* + u_2^* + \ldots + u_j^* = e^{id} \frac{e^{ijd} - 1}{e^{id} - 1}$$

As before

$$|\vec{U}_j^*| \le \frac{1}{|\sin(d/2)|}$$

Finally, the boundedness of

$$\sum_{j=m}^{n} |v_j^* - v_{j+1}^*|$$

is needed. This shall be obtained from the convergence of

$$\sum_{j=m}^{\infty} |v_j^* - v_{j+1}^*|$$

When ϵ_k is positive and decreasing monotonically to zero

$$\sum_{j=m}^{\infty} |v_j^* - v_{j+1}^*| = \sum_{j=m}^{\infty} |e^{i\epsilon_j} - e^{i\epsilon_{j+1}}|$$

$$= \sum_{j=m}^{\infty} 2 \sin\left(\frac{\epsilon_j - \epsilon_{j+1}}{2}\right)$$

provided m is large enough to insure that $(\epsilon_j - \epsilon_{j+1}) < 2\pi$. Thus

$$\sum_{j=m}^{\infty} |v_j^* - v_{j+1}^*| < \sum_{j=m}^{\infty} \left(\epsilon_j - \epsilon_{j+1}\right)$$

$$< \epsilon_m$$

When ϵ_k is negative and increasing monotonically to zero

$$\sum_{j=m}^{\infty} |v_j^* - v_{j+1}^*| = \sum_{j=m}^{\infty} 2\sin\frac{\epsilon_{j+1} - \epsilon_j}{2} < \sum_{j=m}^{\infty} \left(\epsilon_{j+1} - \epsilon_j\right) < -\epsilon_m$$

It may thus be concluded that

$$\sum_{j=m}^{\infty} |v_j^* - v_{j+1}^*| < |\epsilon_m|$$

Applying the Abel transformation

$$\left| \sum_{j=m}^{\infty} u_j^* \, v_j^* \right| \leq \sum_{j=m}^{n-1} |\bar{U}_j^*| \; |v_j^* - v_{j+1}^*| + |\bar{U}_{m-1}^*| \; |v_m^*| + |\bar{U}_n^*| \; |v_n^*|$$

$$\leq \frac{1}{|\sin(d/2)|} \left(\sum_{j=m}^{n-1} |v_j^* - v_{j+1}^*| + |v_m^*| + |v_n^*| \right)$$

$$\leq \frac{1}{|\sin(d/2)|} \left(|\epsilon_m| + |v_m^*| + |v_n^*| \right)$$

Since $|v_m^*| \rightarrow 0$, the convergence of $\bar{U}_k$ in Equation (I-2) is obtained and hence $|\bar{U}_k|$ is bounded.

If d is an integral multiple of 2π and $\epsilon_k = 0$ for all k then the expontial in Equation (I-1) disappears and the series becomes

$$\sum_{k=1}^{\infty} a_k \qquad\qquad (I-3)$$

Thus the convergence of the original series depends on the convergence of the series given by Equation (I-3).

This completes the proof of the theorem. It is to be noted, of course, that the requirements on a_k and ϵ_k need only be valid from a certain point on, not for k at the beginning. It is important also to note the necessity for the requirements on a_k and ϵ_k.

LITERATURE CITED

1. Paul, W. F., "A Self-Excited Rotor Blade Oscillation at High Subsonic Mach Numbers," Journal of the American Helicopter Society, Vol. 14, No. 1, January 1969, pp. 38-48.

2. Loewy, R. G., "A Two Dimensional Approximation to the Unsteady Aerodynamics of Rotary Wings," Journal of the Aerospace Sciences, Vol. 24, No. 2, February 1957, pp. 81-92, 144.

3. Jones, J. P., "The Influence of the Wake on the Flutter and Vibration of Rotor Blades," Aeronautical Quarterly, Vol. IX, 1958, pp. 258-286.

4. Timman, R., and van de Vooren, A. I., "Flutter of a Helicopter Rotor Rotating in Its Own Wake," Journal of the Aerospace Sciences, Vol. 24, No. 9, September 1957, pp. 694-702.

5. Theodorsen, T., "General Theory of Aerodynamic Instability and the Mechanism of Flutter," NACA TR 496, 1949.

6. Hammond, C. E., "A Parametric Study of Helicopter Rotor Blade Flutter Under Low Inflow Conditions, Using Incompressible Aerodynamics," Georgia Institute of Technology, School of Aerospace Engineering, Student Special Problem, June 1968.

7. Miller, R. H., "Theoretical Determination of Rotor Blade Harmonic Airloads," Massachusetts Institute of Technology, Aeroelastic and Structures Research Laboratory, TR 107-2, AD-619048, August 1964.

8. Ichikawa, T., "Linear Aerodynamic Theory of Rotor Blades," Journal of Aircraft, Vol. 4, No. 3, May-June 1967, pp. 210-218.

9. Weissinger, J., "The Lift Distribution of Swept-Back Wings," NACA TM 1120, 1947.

10. Landgrebe, A. J., "An Analytical Method for Predicting Rotor Wake Geometry," AIAA Paper No. 69-196, Presented at the AIAA/AHS VTOL Research, Design, and Operations Meeting, Georgia Institute of Technology, Atlanta, Georgia, February 17-19, 1969.

11. Possio, C., "L'Azione Aerodinamica sul Profilo Oscillante in un Fluido Compressibile a Velocità Iposonora," L'Aerotecnica, t. XVIII, fasc. 4, April 1938. (Also available as British Ministry of Aircraft Production R.T.P. Translation 987.)

12.   Dietze, F., "The Air Forces of the Harmonically Vibrating Wing at Subsonic Velocity (Plane Problem), Parts I and II," U. S. Air Force Translations F-TS-506-RE and F-TS-948-RE, 1947. (Originally, Luftfahrtforschung, Bd. 16, Lfg. 2, 1939, S. 84-86.)

13.   Schade, Th., "Numerische Loesung der Possioschen Integralgleichung der schwingenden Tragflaeche in ebener Unterschallstroemung - I: Analytischer Teil," AVA/44/J/27, 1944. ("Numerical Solution of Possio's Integral Equation for a Vibrating Wing in Two-Dimensional Subsonic Flow - I: Analytical Part," ATI-44523.)

14.   Küssner, H. G., "General Airfoil Theory," NACA TM 979, 1941. (From Luftfahrtforschung, Bd. 17, Lfg. 11/12, 1940, pp. 370-378.)

15.   Karp, S. N., Shu, S. S., and Weil, H., "Aerodynamics of the Oscillating Airfoil in Compressible Flow," U. S. Air Force, Air Materiel Command, Technical Report F-TR-1167-ND, 1947.

16.   Fettis, H. E., "An Approximate Method for the Calculation of Nonstationary Air Forces at Subsonic Speeds," U. S. Air Force, WADC TR 52-56, 1952.

17.   Frazer, R. A., "Possio's Subsonic Derivative Theory and Its Application to Flexural-Torsional Wing Flutter," British Aeronautical Research Council, R & M 2553, 1951.

18.   Jordan, P. F., "Aerodynamic Flutter Coefficients for Subsonic, Sonic, and Supersonic Flow (Linear Two-Dimensional Theory)," British Aeronautical Research Council, R & M 2932, 1953.

19.   Jones, W. P., "The Oscillating Airfoil in Subsonic Flow," British Aeronautical Research Council, R & M 2921, 1956.

20.   Reissner, E., and Sherman, S., "Compressibility Effects in Flutter," Curtiss-Wright Corporation, Airplane Division, Report No. S. B. 240-S-1, 1944.

21.   Haskind, M. D., "Oscillations of a Wing in a Subsonic Gas Flow," Brown University, Translation No. A9-T-22, 1948. [Originally Prinkl. Mat. i Mekh. (Moscow), Vol. XI, No. 1, pp. 129-146, 1947.]

22.   Timman, R., and van de Vooren, A. I., "The Oscillating Wing with Aerodynamically Balanced Control Surface in a Two-Dimensional Subsonic Compressible Flow," National Luchtvaartlaboratorium, Amsterdam, Report F.54, 1949.

23. Timman, R., van de Vooren, A. I., and Greidanus, J. H., "Aerodynamic Coefficients of an Oscillating Airfoil in Two-Dimensional Subsonic Flow," Journal of the Aeronautical Sciences, Vol. 18, No. 12, December 1951, pp. 797-802,834.

24. Jones, W. P., and Rao, B. M., "Compressibility Effects on Oscillating Rotor Blades in Hovering Flight," Volume of Technical Papers on Structural Dynamics, Presented at the AIAA Structural Dynamics and Aeroelasticity Specialist Conference, New Orleans, Louisiana, April 16-17, 1969.

25. Runyan, H. L., and Watkins, C. E., "Considerations on the Effect of Wind-Tunnel Walls on Oscillating Air Forces for Two-Dimensional Subsonic Compresible Flow," NACA TN 2552, 1951.

26. Carta, F. O., "Unsteady Aerodynamic Theory of a Staggered Cascade of Oscillating Airfoils in Compressible Flow," United Aircraft Corporation, Research Department Report R-0582-19, August 1957.

27. Baker, W. E., Woolam, W. E., and Young, D., "Air and Internal Damping of Thin Cantilever Beams," International Journal of Mechanical Sciences, Vol. 9, 1967, pp. 743-766.

28. Scanlan, R. H., and Rosenbaum, R., Introduction to the Study of Aircraft Vibration and Flutter, The Macmillan Company, New York, 1951.

29. Smilg, B., and Wasserman, L. S., "Application of Three-Dimensional Flutter Theory to Aircraft Structures," Air Force Technical Report 4798, ATI-28690, 1942.

30. Hsu, P. T., "Flutter of Low Aspect Ratio Wings. Part I: Calculation of Pressure Distributions for Oscillating Wings of Arbitrary Planform in Subsonic Flow by the Kernel-Function Method," Massachusetts Institute of Technology, Aeroelastic and Structures Research Laboratory, Technical Report 64-1, October 1957.

31. Fung, Y. C., An Introduction to the Theory of Aeroelasticity, John Wiley and Sons, Inc., New York, N. Y., 1955.

32. Infeld, L., Smith, V. G., and Chen, W. Z., "On Some Series of Bessel Functions," Journal of Mathematics and Physics, Vol. 26, No. 1, April 1947, pp. 22-28.

33. Hurwitz, H., Jr., and Zweifel, P. F., "Numerical Quadrature of Fourier Transform Integrals," Mathematics of Computation, Vol. 10, No. 55, July 1956, pp. 140-149.

34. Lebedev, N. N., Special Functions and Their Applications, Prentice-Hall, Inc., Englewood Cliffs, N. J., 1965.

35. Todd, J., "Evaluation of the Exponential Integral for Large Complex Arguments," Journal of Research of the National Bureau of Standards, Vol. 52, No. 6, June 1954, pp. 313-317.

36. Bisplinghoff, R. L., Ashley, H., and Halfman, R. L., Aeroelasticity, Addison-Wesley Publishing Company, Inc., Reading, Massachusetts, 1955.

37. Erdélyi, A., Magnus, W., Oberhettinger, F., and Tricomi, F. G., Higher Transcendental Functions, Vol. II, Bateman Manuscript Project, McGraw-Hill Book Company, New York, New York, 1953.

38. Dwight, H. B., Tables of Integrals and Other Mathematical Data, The Macmillan Company, New York, New York, 1961.

39. Abramowitz, M., and Stegun, I. A., Handbook of Mathematical Functions with Formulas, Graphs, and Mathematical Tables, National Bureau of Standards, Applied Mathematics Series 55, 1964.

40. Fanti, R., and Carta, F. O., "Aerodynamic Interaction Effects on a Staggered Cascade of Airfoils Oscillating in Two-Dimensional Compressible Flow," United Aircraft Corporation, Research Department Report R-0582-17, August, 1957.

VITA

Charles Eugene Hammond was born December 21, 1940, the son of Homer E. and Margaret B. Hammond. After attending elementary schools in Lithonia, Georgia, Macon, Georgia, and Warner Robins, Georgia, he was graduated from the Warner Robins Senior High School in June, 1958. He entered the Georgia Institute of Technology in the fall of that year and in December, 1962, completed the requirements for the degree Bachelor of Aerospace Engineering.

Upon graduation he was commissioned a Second Lieutenant in the United States Air Force. After serving two and one-half years in the Service Engineering Division at Robins, AFB, Georgia, he was awarded the Air Force Commendation Medal and released from active duty in August, 1965, with the rank of First Lieutenant.

After release from active duty he accepted a position with the U.S. Naval Weapons Laboratory, Dahlgren, Virginia. One year later he returned to the Georgia Institute of Technology under the Naval Weapons Laboratory's Full Time Advanced Study Program and was awarded the degree Master of Science in Aerospace Engineering in June, 1968.

A member of Sigma Gamma Tau, Mr. Hammond was the first recipient of the Howard Hughes Fellowship from the Vertical Flight Foundation.

He is married to the former Mae Cauley and they have one daughter, Cynthia Lynn.